GRADUATE AERONAUTICAL LABORATORIES
CALIFORNIA INSTITUTE OF TECHNOLOGY

FM 91 – 1

Partial Chemical Equilibrium: Theory and Implementation in the Program Surf

by

Martin Rein

Firestone Flight Sciences Laboratory

Guggenheim Aeronautical Laboratory

Karman Laboratory of Fluid Mechanics and Jet Propulsion

Pasadena

FM 91 – 1

Partial Chemical Equilibrium:
Theory and Implementation in the Program Surf

by

Martin Rein

Graduate Aeronautical Laboratories
California Institute of Technology
Pasadena, CA 91125

April 1991

Table of Contents

List of Symbols

Only symbols introduced for describing partial equilibrium flows are included in the following list. For symbols not listed here, see Surf report (Rein, 1989).

a_{ij}	coefficients of matrix in eq. (4.5)
a_{pf}	partially frozen sound speed
dE_{jk}	contribution of equilibrium reaction k to the rate of change of dependent species j
dN_{jk}	contribution of nonequilibrium reaction k to the rate of change of dependent species j
F_j	reaction vector of formation reaction for dependent species Y_j
H	defined by eq. (3.12)
$I_{r,k}$	defined by eq. (3.2)
n_e	number of linearly independent equilibrium reactions
$n_{j,l}$	multiplier for rate equation for dependent species Y_j $(l = 1, ..., (s-c) - n_e)$
N_e	set containing the indices of all equilibrium reactions
$\overline{N_e}$	set containing the indices of n_e linearly independent equilibrium reactions
N_{neq}	set containing the indices of all nonequilibrium reactions
$\overline{N_{neq}}$	set containing the indices of all nonequilibrium reactions which are linearly independent of equilibrium reactions
R	reaction vector, universal gas constant
$\tilde{R}$	reduced reaction vector (cf. chapter 4.3.)
S_k	defined by eq. (3.14)
T_{fit}	switch temperature at which thermodynamic model is switched from polynomial fit to statistical mechanics formulation
β_{jk}	$:= \nu'_{jk} - \nu_{jk}$, components of reaction vector
λ	proportionality factor (cf. eq. (3.17))
λ_k	characteristic relaxation length of reaction k, defined by eq. (4.4)
τ_k	characteristic relaxation time of reaction k, defined by eq. (4.3)

subscripts:

e, eq	equilibrium
f	frozen, forward
neq	nonequilibrium
peq	partial equilibrium
pf	partially frozen/equilibrium
$\perp$	orthogonal

superscripts:

e	equilibrium
neq	nonequilibrium
$*$	cf. eq. (2.34)
$\perp$	orthogonal

1. Introduction

Surf is a program for computing steady and inviscid, supersonic reacting flows in planar and axisymmetric nozzles. The program which was described in a previous report (Rein, 1989, named Surf report hereafter), has options for determining nonequilibrium, equilibrium and frozen flows, respectively. Further, the possibility of switching the computation from a fully equilibrium to a fully nonequilibrium flow calculation was introduced. This latter option aimes at decreasing the CPU-time by reducing the stiffness inherent to the partial differential equation system used for modeling the flow. Exploring this concept more deeply, one eventually ends up with the idea of introducing partial equilibrium into Surf. The realization of this idea, both theoretically and practically, is subject of the present report.

The stiffness of the governing equations which often complicates the computation of non-equilibrium reacting flows, is due to characteristic time constants of very different order of magnitudes being present at the same time. Reactions, for example, which are close to equilibrium, have very short time constants, while time constants of reactions which are far from equilibrium, and characteristic times of the flow itself, can be large. A remedy for circumventing, or at least for reducing, the stiffness is to consider those reactions which are close to equilibrium, as actually being in equilibrium. Contributions of these fast reactions to the rate equations can then be replaced by some equilibrium constraints. In this manner the very short characteristic times of close to equilibrium reactions are eliminated.

Ramshaw (1980) proposed two different equation systems for partial chemical equilibrium in fluid dynamics. In the first equation system the contributions of equilibrium reactions to the rate equations are eliminated by suitably combining these equations. In the derivation of this system, however, statements are made which are not clear. Further, Ramshaw does not distinguish between linearly dependent and independent reactions. This point is of great importance in the present theory of partial equilibrium. In deriving the second equation system which is used in the KIVA-code of Amsden *et al.* (1985), additional equations expressing the conservation of mass and energy are needed. The equilibrium conditons are applied in differential form. As Ramshaw (1980) quoted, the resulting equations will only "preserve partial equilibrium if it is initially present but will not establish it if it is not". Further, Ramshaw (1980) states that the concept of partial equilibrium flow is especially useful when the reactions can be classified in equilibrium and nonequilibrium reactions independently of space and time.

In the present report a more straightforward approach, reminding of the one leading to the first equation system of Ramshaw (1980), is used. A general formulation is introduced which is accessible to a mathematical treatment of arbitrary reactive systems. The formulation is in no way limited to cases where all close to equilibrium reactions are *a priori* known. It is thus easily applicable to nozzle flows where the flow conditions range from equilibrium to frozen, enclosing a nonequilibrium regime.

In the following chapters firstly the theory of partial chemical equilibrium in arbitrary reactive systems is formulated. This part provides also a formulation for the partially frozen sound speed. The formulation includes the nonequilibrium and equilibrium sound speeds as limiting cases. In the Surf report the expression for the equilibrium sound speed is in error and needs to be replaced by the present formulation. Subsequently the implementation of the concept of

partial equilibrium in Surf is described and illustrated by sample computations. The theoretical part concerning partial equilibrium is self-contained, whereas the more practical part on the implementation is not. In this latter part reference will often be made to the Surf report cited above. It should be mentioned that the new version of Surf including the partial equilibrium option, works in quite the same manner as the old version. In particular, the input and output formats have not been changed. Actually, on input the new version no longer needs the 'third body vector' (cf. Surf report) to be provided. If, however, this vector is nevertheless provided, this will not lead to an error. The new version is thus compatible with old input data files. On output, some additional information concerning partial chemical equilibrium is written to output file 'outpt2' which contains the detailed results of the computation (cf. Surf report). This happens again in such a way that old evaluation programs should not need to be changed. They can thus be used for both versions of Surf.

The program Surf computes reacting nozzle flows by a method of lines. The initial conditions are usually approximated using a one-dimensional flow solution. The dependence of the solution obtained by Surf, on the resolution in cross direction and on the initial conditions was not considered in the Surf report. It is now discussed in chapters 6.4. and 6.5. .

2. Partial equilibrium in reactive systems

In the following a general formulation for partial chemical equilibrium is introduced. This is done with an application in the field of gas dynamics in mind. For that reason, then and now reference will be made to expressions like 'gas', 'flow', etc. The mathematical formulation, however, can be applied to any reactive system, as long as the reactants are premixed.

2.1. Linearly independent and dependent species

A mixture of s different species is considered. The species can be divided into c linearly independent species Y_i, $i = 1,...,c$, and $(s-c)$ linearly dependent species Y_j, $j = c+1,...,s$ (cf. Lordi *et al.*, 1966). The dependent species are defined by:

$$Y_j = \sum_{i=1}^{c} \alpha_{ji} \cdot Y_i \quad , \qquad j = c+1,...,s \quad . \tag{2.1}$$

Here, α_{ji} denotes the number of atoms or molecules of the independent species Y_i per atom or molecule of the dependent species Y_j, respectively. In the present formulation the α_{ji} may be real numbers. Equations (2.1) represent the so-called formation reactions of the dependent species. The concentrations of the independent species satisfy conservation equations. If the concentrations γ_l, $l = 1,...,s$, are expressed in units of moles per mass the conservation equations are given by:

$$\sum_{l=1}^{s} \alpha_{li} \cdot \gamma_l = \gamma_i^{\circ} \quad , \qquad i = 1,...,c \quad , \tag{2.2}$$

where $\alpha_{li} = \delta_{li}$ for $l = 1,...,c$, $i = 1,...,c$, and δ_{li} is Kronecker's δ. The γ_i°, $i = 1,...,c$, denote the concentrations of the independent species in the special case, where only independent species are present.

At a thermodynamic state specified by two quantities, e.g. temperature and pressure, the equilibrium species concentrations are determined by the conservation equations for the independent species, and by the law of mass action formulated for the formation reactions of the dependent species:

$$\prod_{i=1}^{c} \gamma_i^{\alpha_{ji}} \cdot \gamma_j^{-1} = K_{\gamma_j}(T,p;\gamma_{l,l=1,...,s}) \quad , \qquad j = c+1,...,s \quad . \tag{2.3}$$

T and p denote the temperature and the pressure, respectively. The so-called equilibrium constant K_{γ_j} expressed in terms of the species concentrations in moles per mass, is defined by

$$K_{\gamma_j}(T,p;\gamma_{l,l=1,...,s}) = \Big(\frac{p}{\Gamma\, p_0}\Big)^{-(\sum_{i=1}^{c} \alpha_{ji})+1} \cdot exp\Big(-\frac{1}{RT}\Big(\sum_{i=1}^{c}(\alpha_{ji}\,\hat{\mu}_i^{\circ}) - \hat{\mu}_j^{\circ}\Big)\Big) \quad , \tag{2.4}$$

where p_0 is the reservoir pressure and R the universal gas constant. The chemical potentials per mole, $\hat{\mu}_j^{\circ}$, at this pressure can be calculated using a thermodynamic model as the one provided in the Surf report.

2.2. Linearly independent and dependent reactions

Chemical reactions are always composed of a forward and backward reaction taking place simultaneously. A reaction among the species Y_l, $l = 1, ..., s$, is usually specified in the following manner:

$$\sum_{l=1}^{s} \nu_l \, Y_l \;\rightleftharpoons\; \sum_{l=1}^{s} \nu_l' \, Y_l \;, \tag{2.5}$$

where ν_l and ν_l', $l = 1, ..., s$, are the stoichiometric coefficients of the reactants and products. Here, a reaction vector $R = (\beta_l)_{l=1,...,s}$ is introduced for representing this reaction. The components of the vector R are defined by $\beta_l = \nu_l' - \nu_l$. Third bodies are thus not taken into account in the present reaction vector formulation. They can, however, be easily incorporated by defining extended reaction vectors $R' = (\beta_l')_{l=1,...,2s}$ where $\beta_l' = \nu_l'$ for $l = 1, ..., s$ and $\beta_l' = -\nu_l$ for $l = s+1, ..., 2s$. For the present purpose of describing partial chemical equilibrium the extended form of the reaction vector is not needed. Using the reaction vector notation the condition for a reaction to be in equilibrium can be expressed in the following manner:

$$\sum_{l=1}^{s} \beta_l \cdot \hat{\mu}_l = 0 \quad , \tag{2.6}$$

where $\hat{\mu}_l$ is the chemical potential per mole of species Y_l, $l = 1, ..., s$.

Different reactions are said to be linearly dependent or independent, if their reaction vectors are linearly dependent or independent, respectively. The formation reactions provide a basis for all reactions that can occur. This yields $(s - c)$ linearly independent reaction vectors which span a subspace of the s-dimensional space of reaction vectors. This subspace contains all reactions which do not violate the c constraints which are present due to the conservation equations (2.2) for independent species. It will be called reaction subspace.

2.3. Equilibrium and finite rate reactions

If a reaction is in equilibrium the forward and backward reactions balance each other. Thus an equilibrium reaction does not change the concentrations of the species involved in the reaction. Further, the law of mass action corresponding to the reaction considered, is satisfied. In the present formulation (cf. eq. (2.4)) the so-called equilibrium constant of the law of mass action is a function of the temperature, the pressure and the species concentrations. In steady reacting flows a change of the thermodynamic state may be caused both, by the heat of reaction of a nonequilibrium reaction and by a changing geometry as, for example, in nozzle flows. If the thermodynamic state is changed due to geometrical effects, a reaction which is in equilibrium at first, will get out of equilibrium. It takes a finite time to reestablish equilibrium. Within this time a 'flow particle' usually moves to a new location and the thermodynamic state is changed again, etc. For that reason reactions which are truly in equilibrium will normally not be found in nozzle flows (exceptions may be cases where the thermodynamic state is constant within wide parts of the flow field). Thus, a flow in which all reactions are in equilibrium, represents an ideal case.

This ideal case, however, is the limiting case which is present if the characteristic relaxation times τ_k of all reactions k, $k = 1, ..., r$, are much smaller than a typical time constant τ_f of the flow. The characteristic relaxation time of a reaction k can, e.g., be defined as $\tau_k = max\ (\tau_{jk})$ where the maximum is formed with respect to different j, $j = c+1, ..., s$. The characteristic relaxation times τ_{jk} associated with the rate of change of each of the dependent species concentrations, due to reaction k, were introduced in the Surf report (eq. (2.18)). Henceforth, a reaction with $\tau_k \ll \tau_f$ will be called equilibrium reaction. All other reactions are finite rate reactions which will also be called nonequilibrium reactions.

Within the reaction subspace the equilibrium reactions span a subspace which will be called equilibrium reaction subspace. The reaction subspace can be represented by the direct sum of this equilibrium reaction subspace and another subspace. Here, the orthogonal complement of the equilibrium reaction subspace is chosen as the other subspace. Every reaction vector R can thus be decomposed in two vectors, $R = R_{eq} + R_{neq}$, R_{eq} being an element of the equilibrium reaction subspace, R_{neq} of its orthogonal complement. The contribution to the reaction vector of R_{neq} is responsible for the nonequilibrium properties of a reaction. Therefore the orthogonal complement of the equilibrium reaction subspace will be called nonequilibrium reaction subspace hereafter.

In the case of nonequilibrium flows all reactions considered need to be specified. The rate of change of the species concentrations due to nonequilibrium reactions is described by rate equations (cf. Surf report, eq. (2.15)). In order to approach an equilibrium state by nonequilibrium reactions it is necessary that at least $(s - c)$ linearly independent nonequilibrium reactions are present. Otherwise, an equilibrium state as described above can never be obtained. Strictly speaking, a system of reactions can only yield the equilibrium state if it contains a basis of exactly $(s-c)$ vectors from which all formation reactions can be formed. This condition which is necessary to include the limiting case of equilibrium, is usually never stated explicitly.

2.4. Changes in species concentrations

Changes in the species concentrations are considered to occur only due to chemical reactions. Hence, the concentrations are always positive and there exists a maximum for every concentration. The conservation equations for the independent species limit the concentrations to an even smaller domain.

The species concentrations can be written as a vector $(\gamma_l)_{l=1,...,s}$ which will be called concentration vector hereafter. A reaction changes the concentration vector in the direction of the corresponding reaction vector (except for the sign). Changes in the concentration vector can thus be decomposed into changes in the equilibrium and nonequilibrium reaction subspaces. This decomposition will become important in the formulation of the partially frozen sound speed (cf. chapter 2.7.).

2.5. Example

To elucidate the concept of linearly dependent or independent species and reactions, respectively, an example with $s = 5$ species of which $c = 2$ species are independent, is provided. The

gas considered is composed of the independent species $Y_1 = N_2$, $Y_2 = O_2$ and of the dependent species $Y_3 = N$, $Y_4 = O$, $Y_5 = NO$. The formation reactions are given by:

1) $N \rightleftharpoons 1/2\ N_2$
2) $O \rightleftharpoons 1/2\ O_2$
3) $NO \rightleftharpoons 1/2\ N_2 + 1/2\ O_2$,

i.e. all non-zero α_{ji} are real. The reaction vectors $F_i, i = 1, ..., 3$, of these formation reactions are thus:

$$F_1 = \begin{pmatrix} 1/2 \\ 0 \\ -1 \\ 0 \\ 0 \end{pmatrix} , \quad F_2 = \begin{pmatrix} 0 \\ 1/2 \\ 0 \\ -1 \\ 0 \end{pmatrix} , \quad F_3 = \begin{pmatrix} 1/2 \\ 1/2 \\ 0 \\ 0 \\ -1 \end{pmatrix} . \tag{2.7}$$

The following finite rate reactions are taken into account (not all of these reactions appear in the following example, but they will be used later):

1) $N_2 + M \rightleftharpoons 2N + M$
2) $O_2 + M \rightleftharpoons 2O + M$
3) $NO + M \rightleftharpoons N + O + M$
4) $O_2 + N \rightleftharpoons O + NO$
5) $N_2 + O \rightleftharpoons N + NO$
6) $N_2 + O_2 \rightleftharpoons 2NO$

M denotes an arbitrary third body. The corresponding reaction vectors R_k, $k = 1, ..., 6$, are then given by:

(2.8)

$$R_1 = \begin{pmatrix} -1 \\ 0 \\ 2 \\ 0 \\ 0 \end{pmatrix} , \ R_2 = \begin{pmatrix} 0 \\ -1 \\ 0 \\ 2 \\ 0 \end{pmatrix} , \ R_3 = \begin{pmatrix} 0 \\ 0 \\ 1 \\ 1 \\ -1 \end{pmatrix} , \ R_4 = \begin{pmatrix} 0 \\ -1 \\ -1 \\ 1 \\ 1 \end{pmatrix} , \ R_5 = \begin{pmatrix} -1 \\ 0 \\ 1 \\ -1 \\ 1 \end{pmatrix} , \ R_6 = \begin{pmatrix} -1 \\ -1 \\ 0 \\ 0 \\ 2 \end{pmatrix} .$$

It can be seen that R_3 and R_4 are linearly independent, but R_2 is not: $R_2 = R_3 + R_4$. Further, $R_2 = -2 \cdot F_2$. Thus, let reaction (3) and (4) be in equilibrium, then the equilibrium conditions

$$\begin{aligned} \hat{\mu}_{NO} - \hat{\mu}_N - \hat{\mu}_O &= 0 \\ \hat{\mu}_{O_2} + \hat{\mu}_N - \hat{\mu}_O - \hat{\mu}_{NO} &= 0 \end{aligned} \tag{2.9}$$

hold. Adding these equations yields:

$$\hat{\mu}_{O_2} - 2\hat{\mu}_O = 0 \ . \tag{2.10}$$

This is the condition for the concentrations of O_2 and O to be in mutual equilibrium. Thus, even though finite rate reaction (2) may be in nonequilibrium it does not play a role and can be neglected. It should be mentioned that the total amount of O and O_2 may change, i.e. $\gamma_O + 2 \cdot \gamma_{O_2} \neq const$ (e.g. reactions (5) and (6) can still change the total amount of mon-atomic and di-atomic oxygen).

2.6. Partial chemical equilibrium

The rate of change of the concentration of a species is due to contributions of the individual reactions. This is expressed by the rate equations for the dependent species:

$$\frac{d\gamma_j}{dt} = \sum_{k=1}^{r} \left(\frac{d\gamma_j}{dt}\right)_k \quad , j = c+1, ..., s \quad , \tag{2.11}$$

where $(d\gamma_j/dt)_k$ denotes the contribution of reaction k. The rate of change of the independent species concentrations is easily obtained from the conservation equations (2.2).

Ramshaw (1980), and independently Hornung (1988), proposed to distinguish between contributions of equilibrium and nonequilibrium reactions:

$$\frac{d\gamma_j}{dt} = \sum_{k \in N_{neq}} \left(\frac{d\gamma_j}{dt}\right)_k + \sum_{k \in N_e} \left(\frac{d\gamma_j}{dt}\right)_k \tag{2.12}$$

where $k \in N_{neq}$ denotes nonequilibrium and $k \in N_e$ equilibrium reactions. Considering eq. (2.12) the question arises what the contribution $(d\gamma_j/dt)_{k,k\in N_e}$ of an equilibrium reaction to the rate of change of species concentration γ_j looks like.

Ramshaw (1980) derived explicit expressions for $(d\gamma_j/dt)_{k,k\in N_e}$ by taking the derivative of the equilibrium conditions in the form $\sum_{l=1}^{s} \beta_{lk}\, \hat{\mu}_l = 0$ (this is practically the law of mass action). He further needs the continuity equations, written for the partial mass densities ρ_l of the species, and the energy equation. This leads to his second equation system. Since Ramshaw chose the temperature T and the densities ρ_l, $l = 1, ..., s$, as independent variables (instead of p, ρ and γ_j, $j = c+1, ..., s$) this approach is not straightforwardly applicable in the present case.

A different approach is to use the equilibrium condition for each linearly independent equilibrium reaction to replace a rate equation. At the same time, in the rate equations the contributions of equilibrium reactions to the rate of change are eliminated by suitably adding these rate equations.

To elucidate this procedure an example basing on the one of chapter 2.5. is given first. For simplicity, the rate equations (2.12) are expressed using total differentials:

$$d\gamma_j = \sum_{k \in N_{neq}} dN_{jk} + \sum_{k \in N_e} dE_{jk} \ , \quad j = c+1, ..., s \tag{2.13}$$

where dN_{jk} and dE_{jk} represent the contributions of nonequilibrium and equilibrium reactions k, respectively, to the change of species concentration γ_j. The dN_{jk} are well known expressions (cf. Surf report, eq. (2.12)) whereas the dE_{jk} are unknown.

Consider again the example of 2.5. where reactions (3) and (4) are in equilibrium. The rate equations for the dependent species are then given by:

$$\begin{aligned} d\gamma_N &= dN_{N,1} + dE_{N,3} + dE_{N,4} + dN_{N,5} \\ d\gamma_O &= dN_{O,2} + dE_{O,3} + dE_{O,4} + dN_{O,5} \\ d\gamma_{NO} &= dE_{NO,3} + dE_{NO,4} + dN_{NO,5} + dN_{NO,6} \quad . \end{aligned} \tag{2.14}$$

Considering reactions (3) and (4) it can be seen that

$$
\begin{aligned}
dE_{N,3} &= dE_{O,3} = -dE_{NO,3} \ , \\
-dE_{N,4} &= dE_{O,4} = dE_{NO,4} \ ,
\end{aligned}
\tag{2.15}
$$

because the forward and backward reactions balance each other. Thus, adding the first and last equation of (2.14) yields an equation which no longer contains contributions of equilibrium reactions:

$$
d\gamma_N + d\gamma_{NO} = dN_{N,1} + dN_{N,5} + dN_{NO,5} + dN_{NO,6} \ . \tag{2.16}
$$

The law of mass action formulated for reaction (3) and (4) provides two more equations:

$$
\begin{aligned}
\hat{\mu}_N + \hat{\mu}_O - \hat{\mu}_{NO} &= 0 \quad , \\
-\hat{\mu}_{O_2} - \hat{\mu}_N + \hat{\mu}_O + \hat{\mu}_{NO} &= 0 \quad .
\end{aligned}
\tag{2.17}
$$

Equation (2.16) and equations (2.17) form a determinate system for the concentrations γ_N, γ_O and γ_{NO}.

It can easily be shown that eq. (2.16) is the only independent combination of (2.14) which does not contain 'equilibrium contributions'. First, equations (2.14) are multiplied by factors n_1,n_2 and n_3, respectively. The resulting equations are added. Considering eq. (2.15) this yields:

$$
\begin{aligned}
& n_1 \cdot d\gamma_N + n_2 \cdot d\gamma_O + n_3 \cdot d\gamma_{NO} = \\
& \qquad n_1 \cdot dN_{N,1} + n_2 \cdot dN_{O,2} + (n_1 + n_2 - n_3) \cdot dE_{N,3} + (-n_1 + n_2 + n_3) \cdot dE_{N,4} + \\
& \qquad n_1 \cdot dN_{N,5} + n_2 \cdot dN_{O,5} + n_3 \cdot dN_{NO,5} + n_3 \cdot dN_{NO,6} \ .
\end{aligned}
\tag{2.18}
$$

The conditons for the equilibrium contributions to disappear are thus:

$$
\begin{aligned}
n_1 + n_2 - n_3 &= 0 \\
-n_1 + n_2 + n_3 &= 0 \ .
\end{aligned}
\tag{2.19}
$$

The only non-trivial solution of this system is $n_1 = n_3$, $n_2 = 0$. Hence, reaction (2) is not contained in the new rate equation which is obtained by a linear combination of the original ones and no longer contains contributions of equilibrium reactions. Reaction (2) is redundant, because the concentrations of O and O_2 which are the ones changed by reaction (2), are already in mutual equilibrium due to equilibrium reactions (3) and (4) (cf. example in 2.5.).

In the following a general formulation for partial chemical equilibrium will be given. Consider n_e, $n_e \leq s - c$, linearly independent reactions to be in equilibrium. This yields n_e equilibrium constraints. $(s - c) - n_e$ additional equations which do not contain equilibrium contributions to the rate of change, can be obtained by linear combinations of the rate equations. In the rate equations it is sufficient to consider only those nonequilibrium reactions which are linearly independent of the equilibrium reactions. The set of these equations will be denoted $\overline{N_{neq}}$ hereafter. Changes in the species concentrations due to nonequilibrium reactions which depend linearly on equilibrium ones, will be instantaneously corrected by the equilibrium reactions. Similarly, only those equilibrium reactions whose basis vectors span the space of equilibrium reactions need

to be taken into account in the rate equations. This leads to the following form of the linear combination of the rate equations:

(2.20)

$$\sum_{j=c+1}^{s} n_{j,l} \cdot \frac{d\gamma_j}{dt} = \sum_{j=c+1}^{s} n_{j,l} \cdot \Big[\sum_{k \in \overline{N_{neq}}} \Big(\frac{d\gamma_j}{dt}\Big)_k \Big] + \sum_{j=c+1}^{s} n_{j,l} \cdot \Big[\sum_{k \in \overline{N_e}} \Big(\frac{d\gamma_j}{dt}\Big)_k \Big] \quad , \quad l = 1, ..., (s-c) - n_e \ ,$$

where $\overline{N_e}$ denotes a set of n_e linearly independent equilibrium reactions. The multipliers $n_{j,l}$ are subject to n_e constraints:

$$\sum_{j=c+1}^{s} n_{j,l} \cdot \beta_{jk} = 0 \ , \quad k \in \overline{N_e} \ . \tag{2.21}$$

The constraints admit $(s-c) - n_e$ linearly independent solutions for the multipliers $n_{j,l}$. These solutions have been labeled by the index l, $l = 1, ..., s-c-n_e$. In deriving the constraints (2.21) use was made of the relation

$$\Big(\frac{d\gamma_j}{dt}\Big)_k \cdot \frac{1}{\beta_{jk}} = const_k \quad , \quad j = c+1, ..., s \ \text{ if } \ \beta_{jk} \neq 0 \ \text{ and } \ k \in N_e \ , \tag{2.22}$$

which expresses the balance of forward and backward reactions in the equilibrium case.

This formulation is based on the same idea as Ramshaw's first equation system, namely on the elimination of the equilibrium contributions in the rate equations by suitable combinations of these equations. Ramshaw does not, however, distinguish between linearly dependent and independent reactions. He even states that every equilibrium reaction provides an independent equation (this is true under certain circumstances only!). His arguments following this statement are therefore not clear. – In comparison with Ramshaw's second equation system the present formulation has the advantage that the equilibrium constraints need not be differentiated. Further, no additional equations such as the energy equation, are needed.

2.7. Frozen, partially frozen and equilibrium sound speed

In this paragraph, the partially frozen sound speed which could be equally called partial equilibrium sound speed, will be introduced. The definition of the partially frozen sound speed includes the frozen and equilibrium sound speeds as limiting cases. In general, the sound speed a can be defined by

$$a^2 = -\frac{h_\rho}{h_p - 1/\rho} \quad , \tag{2.23}$$

where the indices denote partial derivatives. The enthalpy is a function of the pressure, the density and the species concentrations. Its total differential is given by:

$$dh = \frac{\partial h}{\partial p}\, dp + \frac{\partial h}{\partial \rho}\, d\rho + \sum_{l=1}^{s} \frac{\partial h}{\partial \gamma_l}\, d\gamma_l \quad . \tag{2.24}$$

Depending on how the partial derivatives are formed in eq. (2.23), the equilibrium, frozen or partially frozen sound speed will be obtained. In equilibrium the concentrations depend on two

thermodynamic variables, e.g., on the pressure and the density. The concentrations are thus no longer independent variables. In nonequilibrium, however, the $(s-c)$ concentrations of the dependent species are independent variables. Hence, the equilibrium sound speed is obtained, if the partial derivatives of the enthalpy are taken with the concentrations being in equilibrium, and the pressure or density, respectively, being constant. Taking the partial derivatives with respect to pressure or density, with all other variables, including the concentrations, being constant, yields the frozen sound speed.

If partial equilibrium is considered, the number of independent variables depends on the degree of equilibrium. In the limiting case of nonequilibrium there exist $(s-c)$ independent concentration variables in addition to pressure and density. Each linearly independent equilibrium reaction reduces the number of independent variables by one. The equilibrium reactions define the equilibrium and nonequilibrium reaction subspace. In the equilibrium reaction subspace changes of the concentration vector need to satisfy the equilibrium constraints, whereas changes of the concentrations are independent in the nonequilibrium reaction subspace. The dimension of the nonequilibrium reaction subspace is equal to the number of independent concentration variables. Usually, an orthogonal basis of this subspace does not coincide with basis vectors of the normal coordinate system of the reaction space (i.e. the coordinate system which is consistent with the definition of the reaction vectors in chapter 2.2.). In the case of partial equilibrium the remaining independent concentration variables are then no longer individual concentrations of the dependent species.

For forming the partial derivatives of the enthalpy in eq. (2.23), it is important to look at the changes in the concentration vector. In the case of partial equilibrium these changes can be devided into changes in the equilibrium and nonequilibrium reaction subspaces. The derivative of the enthalpy with respect to pressure or density needs to be taken with changes of the concentration vector in the equilibrium subspace satisfying the corresponding equilibrium constraints. In the nonequilibrium reaction subspace changes in the concentration vector are zero. Changes of the concentration vector defined in this manner, are denoted by $(d\gamma_l)_{\gamma_m^*}$ in the following. The independent changes (i.e. those which are not functions of the pressure and density) are $(d\gamma_l)_{ind}$. The total differential of the enthalpy can then be written:

$$
\begin{aligned}
dh &= \frac{\partial h}{\partial p}\,dp + \frac{\partial h}{\partial \rho}\,d\rho + \sum_{l=1}^{s} \frac{\partial h}{\partial \gamma_l}\left((d\gamma_l)_{\gamma_m^*} + (d\gamma_l)_{ind}\right) \\
&= \frac{\partial h}{\partial p}\,dp + \frac{\partial h}{\partial \rho}\,d\rho + \sum_{l=1}^{s} \frac{\partial h}{\partial \gamma_l}\left(\left(\frac{\partial \gamma_l}{\partial p}\right)_{\rho,\gamma_m^*} dp + \left(\frac{\partial \gamma_l}{\partial \rho}\right)_{p,\gamma_m^*} d\rho\right) + \sum_{l=1}^{s} \frac{\partial h}{\partial \gamma_l}\,(d\gamma_l)_{ind} \quad ,
\end{aligned}
\tag{2.25}
$$

In the equilibrium subspace concentration changes depend on pressure and density. This was used in writing the second line of eq. (2.25). Considering eq. (2.25), the partially frozen sound speed a_{pf} is defined as

$$
a_{pf}^2 = -\frac{h_\rho + \sum_{l=1}^{s} \frac{\partial h}{\partial \gamma_l}\left(\frac{\partial \gamma_l}{\partial \rho}\right)_{p,\gamma_m^*}}{h_p + \sum_{l=1}^{s} \frac{\partial h}{\partial \gamma_l}\left(\frac{\partial \gamma_l}{\partial p}\right)_{\rho,\gamma_m^*} - 1/\rho} \quad .
\tag{2.26}
$$

The s components of the derivatives of the concentration vector with respect to pressure and density, $(\gamma_{l/p})_{\rho,\gamma_m^*}$ and $(\gamma_{l/\rho})_{p,\gamma_m^*}$, are implicitly given by an equation system. – In the

equilibrium subspace changes of the concentration vector satisfy the equilibrium constraints. These constraints provide n_e equations for the derivatives of the concentrations. Additional $s-c-n_e$ equations are obtained from the constraint that changes in the concentrations are zero in the nonequilibrium subspace. The conservation equations (2.2) for independent species concentrations provide the remaining c equations. The $(\gamma_{l/p})_{\rho,\gamma_m^*}$ and $(\gamma_{l/\rho})_{p,\gamma_m^*}$, $l=1,...,s$, can thus be determined.

For actually calculating the partially frozen sound speed some further information is needed. As in the Surf report the gas is assumed to be thermally perfect. Then the thermal and caloric state equation of the gas which is composed of s different species, read as follows:

$$\begin{aligned} p &= \rho \cdot \Gamma \cdot R \cdot T \quad , \qquad \Gamma := \sum_{l=1}^{s} \gamma_l \quad , \\ h &= \sum_{l=1}^{s} \gamma_l \cdot \hat{h}_l \quad , \end{aligned} \tag{2.27}$$

where Γ is the sum of the species concentrations. The molar enthalpies $\hat{h}_l$ which are functions only of the temperature, can be determined using a thermodynamic model as the one provided in the Surf report.

Considering the thermal and caloric state equations (2.27), the total differential of the enthalpy can be written as

$$dh = c_p \frac{1}{\rho R \Gamma} dp - c_p \frac{p}{\rho^2 R \Gamma} d\rho + \sum_{l=1}^{s} \Big[\hat{h}_l - c_p \frac{p}{\rho R \Gamma^2}\Big] d\gamma_l \quad , \tag{2.28}$$

where the specific heat c_p (per mass) at constant pressure is defined by:

$$c_p := \sum_{l=1}^{s} \gamma_l \cdot \hat{c}_{p,l} = \sum_{l=1}^{s} \gamma_l \cdot \Big(\frac{\partial \hat{h}_l}{\partial T}\Big)_p \quad . \tag{2.29}$$

The equilibrium constraints corresponding to the n_e linearly independent equilibrium reactions are the corresponding laws of mass action. The species concentrations satisfy these laws of mass action. To obtain n_e equations for the derivatives of the species concentrations which express the equilibrium constraints, the laws of mass action are used in differential form:

$$\begin{aligned} &\sum_{l=1}^{s} \frac{\beta_{lk}}{\gamma_l} d\gamma_l + \sum_{l=1}^{s} \Big[\frac{1}{\Gamma}\Big(\frac{\Delta \hat{h}_k}{RT} - \sum_{l=1}^{s} \beta_{lk}\Big)\Big] d\gamma_l + \Big[\sum_{l=1}^{s} \beta_{lk} - \frac{\Delta \hat{h}_k}{RT}\Big] \frac{1}{p} dp + \frac{\Delta \hat{h}_k}{RT} \frac{1}{\rho} d\rho = 0 \quad , \\ &\qquad \text{where} \quad \Delta \hat{h}_k := \sum_{l=1}^{s} \beta_{lk} \hat{h}_l \quad , \qquad k \in \overline{N_e} \quad . \end{aligned} \tag{2.30}$$

The differentials of the independent species concentrations are replaced by the expression

$$d\gamma_i = - \sum_{j=c+1}^{s} \alpha_{ji} \, d\gamma_j \quad , \qquad i = 1,...,c \quad , \tag{2.31}$$

which follows from the conservation equations (2.2) for independent species. This, and rearranging the terms in eq. (2.30), eventually yields:

$$\sum_{j=c+1}^{s}\Big\{\frac{1}{\Gamma}\Big[\frac{\Delta\hat{h}_k}{RT}-\sum_{l=1}^{s}\beta_{lk}\Big]\cdot\Big(1-\sum_{i=1}^{c}\alpha_{ji}\Big)+\frac{\beta_{jk}}{\gamma_j}-\sum_{i=1}^{c}\Big(\frac{\beta_{ik}}{\gamma_i}\alpha_{ji}\Big)\Big\}d\gamma_j-$$

$$-\Big[\frac{\Delta\hat{h}_k}{RT}-\sum_{l=1}^{s}\beta_{lk}\Big]\frac{1}{p}dp+\frac{\Delta\hat{h}_k}{RT}\frac{1}{\rho}d\rho=0\quad,\qquad k\in\overline{N_e}\quad. \tag{2.32}$$

The remaining $s-c-n_e$ equations for determining the derivatives of the dependent species concentrations with respect to presssure and density are obtained from the constraint that changes of the concentrations are zero in the nonequilibrium reaction subspace. This condition can be expressed by equating the scalar product of the basis vectors $(R^{neq}_{l,k})_{(l=1,...,s)}$, $k=1,...,s-c-n_e$ of the nonequilibrium subspace and the difference vector of the concentrations to zero. Considering again relation (2.31) this yields the following additional $s-c-n_e$ equations:

$$\sum_{j=c+1}^{s}\Big[(R^{neq}_{j,k})-\sum_{i=1}^{c}(R^{neq}_{i,k})\cdot\alpha_{ji}\Big]\cdot d\gamma_j=0\qquad,\quad k=1,...,s-c-n_e\quad. \tag{2.33}$$

The derivatives of the species concentrations with respect to pressure and density under the conditions of partial equilibrium are now easily obtained. Here, this is demonstrated for the derivatives with respect to the pressure.

$$\sum_{j=c+1}^{s}\Big\{\frac{1}{\Gamma}\Big[\frac{\Delta\hat{h}_k}{RT}-\Big(\sum_{l=1}^{s}\beta_{lk}\Big)\Big]\cdot\Big(1-\sum_{i=1}^{c}\alpha_{ji}\Big)+\frac{\beta_{jk}}{\gamma_j}-\sum_{i=1}^{c}\Big(\frac{\beta_{ik}}{\gamma_i}\alpha_{ji}\Big)\Big\}\cdot\Big(\frac{\partial\gamma_j}{\partial p}\Big)_{\rho,\gamma^*_m}=$$

$$=\Big[\frac{\Delta\hat{h}_k}{RT}-\sum_{l=1}^{s}\beta_{lk}\Big]\cdot\frac{1}{p}\quad,\qquad k\in\overline{N_e}\quad, \tag{2.34}$$

$$\sum_{j=c+1}^{s}\Big[(R^{neq}_{j,k})-\sum_{i=1}^{c}(R^{neq}_{i,k})\cdot\alpha_{ji}\Big]\cdot\Big(\frac{\partial\gamma_j}{\partial p}\Big)_{\rho,\gamma^*_m}=0\quad,\quad k=1,...,s-c-n_e\quad.$$

The '$*$' denotes the special conditions concerning the concentrations in the partial equilibrium case. There is exactly one equation for each of the dependent species concentrations. This system of linear equations for the derivatives of species concentrations in partial equilibrium can thus be analytically solved for the derivatives $(\partial\gamma_l/\partial p)_{\rho,\gamma^*_j}$. The derivatives with respect to the density are obtained analogous.

In the case of full equilibrium no basis for the equilibrium reactions will be determined. Then, the concentrations of the dependent species satisfy the laws of mass action formulated for the corresponding formation reactions. To obtain the derivatives of the species concentration this law of mass action is used in differential form:

$$\sum_{l=c+1}^{s}\Big\{\frac{1}{\Gamma}\Big[\frac{\Delta\hat{h}_j}{RT}-\Big(\sum_{i=1}^{c}\alpha_{ji}-1\Big)\Big]\cdot\Big(1-\sum_{i=1}^{c}\alpha_{li}\Big)-\frac{\delta_{lj}}{\gamma_j}-\sum_{i=1}^{c}\Big(\frac{\alpha_{ji}}{\gamma_i}\alpha_{li}\Big)\Big\}d\gamma_l-$$

$$-\Big[\frac{\Delta\hat{h}_j}{RT}-\Big(\sum_{i=1}^{c}\alpha_{ji}-1\Big)\Big]\frac{1}{p}dp+\frac{\Delta\hat{h}_j}{RT}\frac{1}{\rho}d\rho=0\quad,\qquad j=c+1,...,s\quad, \tag{2.35}$$

$$\text{where}\quad\Delta\hat{h}_j:=\sum_{i=1}^{c}\alpha_{ji}\hat{h}_i-\hat{h}_j\quad.$$

No additional equations are needed, since these are already $(s - c)$ independent equations. The derivatives of the species concentrations are obtained in the same manner as in the case discussed above.

3. Partial equilibrium in reacting flows

In the Surf report equations describing nonequilibrium reacting flows were provided. In comparison with these equations the rate equations (eqs. (2.15) of the Surf report) will be changed in a formulation considering partial equilibrium. Further, the energy equation is affected by a partial equilibrium formulation since it is formulated for the enthalpy. In the program Surf, however, pressure, density and species concentration were chosen as dependent variables. Derivatives of the enthalpy are thus replaced, considering the total differential of the enthalpy. Thereby it should be distinguished between changes of the concentration vector in the equilibrium and nonequilibrium reaction subspace. This was expressed in eq. (2.25) which is repeated here:

$$dh = h_p\ dp + h_\rho\ d\rho + \sum_{l=1}^{s} h_{\gamma_l} \left((d\gamma_l)_{\gamma_m^*} + (d\gamma_l)_{ind} \right) \quad . \tag{3.1}$$

The equations will be transformed to characteristic form. In this, the term $\sum_{l=1}^{s} h_{\gamma_l}\ (d\gamma_l)_{\gamma_m^*}$ can be eliminated by using the definition of the partially frozen sound speed. This results in C^+ and C^- characteristics which are defined by the partially frozen sound speed as to be expected in partial equilibrium flows. It turns out to be difficult, however, to find an expression for the remaining last term in eq. (3.1). For that reason, in the following characteristic formulation the frozen sound speed is used (as in the Surf report).

The $(s-c)$ rate equations for the dependent species are now replaced by $(s-c)-n_e$ linear combinations of these equations which do not contain contributions of equilibrium reactions, and by n_e equilibrium constraints for n_e linearly independent equilibrium reactions. First, however, a parameter $I_{r,k}$ is introduced so that:

$$I_{r,k} = \begin{pmatrix} 1 \\ 0 \end{pmatrix} \text{ if reaction } k \begin{pmatrix} \text{is in the equilibrium reaction subspace} \\ \text{is not in the equilibrium reaction subspace} \end{pmatrix} . \tag{3.2}$$

In this, $k \ni \overline{N_e}$ means that reaction k is not one of the basis reactions for the equilibrium reactions. The combinations of the rate equations can now be written as follows:

$$\sum_{j=c+1}^{s} n_{j,l} \cdot \frac{d\gamma_j}{dt} = \sum_{j=c+1}^{s} n_{j,l} \cdot \left(\sum_{k=1}^{r} (1 - I_{r,k}) P_{jk} \right) \quad , \quad l = 1, ..., (s-c) - n_e \ , \tag{3.3}$$

where the contribution P_{jk} of the nonequilibrium reaction k to the rate of change of the dependent species Y_j is given by (cf. Surf report, eq. (2.12)):

$$P_{jk} = \rho^{(\sum_{l=1}^{s} \nu_{lk})-1}\ \beta_{jk}\ k_{f,k} \left[\prod_{l=1}^{s} \gamma_l^{\nu_{lk}} - \frac{1}{K_{\gamma,k}} \prod_{l=1}^{s} \gamma_l^{\nu'_{lk}} \right] \quad , \quad j = c+1, ..., s \ , \quad k = 1, ..., r \ . \tag{3.4}$$

$k_{f,k}$ is the rate constant of the forward reaction of reaction k. In the numerical computation it is approximated by a modified Arrhenius equation. The laws of mass action formulated for the n_e linearly independent equilibrium reactions, provide the equilibrium constraints:

$$\prod_{l=1}^{s} \gamma_l^{\nu_{lk}} = \frac{1}{K_{\gamma_k}} \cdot \prod_{l=1}^{s} \gamma_l^{\nu'_{lk}} \quad , \quad k \in \overline{N_e} \ . \tag{3.5}$$

Here, the equilibrium constant K_{γ_k} is defined by:

$$K_{\gamma_k} = \left(\frac{p}{\Gamma\, p_0}\right)^{-\sum_{l=1}^{s} \beta_{jk}} \cdot exp\left(-\frac{1}{RT}\sum_{l=1}^{s} \beta_{lk}\ \hat{\mu}_l^{\circ}\right) \quad . \tag{3.6}$$

The program Surf computes stationary flows in planar and axisymmetric nozzles. The nozzle geometry is specified in terms of two functions $y_+(x)$ and $y_-(x)$, $y_+ > y_-$. The throat is located at $x = 0$ and the flow is in the positive x-direction. In the planar case, y_+ and y_- denote the location of the upper and lower wall, respectively, whereas in the axisymmetric case y_+ is the nozzle radius and $y_- \geq 0$. Usually $y_- = 0$, but also centerbodies can be taken into account by choosing $y_- > 0$. In the Surf report new coordinates (ξ, η) were introduced to transform the nozzle geometry into a rectangular: $\xi = x$ and $\eta = (y - y_-)/(y_+ - y_-)$. Due to this transformation additional terms appear in the transformed equations:

$$a := \frac{\partial \eta}{\partial x} \quad , \quad b := \frac{\partial \eta}{\partial y} \quad \text{and} \quad d := a\ u + b\ v \quad , \tag{3.7}$$

where u and v are the components of the velocity in $x-$ and $y-$direction, respectively. The resulting differential equations are solved by the method of lines. In using this method the derivatives in $\eta-$direction are replaced by finite differences. The finite difference scheme chosen in the Surf report, is based on a characteristic formulation of the equations. One-sided difference formulas are used to approximate derivatives with respect to η. In this, the finite differences are taken in the direction of the characteristic direction of the compatibility equation considered. In this manner a kind of "up-information" differencing is obtained. This formulation has several advantages (cf. Moretti, 1979), one of them being a simple physical formulation of the boundary conditions. The derivative of some arbitrary function f is thus replaced by:

$$\left(\frac{\partial f}{\partial \eta}\right)_i \longrightarrow \quad \left(\frac{\Delta f}{\Delta \eta_n}\right)_i := \frac{(1 - s_i)\cdot f_{n+1} + 2\cdot s_i \cdot f_n - (1 + s_i)\cdot f_{n-1}}{(1 - s_i)\cdot \eta_{n+1} + 2\cdot s_i \cdot \eta_n - (1 + s_i)\cdot \eta_{n-1}} \quad , \tag{3.8}$$

$$s_i = \text{sign}\left[\left(\frac{\partial \eta_n}{\partial \xi}\right)_i\right] \quad , \quad \eta_{n+1} > \eta_n > \eta_{n-1} \quad ,$$

where the index i denotes a characteristic direction and n is an index representing the discretization of the $\eta-$coordinate.

The rate equations, and thus linear combinations thereof, are already in characteristic form. In transforming the continuity, momentum and energy equations into characteristic form some coupling terms containing derivatives of the species concentrations were treated as "forcing terms" (cf. Surf report). In the case of purely nonequilibrium flows, however, the complete characteristic equations (i.e. without forcing terms) can be easily obtained. A sample computation using the two different formulations yielded practically the same results in both cases.

In the present formulation of partial equilibrium flows only the rate equations and the equilibrium constraints are different from the equations listed in the Surf report. For completeness, however, all equations, together with the corresponding characteristic equations, are listed in the following:

$$-\frac{H}{{a_f}^2}\,\frac{dp}{d\xi} + H\,\frac{d\rho}{d\xi} + \sum_{l=1}^{s} h_{\gamma_l}\frac{d\gamma_l}{d\xi} = 0 \qquad \text{along} \quad \left(\frac{d\eta}{d\xi}\right)_1 = \frac{d}{u} \quad , \tag{3.9}$$

$$\frac{du}{d\xi} + \frac{v}{u}\frac{dv}{d\xi} + \frac{1}{\rho u}\frac{dp}{d\xi} = 0 \qquad \text{along} \quad \left(\frac{d\eta}{d\xi}\right)_1 = \frac{d}{u} \quad , \tag{3.10}$$

$$\begin{aligned} v\frac{du}{d\xi} - u\frac{dv}{d\xi} \mp \frac{\sqrt{u^2+v^2-{a_f}^2}}{\rho a_f}\frac{dp}{d\xi} &= \frac{{a_f}^2}{{a_f}^2-u^2}\ \frac{1}{\rho}\left[-\frac{I_p\ \rho\ v}{y} + \right. \\ &\left. + \frac{1}{H}\sum_{l=1}^{s} h_{\gamma_l}\left(u\ \gamma_{j_\xi} + d\ \gamma_{j_\eta}\right)\right] \cdot \left[v \pm \frac{u}{a_f}\sqrt{u^2+v^2-{a_f}^2}\ \right] \\ \text{along} \quad \left(\frac{d\eta}{d\xi}\right)_{2,3} &= \frac{1}{{a_f}^2-u^2}\ \left[a\ ({a_f}^2-u^2) - buv \mp \sqrt{u^2+v^2-{a_f}^2}\ \ a_f b\right] \quad . \end{aligned} \tag{3.11}$$

In this H denotes

$$H := h_\rho \quad . \tag{3.12}$$

At this place it should be mentioned that in the compatibility equation (5.17) of the Surf report the first term within the first square bracket on the right hand side should be multiplied by the density. The correct form of this term is: $-I_p\ \rho\ v/y$.

The $(s-c)-n_e$ different linear combinations of the rate equations in characteristic form are given by:

$$\begin{aligned} \sum_{j=c+1}^{s} n_{j,l}\cdot\frac{d\gamma_j}{d\xi} &= \frac{1}{u}\cdot\sum_{j=c+1}^{s} n_{j,l}\cdot\left(\sum_{k=1}^{r}(1-I_{r,k})P_{jk}\right) \quad , \quad l=1,...,s-c-n_e \quad , \\ &\text{along} \quad \left(\frac{d\eta}{d\xi}\right)_1 = \frac{d}{u} \quad . \end{aligned} \tag{3.13}$$

To facilitate the implementation of the equations for partial equilibrium flows in the program Surf, the n_e equilibrium constraints (3.5) are used in differential form. In this manner the number of ordinary differential equations to be solved remains constant throughout the flow field. As quoted in the introduction, the drawback of this formulation is that the equilibrium conditions in differential form cannot establish partial equilibrium. In the course of stationary nozzle flow calculations considered here, however, the computation proceeds in downstream direction. In this direction the flow will depart more and more from equilibrium. At the upstream boundary the program Surf permits boundary conditions which are in accordance to equilibrium or frozen flows, respectively. The former case should always be considered when equilibrium or partial equilibrium flows are calculated. Then, equilibrium is initially present and needs not be established.

In some computations it turned out that a stabilized form of the differentiated law of mass yields better results. To stabilize the differential form of the law of mass action a source term which is proportional to the departure S_k from equilibrium S_k, is introduced. Here, S_k is defined by

$$S_k = 1 - \frac{1}{K_{\gamma_k}}\cdot\prod_{l=1}^{s}\gamma_l^{\beta_{lk}} \quad , \quad k \in \overline{N_e} \quad . \tag{3.14}$$

In the new version of Surf which includes the partial equilibrium option, the equilibrium conditions corresponding to the n_e linearly independent equilibrium reactions k, $k \in \overline{N_e}$, are used in the following form:

$$
\begin{aligned}
\frac{dS_k}{d\xi} = & -\Big(\sum_{l=1}^{s}\beta_{lk} - \frac{\Delta\hat{h}_k}{R\,T}\Big)\cdot\frac{1}{p}\frac{dp}{d\xi} - \frac{\Delta\hat{h}_k}{R\,T}\cdot\frac{1}{\rho}\frac{d\rho}{d\xi} \\
& - \sum_{j=c+1}^{s}\Big[\beta_{jk}\frac{\Gamma}{\gamma_j} - \sum_{l=1}^{s}\beta_{lk} + \frac{\Delta\hat{h}_k}{R\,T} - \sum_{i=1}^{c}\Big(\beta_{ik}\frac{\Gamma}{\gamma_i} - \sum_{l=1}^{s}\beta_{lk} + \frac{\Delta\hat{h}_k}{R\,T}\Big)\cdot\alpha_{ji}\Big]\cdot\frac{1}{\Gamma}\frac{d\gamma_j}{d\xi} \\
= & -\lambda\cdot S_k \;,\quad k\in\overline{N_e} \quad,\quad \text{along} \quad \Big(\frac{d\eta}{d\xi}\Big)_1 = \frac{d}{u}
\end{aligned}
\tag{3.15}
$$

$$
\text{where}\quad \Delta\hat{h}_k := \sum_{l=1}^{s}\beta_{lk}\hat{h}_l \quad .
$$

A suitable value for the proportionality factor λ is to be determined from sample calculations. A comparison of the results for purely equilibrium flows obtained from both, calculations using the stabilized differential form (3.15) and the original law of mass action (3.5) has shown, that $\lambda = 0$ is usually sufficient to obtain good agreement. In some cases, however, $\lambda = 10$ yields better agreement. For that reason, in the new version of the program Surf λ is always taken $\lambda = 10$.

4. Determination of equilibrium reactions, multipliers for the rate equations and reduced reaction vectors

4.1. Equilibrium reactions

Reactions having characteristic relaxation times which are much smaller than a typical fluid mechanical time were called equilibrium reactions (cf. chapter 2.3.). In the following, an expression for the characteristic relaxation time of a reaction will be derived. Only a brief explanation is given, because a more detailed derivation is contained in the Surf report.

Consider r different reactions to be present among the species. The contribution of reaction k to the rate of change of concentration γ_j can be written as

$$(4.1) \qquad \frac{1}{\gamma_j} \cdot \left[\frac{d\gamma_j}{dt}\right]_k = \frac{1 - \frac{1}{K_{\gamma,k}} \prod_{l=1}^{s} \gamma_l^{\beta_{lk}}}{\tau_{jk}} \quad , \quad j = c+1, ..., s, \quad k = 1, ..., r \quad ,$$

where $K_{\gamma,k}$ is the equilibrium constant of the law of mass action corresponding to reaction k. The τ_{jk} are local characteristic relaxation times associated with the rate of change of species Y_j. Considering the full expression for the rate of change of γ_j due to reaction k, the following equation was derived for τ_{jk} in the Surf report:

$$(4.2) \quad \tau_{jk} = \left[\rho^{(\sum_{l=1}^{s} \nu_{lk})-1} \cdot \beta_{jk} \cdot k_{f,k} \cdot \prod_{l=1}^{s} \gamma_l^{\nu_{lk}} \cdot \frac{1}{\gamma_j}\right]^{-1} \quad , \quad \beta_{jk} \neq 0 \ , \quad j = c+1, ..., s, \quad k = 1, ..., r \ .$$

As suggested in chapter 2.3. the characteristic relaxation time τ_k of reaction k is defined as the maximum of the absolute τ_{jk}:

$$(4.3) \qquad \tau_k = \max_{j=c+1,...,s} (|\tau_{jk}|) \ , \quad k = 1, ..., r \ .$$

Within the program Surf characteristic relaxation lengths are considered. The characteristic relaxation length λ_k of reaction k is defined as the product of the corresponding relaxation time and the local flow velocity w:

$$(4.4) \qquad \lambda_k = w \cdot \tau_k \quad .$$

As long as this characteristic length is smaller than a critical relaxation length λ_{crit} which is chosen by the user of the program Surf, reaction k is considered to be in equilibrium.

In the formulation of partial chemical equilibrium, a basis for all equilibrium reactions needs to be determined. This is accomplished as follows. The first equilibrium reaction is always considered to be independent. Now it is searched for the next equilibrium reaction whose reaction vector is linearly independent of the reaction vector of the first equilibrium reaction. Then it is searched for the next equilibrium reaction which is linearly independent of the first two ones, etc.. The linear independence of different reaction vectors is examined by checking whether the Gram determinant formed by the corresponding reaction vectors, is positive definite ($\hat{=}$ linearly dependent) or not ($\hat{=}$ linearly independent).

4.2. Multipliers for rate equations

The equation system (2.21) for the multipliers $n_{j,l}$, $j = c+1,...,s$, which can be expressed as $\beta^t_{jk}\, n_{j,l} = 0$, is normally underdetermined, since usually $n_e < s-c$. In this case a fundamental solution for the multipliers is determined in the following manner. Firstly, the first n_e columns of the $n_e \times (s-c)$ matrix $(\beta_{jk})^t, j = c+1,...,s, \quad k \in \overline{N_e}$ is transformed into an upper triangular form by Gaussian elimination, using column pivoting and interchanging columns. This yields an expression like:

$$(4.5) \qquad \begin{pmatrix} a_{1,1} & \dots & a_{1,n_e} & \dots & a_{1,s-c} \\ \vdots & \ddots & \vdots & & \vdots \\ 0 & \dots & a_{n_e,n_e} & \dots & a_{n_e,s-c} \end{pmatrix} \begin{pmatrix} n_{1,l} \\ \vdots \\ n_{n_e,l} \\ n_{n_e+1,l} \\ \vdots \\ n_{s-c,l} \end{pmatrix} = 0 \quad , \quad l = 1,...,(s-c)-n_e \ .$$

A fundamental solution $N_l = (n_{j,\ j=1,...,s-c})_l$, $l = 1,...,(s-c)-n_e$ of eq. (4.5) is now obtained by considering the elements $n_{n_e+1,l}\ ,...,\ n_{s-c,l}$ of the solution vector N_l to be given by

$$(4.6) \qquad n_{n_e+j,l} = \delta_{j,l-n_e} \quad , \quad j = 1,...,s-c-n_e \ .$$

This yields the following recursive formulas for the other elements $n_{i,l}, i \le n_e$, of the vector N_l:

$$(4.7) \qquad \begin{aligned} n_{n_e,l} &= -\frac{1}{a_{n_e,n_e}} \cdot a_{n_e,n_e+l} \\ n_{n_e-i,l} &= -\frac{1}{a_{n_e-i,n_e-i}} \cdot \Big(\sum_{j=n_e-i+1}^{n_e} a_{n_e-i,j} \cdot n_{j,l} + a_{n_e-i,n_e+l} \Big) \end{aligned} \qquad l = 1,...,(s-c)-n_e \ .$$

In case $n_e = 0$, all reactions are in nonequilibrium and the ordinary set (2.11) of rate equations is obtained. If $n_e = s-c$, all species concentrations are in equilibrium and only equilibrium constraints are needed for calculating the species concentrations.

4.3. Reduced reaction vectors

Within the program Surf reduced reaction vectors are used. The definition of these vectors differs slightly from the one of the reaction vectors (cf. chapter 2.2.). Following the definiton of chapter 2.2. reaction vectors are elements of an s–dimensional vector space. Here, however, only reactions satisfying the constraints given by the conservation equations (2.2) for the independent species are admitted. The corresponding reaction vectors are therefore elements of an $(s-c)$–dimensional subspace of the s–dimensional vector space. This $(s-c)$–dimensional subspace is spanned by the reaction vectors F_j, $j = c+1,...,s$, of the formation reactions which thus form a basis for this subspace. With regard to later applications this basis is orthonormalized by the Gram-Schmidt procedure. The resulting basis is denoted by $F^{\perp}_j$, $j = 1,...,s-c$. All reaction vectors R_k, $k = 1,...,r$, considered can be constructed from this orthonormal basis:

$$(4.8) \qquad R_k = \sum_{j=c+1}^{s} f_{k,j} \cdot F^{\perp}_j \quad , \quad k = 1,...,r \ .$$

This representation suggests the definition of reduced reaction vectors $\tilde{R}_k$ which are elements of an $(s-c)$–dimensional space, by $\tilde{R}_k := (f_{k,l})_{l=1,...,s-c}$. These reduced reaction vectors are used throughout the program Surf. They are easily obtained. Equation (4.8) can be written as $F\ \tilde{R}_k = R_k$ where F is a matrix which contains the basis vectors $F_j^{\perp}$, $j = 1, ..., s-c$, of the orthonormal basis as columns. This equation is multiplied from the left by the transpose of F, resulting in $F^t\ F\ \tilde{R}_k = I\ \tilde{R}_k = F^t\ R_k$ where I is the identity matrix. The components $f_{k,l}$, $l = 1, ..., s-c$, of the reduced reaction vector $\tilde{R}_k$ are thus determined.

The reduced reaction vectors are used, for example, in determining a basis of the nonequilibrium reaction subspace. This is accomplished as follows. The basis of the equilibrium reaction subspace is already known (cf. chaptert 4.1.). The constraint that the basis vectors of the nonequilibrium reaction subspace are perpendicular to the ones of the equilibrium subspace can be expressed by

$$W^t\ \tilde{R}^{neq} = 0 \tag{4.9}$$

where W is a matrix containing the reduced basis vectors of the equilibrium subspace as columns, and $\tilde{R^{neq}}$ is a reduced basis vector of the nonequilibrium subspace. Determining a fundamental solution of eq. (4.9) yields a basis of the nonequilibrium subspace. The fundamental solution is obtained in the same manner as described in chapter 4.2. . This reduced basis is then transformed to a basis of usual reaction vectors and orthonormalized.

5. Modifications of the program Surf

The implementation of the option for computing partial equilibrium flows into Surf is accomplished in such a way that the user accustomed to the first version of Surf, will not notice it. Some insignificant changes of the input and output data are discussed in the next section. New Fortran subroutines needed for controlling the computation of partial equilibrium flows, and modifications of already existing routines are briefly explained in chapter 5.2. which is a supplement to chapter 6.4. of the Surf report. Some of the more important Fortran variables used in these subroutines are listed in appendix **B** which completes appendix **C** of the Surf report.

5.1. Input and output data

The number of input data needed for running Surf has been reduced. The new version of Surf no longer needs reactions which differ from each other only in having different third bodies, being specified. This information was transfered to the program Surf via a so-called third body vector in the last data set of the input data file. Thus, this data set (labeled by 32 and 33 in chapter 6.2. of the Surf report) no longer needs to be provided. If an input data file still contains the third body vector, a comment will be written to output file 'outpt1' (cf. below) reminding the user that the third body vector is no longer needed. This does not affect the computation.

The meaning of the critical relaxation length λ_{crit} has slightly changed. As in the old version of Surf, it is provided as 'dcrit' in data set number 17 of the input data file. If dcrit< 0 or dcrit $= 0$, a two-dimensional nonequilibrium or equilibrium flow, respectively, will be computed. These options remained unchanged. If, however, dcrit> 0, a partial equilibrium flow is now calculated. All reactions with characteristic lengths $\lambda_k < \lambda_{crit}$ will be considered to be in equilibrium. Reactions with $\lambda_k > \lambda_{crit}$ are treated as finite rate reactions. There is thus no longer a switch from a fully equilibrium to a fully nonequilibrium flow calculation, as soon as any of the reactions gets out of equilibrium. A good choice of the critical relaxation length is crucial for obtaining a reasonable reduction of the CPU time. If the critical length is chosen too large, the results of the partial equilibrium flow computation will deviate noticably from a nonequilibrium flow and approach an equilibrium flow.

The results of a computation by Surf are stored in two output files, called 'outpt1' and 'outpt2' (cf. Surf report). Output file 'outpt1' containes formatted data in a self explanatory manner. Some new comments concerning the computation of partial equilibrium flows can be present in this output file. The second output file, 'outpt2', which is a direct access file and contains unformatted data, provides detailed results of the computation. In the old version of Surf those records containing the results of a 2-D nonequilibrium calculation are not filled up to the end. The new version of Surf writes the number n_e of linearly independent equilibrium reactions and the partially frozen sound speed into this free space and thus provides an idea of the degree of equilibrium being present in the partial equilibrium flow. The structure of output file 'outpt2' was explained in the Surf report (cf. chapter 6.3.). Here, only that part which has been changed, is listed again. It should be mentioned that in 'outpt2' real numbers are stored as single precision numbers and that the record length is RECL $= 6 + s - c$. The fourth section of 'outpt2' is now given by:

record number:	content of record:

IV. if 2-D nonequilibrium flow has been calculated:

$i_{2-D} + (m-1) \cdot n_{max} + n$	$u_{(m,n)}$, $v_{(m,n)}$, $p_{(m,n)}$, $\rho_{(m,n)}$, $(\gamma_{j,(m,n)})_{j=c+1,...,s}$, $n_{e_{(m,n)}}$, $a_{pf_{(m,n)}}$
$n = 1, ..., n_{max}$	where the index (m,n) denotes that these are the values
$m = 1, ..., m_{max}$	of u, v, p, ρ γ_j, $j = c+1, ..., s$ and n_e at
	$x_m = x_u + (m-1) \cdot (x_d - x_u)/(m_{max}-)1$
	$y_{(m,n)} = y_-(x_m) + (n-1) \cdot (y_+(x_m) - y_-(x_m))/(n_{max} - 1)$
	the index m runs from $m = 1, ..., m_{max}$ and, for each m,
	index n runs from $n = 1, ..., n_{max}$

i_{2-D} remains to be specified:

a) neither 1-D frozen nor 1-D equilibrium flow has been calculated: $i_{2-D} = 100$
b) 1-D frozen or 1-D equilibrium flow has been calculated: $i_{2-D} = 100 + m_{max}$
c) 1-D frozen and 1-D equilibrium flow have been calculated: $i_{2-D} = 100 + 2 \cdot m_{max}$

5.2. New and changed subroutines

`subroutine coefmt:`

This subroutine determines the formation reaction vectors and stores them as columns of matrix `fm`. Then, an orthonormal basis for the space spanned by the formation reactions, is determined by the Gram-Schmidt procedure, and stored as columns in `fmon(1,k)`. Finally, the coefficients for constructing the reaction vectors from the orthonormal basis are determined and stored as columns of matrix `coevc(idscm,irm)`.

`subroutine gram(rmat,rmatg,nrow,nrowm,ncol,ncolm):`

This subroutine computes the Gram matrix `rmatg := rmatt * rmat` where `rmatt` is the transpose of `rmat`. `rmat` and `rmatg` need to be dimensioned as `rmat(nrowm,ncolm)` and `rmatg(ncolm,nrowm)` in the calling program.

`subroutine iesw(xsl,xsi):`

This subroutine was changed! It determines whether reactions are considered to be in equilibrium (`ie` $= 1$), partial equilibrium (`ie` $= -1$) or in nonequilibrium (`ie` $= -1$) at the position `xsi` $= x_m = x_u + (m-1)(x_d - x_u)/(m_{max} - 1)$. If partial or nonequilibrium flows are considered, the parameter `ie` is set to `ie` $= -1$ and the equations for a two-dimensional partial or nonequilibrium flow are solved.

If partial equilibrium is considered, first all equilibrium reactions and a basis for these reactions are determined. If real partial equilibrium is present (i.e. $0 < n_e < s - c$) a basis for the nonequilibrium reaction subspace is calculated. Then, the multipliers for the rate equations are determined.

Every time when one of the basis vectors of the equilibrium reactions is changed `ie` is set to `ie` $= -10$ (this affects the parameter `info(1)` to be set to `info(1)` $= 0$ in `subroutine intgrtn`).

subroutines called: geomtr, lindep, gram, fndsys, dgeco2

subroutine lindep(vcmat,nrow,mrowm,ncol,ncolm, indvc,ibsvc,idmnsn,wm,wmg,ipvt,wv):

vcmat is a matrix. Its column vectors are divided into different groups. Vectors belonging to one group are marked by assigning the same value to all components of the index vector indvc which have the same index as the columns containing the vectors considered.

The subroutine determines the first idmnsn linearly independent column vectors of vcmat which are also elements of the group with indvc(i) = 1. idmnsn which is the maximum number of independent vectors, is also determined by this routine. The column indices of the linearly independent (i.e. basis) vectors are stored in the first idmnsn components of the vector ibsvc.

vcmat, indvc, ibsvc, and the work arrays wm, wmg, ipvt and wv need to be dimensioned as vcmat(nrowm,ncolm), indvc(ncolm), ibsvc(nrowm), wm(nrowm,nrowm), wmg(nrowm,nrowm), ipvt(nrowm) and wv(nrowm) in the calling program.

subroutines called: gram, dgeco2

subroutine fndsys(a,nr,nrm,mc,mcm,f,iw,rw):

Subroutine fndsys determines a fundamental system for the solution of an equation system $A\,x = 0$ where A is a nr $\times$ mc matrix and x is a vector with mc components. Here, mc $>$ nr, i.e. the system $A\,x = 0$ is underdetermined. The vectors spanning the solution space are stored in the first mc $-$ nr columns of matrix f.

a, f, and the work arrays iw and rw need to be dimensioned as a(nrm,mcm), f(mcm,nrm), iw(mcm,mcm) and rw(mcm,nrm) in the calling program.

subroutine nfsolv(xsi,u,uprime,rpar,ipar):

Same as old subroutine nfsolv. Now this subroutine is called to provide a system of first order differential equations discribing a partial equilibrium flow (formerly: a nonequilibrium flow). The subroutine need not be changed since the modifications were performed in subroutine nmatrix which is called by the present routine.

subroutines called: nmatrix, dgbfa2, dgbsl2

subroutine nmatrix(xsi,abd,a,b,xsl,lda):

Similar to old subroutine nmatrix. Now this subroutine evaluates the coefficient matrix a and the r.h.s. vector b of the system of ordinary differential equations in the case of partial equilibrium where the equation system is of the form 'a uprime = b' (uprime is not used in this routine). The limiting case of total nonequilibrium can also be represented by this routine. For using the LINPACK routines dgbfa2 and dgbsl2 the coefficients of matrix a are stored in a special order in matrix abd. The parameter lda is the leading dimension of array abd.

subroutines called: apf2, geomtr, thdyn

subroutine read:

Same as in old version of Surf (cf. Surf report), except for some minor changes in input and output due to the reaction vector no longer being necessary.

subroutine initial:

Same as in old version of Surf, except for a call to subroutine coefmt being added for determining the reduced reaction vectors.

subroutine intgrtn:

Same as in old version of Surf, except for minor changes concerning the output of the number of linearly independent reactions and the partially frozen sound speed to output file 'outpt2' (cf. chapter 5.1.).

function apf2(n):

This function subroutine calculates the square of the partially frozen sound speed. The parameter `n` denotes the line number (cf. method of lines), i.e. the position in η–direction where the sound speed is to be determined. In the limiting case of equilibrium flows this routine computes the equilibrium sound speed and therefore replaces the function subroutine `ae2(idummy)`, except for subroutines `equil` and `matrix` (cf. Surf report).

subroutines called: dgefa2, dgesl2

function ae2(idummy):

This function subroutine routine computes the equilibrium sound speed. It is called by subroutine equil and matrix. If subroutine equil is correctly changed, function `ae2(idummy)` could be replaced by function `apf2(n)` in subroutine `equil` as well.

subroutines called: dgefa2, dgesl2

LINPACK routines (cf. Dongarra *et al.* (1979):

In addition to the LINPACK routines already listed in the Surf report, the double precision routines dgefa, dgesl and dgeco are used by the new version of Surf. Because some of these routines are also used by SLATEC(DEPAC) routines, e.g. by ddebdf and ddeabm (cf. Surf report), these routines were doublicated to the routines dgefa2, dgesl2 and dgeco2 which are identical to the routines dgefa, dgesl and dgeco.

dgefa2(a,lda,n,ipvt,info):

This routine computes the LU factorization of a matrix A. For details see the LINPACK User's Guide (Dongarra *et al.* (1979).

dgesl2(lua,lda,n,ipvt,b,job):

Using the LU factorization of a matrix (stored in `lua`) this routine solves linear systems of the form $A\,X = B$. For details see the LINPACK User's Guide (Dongarra *et al.* (1979).

dgeco2(a,lda,n,ipvt,rcond,w):

Routine dgeco2 is only used to determine the condition of a matrix A in the course of determining linearly independent vectors (cf. chapter 4.1.). For details see the LINPACK User's Guide (Dongarra *et al.* (1979).

6. Sample computations and discussion

In this chapter the effect of introducing partial equilibrium is demonstrated. Further, some aspects of the program Surf which were not considered in the Surf report, are discussed. In most of the following sample computations the same case as in chapter 7.1. of the Surf report is considered, namely the expansion of high temperature air through the axisymmetric T5/100 nozzle of the GALCIT shock tunnel. The computational domain extends again form $x = 0.01m$ to $x = 1.00m$. As in the Surf report the reservoir temperature and pressure are $T_0 = 9000K$ and $p_0 = 200 \cdot 10^5 Pa$ and the composition of air is represented by eight species: e^-, N_2, O_2, Ar, N, O, NO, NO^+.The first four species are independent species. Among these species 22 reactions are considered:

1-6)	$N_2 + M_i$	$\rightleftharpoons$	$2N + M_i$
	$M_1 = N_2,\ M_2 = N,\ M_3 = O_2,\ M_4 = Ar,\ M_5 = O,\ M_6 = NO$		
7-12)	$O_2 + M_i$	$\rightleftharpoons$	$2O + M_i$
	$M_7 = O_2,\ M_8 = O,\ M_9 = N_2,\ M_{10} = Ar,\ M_{11} = N,\ M_{12} = NO$		
13-18)	$NO + M_i$	$\rightleftharpoons$	$N + O + M_i$
	$M_{13} = N_2,\ M_{14} = O_2,\ M_{15} = Ar,\ M_{16} = N,\ M_{17} = O,\ M_{18} = NO$		
19)	$O_2 + N$	$\rightleftharpoons$	$O + NO$
20)	$N_2 + O$	$\rightleftharpoons$	$N + NO$
21)	$N_2 + O_2$	$\rightleftharpoons$	$2NO$
22)	$e^- + NO^+$	$\rightleftharpoons$	$N + O$.

According to chapter 2.2. the corresponding reaction vectors span a four-dimensional reaction subspace in the eight-dimensional space of reaction vectors. The data describing the thermodynamic properties of the species and the chemical reactions are the same as in the example of the Surf report. The only difference is that the temperature T_{fit} at which the thermodynamic model is switched from a polynomial fit to a statistical mechanics formulation was shifted to $T_{fit} = 3000K$ for all species. This yields a smoother transition between the two models than the switch temperature $T_{fit} = 6000K$ which was previously used. – At the upstream boundary the initial conditions are approximated by the solution of a one-dimensional equilibrium flow.

The parameters which are typically changed in the following computations, are the critical relaxation length λ_{crit} and the number of lines n_{max} used in the method of lines. The value of λ_{crit} determines whether an equilibrium ($\lambda_{crit} = 0m$), nonequilibrium ($\lambda_{crit} < 0m$) or partial equilibrium ($\lambda_{crit} > 0m$) flow is considered. By n_{max} the resolution in radial direction is fixed. In the following a computation with $n_{max} = 20$ and $\lambda_{crit} = 0.1m$ will be regarded as the standard case. In contrast to the example provided in the Surf report the number of lines m_{max} in axial direction at which the solution is printed, is increased from $m_{max} = 150$ to $m_{max} = 200$. This does not affect the solution but yields a better resolution in plotting the x-dependence of any variable. The input data file for the program Surf, corresponding to the standard case, is listed in Fig. 1. Note that the third body vector is no longer provided. Further, the last comment line (`'c.l.: ithb(k),k=1,.,ir:'`) could also be omitted.

For running the program Surf the geometry of the nozzle needs to be specified in subroutine geomtry (cf. Surf report). Thereby it is important that the first derivative of the radius (axisymmetric case) is smooth. This will be demonstrated in chapter 6.6. . The derivatives of the radius of the T5/100 nozzle were not plotted in the Surf report. Therefore, in addition to the nozzle contour of the T5/100 nozzle, the first and second derivative of its radius (as used by Surf) are provided in Fig. 2. The discontinuities in the second derivative are not crucial.

6.1. Expansion of high temperature air: partial equilibrium flow

The expansion of high temperature air through the T5/100 nozzle is computed, assuming all reactions to be in equilibrium whose characteristic relaxation times τ_k, $k = 1, ..., 22$, are shorter than a characteristic fluid dynamic time $\tau_f := \lambda_{crit}/w$. Here, w is the local flow velocity and λ_{crit} is chosen $\lambda_{crit} = 0.1m$ (standard case). Otherwise, reactions are considerd to be finite rate reactions. At the upstream boundary of the computational domain the initial conditions are approximated by a one-dimensional equilibrium flow. Not all reactions satisfy the equilibrium criterion $\tau_k < \tau_f$ right at the upstream boundary. This is shown by the following list in which an equilibrium reaction k is marked by $k(e)$ and a nonequilibrium reaction k by $k(n)$:

$$1(e),\ 2(e),\ 3(n),\ 4(n),\ 5(e),\ 6(n),\ 7(n),\ 8(e),\ 9(e),\ 10(n),\ 11(e),\ 12(n),$$
$$13(e),\ 14(n),\ 15(e),\ 16(e),\ 17(e),\ 18(e),\ 19(e),\ 20(e),\ 21(e),\ 22(e) \quad .$$

However, at the upstream boundary and in a region downstream of it, the dimension n_e of the equilibrium reaction subspace equals the dimension of the reaction subspace: $n_e = s - c$. At the upstream boundary the finite rate equations are thus redundant and the approximation of the initial conditions by an equilibrium flow is self consistent.

In Fig. 3a the regions of the flow field with different degrees of equilibrium are shown by plotting the contour lines of the dimension n_e of the equilibrium subspace. It can be seen that the reactions tend to stay slightly longer in equilibrium on the centerline than at the walls. In a region of constant n_e the basis vectors of the equilibrium subspace (as used by Surf) can change due to a basis reaction becoming a finite rate reaction. This is demonstrated for the case $n_e = 3$ by listing the reaction numbers of the basis vectors on the centerline:

$4.48 \cdot 10^-2m \leq x \leq 4.98 \cdot 10^-2m$:	No.: 2, 8, 13
$4.98 \cdot 10^-2m \leq x \leq 6.97 \cdot 10^-2m$:	No.: 8, 13, 20
$6.97 \cdot 10^-2m \leq x \leq 8.96 \cdot 10^-2m$:	No.: 8, 19, 20.

It should be mentioned that the basis of the equilibrium reaction subspace needs not necessarily be changed every time a basis reaction becomes a finite rate reaction. In other words, as long as a finite rate reaction is an element of the equilibrium reaction subspace (and thus redundant) its reaction vector can also be used as a basis vector of the equilibrium subspace.

The partially frozen sound speed which enters the computation due to the characteristic formulation of the conservation equations, is compared with the equilibrium and frozen sound speed in Fig. 3b. The three sound speeds are plotted along the axis of the nozzle. From the beginning to $x \approx 0.045m$, an equilibrium flow is assumed (i.e. $n_e = 4$) and the partially frozen sound speed equals the equilibrium one. In the region with $n_e = 3$ the only finite rate reaction

which is not in the equilibrium reaction subspace, is reaction $k = 22$. Because the concentrations of the ionized species involved in this reaction are already very small, this nonequilibrium reaction affects the partially frozen sound speed little and the difference between a_{pf} and a_e is not resolved in Fig. 3b. A first noticable increase of the partially frozen sound speed can be observed when the dimension of the equilibrium reaction subspace decreases to $n_e = 2$. The partially frozen sound speed is now really greater than the equilibrium and less than the frozen sound speed. The next decrease in the dimension of the equilibrium subspace is again hardly noticable in the partially frozen sound speed. As soon as the transition to a fully nonequilibrium flow computation takes place the partially frozen sound speed jumps to the value of the frozen sound speed. – At $x \approx 0.54\ m$ another kink is present in both, the equilibrium and frozen/partially frozen sound speed. It is caused by the vibrational degrees of freedom being frozen at $T_v = 3000$ for $T \leq T_v$. The freezing of the vibrational degrees of freedom takes place at just this position. It can be seen that the effect of this freezing is of the same order of magnitude as the decrease of the dimension of the equilibrium reaction subspace by one.

Fig. 3c shows a contour plot of the temperature. All contour lines are smooth. The transition from equilibrium, via partial equilibrium, to nonequilibrium is not reflected in the contour lines. This is also true for the pressure, density and velocity contours.

The species concentrations are those variables which are primarily affected by a change of the dimension of the equilibrium reaction subspace. For that reason it might be expected that the contour lines of the species concentrations are not smooth in regions where partial equilibrium is assumed. This is not the case, however. As an example the contour lines of γ_N, γ_{O_2} and γ_{NO} are plotted in Fig. 3d-f. Only on one contour line of γ_{NO} small wiggles can be seen at $x \approx 0.19\ m$. These are due to the change from partial equilibrium to fully nonequilibrium at about this position (cf. Fig. 3a). Here, on neighboring lines (of the method of lines) the dimension of the equilibrium reaction subspace is different. This directly affects the concentrations because the rates of some reactions are finite on one line and infinit on the neighboring one. The effect, however, is small and local.

A more quantitative comparison of the partial equilibrium flow computation with a nonequilibrium, equilibrium and frozen flow computation is given in Fig. 4. The initial conditions are the same in all cases, i.e. even the frozen flow computation starts from initial conditions which are obtained by assuming an equilibrium flow at the inflow boundary. In Fig. 4a-j the state variables are plotted versus the non-dimensionalized radius (η) at the nozzle exit. The agreement of the partial equilibrium and nonequilibrium solution is excellent. In most cases the two solutions can not be distinguished in Fig. 4. At the nozzle exit, on the axis, the deviation of the partial equilibrium solution from the nonequilibrium solution is given by: temperature: -0.18%, pressure: -0.13%, density: -0.10%, velocity: 0.02%, γ_N: -2.09%, γ_O: -0.07%, γ_{NO}: 0.74%, γ_{NO^+}: -0.42%. The only larger deviation occurs in the concentration of N which is already very small (less than $0.01 mole/kg$). The equilibrium and frozen flow solutions which vary significantly from the nonequilibrium one, provide some idea of how important it is to perform a nonequilibrium/partial equilibrium flow computation. Finally it is noted that density and velocity of the equilibrium solution are very similar to the ones of the nonequilibrium/partial equilibrium solution. This is a typical result in nonequilibrium nozzle flows.

The computation of this partial equilibrium flow took 200 seconds on a VAX 9000.

6.2. Critical relaxation length

The critical relaxation length λ_{crit} determines whether a reaction is considered to be in equilibrium or not. With increasing λ_{crit} a reaction can deviate more and more from equilibrium without being treated as a finite rate reaction. In the limit of $\lambda_{crit} \rightarrow \infty$ a purely equilibrium flow, and in the case $\lambda_{crit} \rightarrow 0$ a purely nonequilibrium flow is obtained. A partial equilibrium flow computation is usually performed in order to save CPU-time by reducing the stiffness of the partial differential equations. In this it will be desired to obtain practically the nonequilibrium flow solution. In order to provide some idea of the influence of the critical relaxation length on the partial equilibrium flow solution, four computations with different λ_{crit} are compared: *a)* $\lambda_{crit} = 0.01m$: this is approximately the radius of the nozzle throat, *b)* $\lambda_{crit} = 0.10m$: this is of the order of magnitude of the radius at the nozzle exit, *c)* $\lambda_{crit} = 1.00m$: this is the distance from the throat to the nozzle exit, *d)* $\lambda_{crit} = 10.00m$: this is large compared with the size of the nozzle.

The regions of the flow field where partial equilibrium is assumed, are shown in Fig. 5. First, in Fig. 5a, the dimension n_e of the equilibrium reaction subspace is plotted along the centerline of the nozzle for all cases considered. The extent of regions with constant n_e increases about linearly with the logarithm of the critical relaxation length. This is not a general result since the characteristic relaxation times τ_k of the reactions depend on the thermodynamic state in a complex manner. For $\lambda_{crit} = 1m$ and $\lambda_{crit} = 10m$ the contour lines of n_e are shown in Fig. 5b and 5c in the same way as this was done for the case $\lambda_{crit} = 0.1m$ in Fig. 3a. The curved lines demonstrate well that the partial equilibrium formulation is locally applied.

In Fig. 6 the temperature on the nozzle axis, obtained from partial equilibrium computations with different λ_{crit}, is compared with the temperature of the nonequilibrium, equilibrium and frozen flow solution. If $\lambda_{crit} = 0.1m$, the difference between the partial and nonequilibrium solution can almost not be resolved (cf. Fig. 6a). The difference between these two solutions is even smaller in the case of $\lambda_{crit} = 0.01m$ which is therefore not considered in Fig. 6. Fig. 6a shows that up to $x \simeq 0.1m$ the partial/nonequilibrium temperature is practically equal to the temperature of an equilibrium flow. In this flow regime the partial equilibrium flow computation (with $\lambda_{crit} = 0.1m$) solves essentially the equilibrium flow equations ($n_e = 4$ for $x \lesssim 0.05m$ and $n_e = 3$ for $x \lesssim 0.1m$). As soon as the nonequilibrium flow deviates from the equilibrium one the partial equilibrium computation is performed with a higher degree of nonequilibrium, though a fully nonequilibrium flow is not assumed before $x \simeq 0.2m$. Fig. 6b displays the temperature curve of a calculation using $\lambda_{crit} = 1.0m$. It can be seen that the temperature T_{peq} of the partial equilibrium solution coincides with the equilibrium temperature T_{eq} longer than does the nonequilibrium temperature T_{neq}. Only behind $x \simeq 0.2m$ where n_e drops to $n_e = 2$, T_{peq} starts to approach rapidly T_{neq}. Despite the distinct difference between T_{peq} and T_{neq} before $x \simeq 0.2m$, this difference becomes eventually very small. In the case of $\lambda_{crit} = 10.m$ (cf. Fig. 6c) T_{peq} stays very long at the equilibrium temperature before decreasing towards T_{neq}. This time, however, the nonequilibrium limit is no longer reached and T_{peq} approaches a value somewhere in between the equilibrium and nonequilibrium solution. This shows that $\lambda_{crit} = 10.0m$ is clearly too large.

As another example one of the species concentrations (γ_O) is also plotted along the nozzle axis in Fig. 7. This time partial equilibrium computations with $\lambda_{crit} = 0.01, 0.10$ and $1.00m$

are compared with the nonequilibrium, equilibrium and frozen flow solution. The main features are similar to those observed in the temperature (cf. Fig. 6). In the case of the small critical relaxation length ($\lambda_{crit} = 0.01m$) the partial equilibrium and nonequilibrium solution agree well everywhere (cf. Fig. 7a). Except for a small region about $x \approx 0.08m$ where partial equilibrium is assumed, the difference is not resolved in Fig. 7a. Fig. 7b shows the concentration γ_O obtained by a computation with $\lambda_{crit} = 0.1m$. As long as the dimension of the equilibrium reaction subspace is greater than 2 the partial equilibrium solution $(\gamma_O)_{peq}$ coincides with the equilibrium solution. Right after the switch from $n_e = 3$ to $n_e = 2$ a strong increase in γ_O takes place which results in a $(\gamma_O)_{peq}$ which is slightly greater than $(\gamma_O)_{neq}$. The next decrease in the dimension, from $n_e = 2$ to $n_e = 1$, is reflected in a small increase in the difference between $(\gamma_O)_{peq}$ and $(\gamma_O)_{neq}$. At the transition to the fully nonequilibrium equations ($x \simeq 0.2m$), $(\gamma_O)_{peq}$ decreases towards $(\gamma_O)_{neq}$ and in the course of the nonequilibrium computation the difference between the partial and nonequilibrium γ_O remains very small. Finally, in Fig 7c the $(\gamma_O)_{peq}$ curve of a calculation with $\lambda_{crit} = 1.0m$ is depicted. At the points where n_e is changed all corresponding increases and decreases in $(\gamma_O)_{peq}$ are qualitatively equal to the case of $\lambda_{crit} = 0.1m$ (cf. Fig. 7b). This time, however, the partial equilibrium solution stays much longer in equilibrium. Due to the strong decrease of $(\gamma_O)_{eq}$ behind $x \simeq 0.1m$ which is not present in $(\gamma_O)_{neq}$, $(\gamma_O)_{peq}$ deviates very much from the nonequilibrium solution. This is even more pronounced in the case of $\lambda_{crit} = 10.0m$ which is not shown in Fig. 7.

Finally, in Fig. 8 the state variables of all partial equilibrium calculations are compared with the fully nonequilibrium solution at the nozzle exit. It can be seen that $\lambda_{crit} = 0.01, 0.10$ and $1.00m$ yields good results, i.e. the corresponding solutions are close to the fully nonequilibrium solution. In the case of $\lambda_{crit} = 1.0m$ some state varibles show already a distinct deviation (e.g. u, γ_{N_2} , γ_{NO}). If $\lambda_{crit} = 10.0m$, however, the deviations from nonequilibrium become very strong. This solution is thus no longer acceptable.

The CPU-times of the partial equilibrium computations are not always shorter than the one of the fully nonequilibrium calculation. In the case of the very small critical relaxation length ($\lambda_{crit} = 0.01m$) the CPU-time is even larger (by about 14%) than in the case of a fully nonequilibrium computation. The reason is not clear, but the following remarks may provide some ideas of what happens. Every time when the dimension of the equilibrium reaction subspace changes, the integration in ξ-direction of the ordinary system of equations is started anew, i.e. the code which performes this integration initializes itself. When the equations are stiff this needs some time. If $\lambda_{crit} = 0.01m$, the equations are still stiff when they are switched to nonequilbrium. Then, restarting the code could lead to a higher consumption of time than is saved by a partial equilibrium computation. The code needs not necessarily to be restarted. However, if it is not restarted at those positions where the dimension of the equilibrium subspace changes, the code has some trouble with the change in the equations. This again leads to larger CPU-times.

In all other cases of partial equilibrium the CPU-times are smaller than in fully nonequilibrium. The savings are about the same in all of these cases (28% ($\lambda_{crit} = 0.10m$), 32% ($\lambda_{crit} = 1.00m$) and 31% ($\lambda_{crit} = 10.00m$)). The savings would be greater if only the time which is needed for computing that part of the flow field where partial equilibrium is actually assumed, is compared. The results of computations with $\lambda_{crit} = 0.01m$ and $0.10m$ are both very close to the nonequilibrium solution. Some more pronounced deviations are present in the

case of $\lambda_{crit} = 1.00m$, the results can still be regarded as close to nonequilibrium though. If $\lambda_{crit} = 10.00m$ this is no longer the case. Among the partial equilibrium computations which provide a saving in CPU-time, the one with $\lambda_{crit} = 0.1m$ yields the best agreement with the nonequilibrium solution. It is therefore suggested that $\lambda_{crit} = 0.10m$ is a good choice of the critical relaxation length. For that reason this case was chosen to be the 'standard case' in the beginning of chapter 6.

6.3. Expansion of an ideal gas

The program Surf can also be used for calculating flows of an ideal gas. In the case of ideal gases the thermal state equation is of the form $p = \rho \cdot R^* \cdot T$, where R^* is a constant. The caloric state equation shows a linear relationship between the enthalpy and the temperature: $h = c_p \cdot T + h^\circ$ where the specific heat at constant pressure, c_p, is constant. The formation enthalpy h° enters the equation due to the special choice of some reference state.

As an example the expansion of an ideal diatomic gas is calculated. Essentially the same case as in the preceding chapters is considered, namely the flow through the T5/100 nozzle at the reservoir temperature and pressure $T_0 = 9000K$ and $p_0 = 200 \cdot 10^5 Pa$. However, in order to model an ideal diatomic gas, the number of species and their thermodynamic properties are changed. Further, a frozen flow computation is performed. In contrast to the frozen flow computation presented in chapter 6.1., the initial conditions are already approximated by a frozen flow. The input data used in this ideal gas computation are listed in Fig. 9. It would be sufficient to consider just one species. The program Surf, however, requires at least one dependent and one independent species to be specified. Here, diatomic and monatomic oxygen are chosen. The formation enthalpy of O_2 is taken as zero as usual, but the formation enthalpy of O is artificially increased by a factor of ten. At the present reservoir conditions this results in a very small equilibrium (= reservoir) concentration of monatomic oxygen ($\gamma_O = 2 \cdot 10^{-11} mole/kg$). A frozen flow computation is performed (i.e. no reactions are considered, on input `ir = 0`) which starts from initial conditions that are obtained by assuming already a frozen flow between the reservoir and the upstream boundary (input parameter `i2d = -1` , cf. Surf report). Hence, pratically the flow of purely diatomic oxygen is calculated and the thermal state equation is of the correct form. The thermodynamic state is modeled using the statistical mechanics formulation. This is done by chosing a negative switch temperature, `TFIT = -3.D3`. Then, no coefficients for a polynomial fit need to be provided (cf. Surf report). In the thermodynamic model vibrational and electronical excitations are neclected. The corresponding characteristic temperatures are assumed to be zero. The caloric state equation is then given by:

$$
\begin{aligned}
h &= \sum_{l=1}^{2} \gamma_l \cdot \hat{h}_l = \gamma_O \cdot \hat{h}_O + \gamma_{O_2} \cdot \hat{h}_{O_2} \\
&\simeq \gamma_{O_2} \cdot \left(\hat{h}^\circ_{O_2} + \left[\frac{5}{2} + (\phi - 1) \right] \cdot R \cdot T \right) = c_p \cdot T + h^\circ_{O_2} \quad ,
\end{aligned}
\tag{6.1}
$$

where the contribution of monatomic oxygen was neglected and '$\hat{h}$' is the molar enthalpy.

The results of the ideal gas computation using the input data discussed in the last paragraph, are compared with the 'standard case' and the frozen flow solution in Fig. 10 and 11. In contrast

to the ideal gas case in which a frozen flow is assumed as well, the frozen flow computation starts at the same initial conditions as the 'standard case' calculation, i.e. from the reservoir to the upstream boundary of the computational domain an equilibrium flow is assumed. Further, in the frozen flow case the electronical and vibrational excitation of the species are taken into account, hence the caloric state equation does not satisfy the conditions of an ideal gas. Fig. 10a shows contour lines of the temperature. These can be compared with Fig. 3c where the corresponding contour lines of the 'standard case' are depicted. In Fig. 10b the temperatures of the three flows considered, are plotted along the nozzle axis. The two frozen flow cases reveal a similar behaviour of the temperature. First it decreases quickly and later an almost constant value is assumed. These final values are very close to each other. This is probably due to the special conditions considered in this example.

Fig. 11 shows the radial variation of the state variables at the nozzle exit. Species concentrations are not plotted, because they are of no importance in an ideal gas flow. In the ideal gas case the flow is frozen everywhere. Hence, no energy is released due to recombination in the convergent part of the nozzle. At the upstream boundary of the computational domain the total energy flux of the gas is therefore not the same in the ideal gas and the other two cases. Further, already in the reservoir the composition of the gas is different. This leads to different reservoir enthalpies ($(h_0)_{id} = 0.8185 \cdot 10^7 J/kg$, $(h_0)_{peq} = 0.2292 \cdot 10^8 J/kg$). The numerical values of the state variables displayed in Fig. 11, can therefore not be exactly compared. It can be seen, however, that in some sense the ideal gas flow is similar to the frozen flow. In particular the strong variation of the density in radial direction is present in both flows.

6.4. Remarks on the initial conditions

At the upstream boundary the initial conditions are approximated by a one-dimensional equilibrium or frozen flow solution. Thereby the state variables are assumed to be constant on the whole inflow cross section. Only the condition of a tangential flow is satisfied at the walls. The radial variation of the flow which is known to be present in nozzle flows, is thus neclected. In this chapter the influence of this approximation on the solution is investigated by considering slightly changed initial conditions in which the state variables are functions of the radius. The results of computations with two different radial variations of the initial conditions are compared with those in which the state variables are constant on the inflow cross section.

The radial variation of the initial conditions is obtained by a modification of subroutine inicond. This subroutine determines the initial data by computing the one-dimensional equilibrium or frozen flow solution at the upstream boundary at x_u (cf. Surf report). Its modified form is listed in Fig. 12. The initial conditions at different radial positions η, but constant $x_u = (x_u)_0$, are obtained by approximating the initial state at different η by an equilibrium solution which corresponds to different cross sectional areas. This is accomplished by a sinusoidal variation with η of that x_u which is used in calculating the one-dimensional equilibrium state:

$$x_u = (x_u)_0 \cdot \left(1 \pm \frac{1}{2} \cdot \left(1 - cos\left(\frac{\pi}{2} \frac{n-1}{n_{max}-1}\right)\right)\right) \quad . \tag{6.2}$$

Here, $(x_u)_0$ is the true position of the upstream boundary and n is the line number (method of lines) corresponding to the radial position. At $\eta = 0$ (i.e. $n = 1$) the cross sectional area assumed,

is always equal to the actual one. Using the plus sign in eq. (6.2) yields a radial variation of the state variables which is qualitatively equal to the one expected in nozzle flows. This case will be called 'physical case'. A minus sign yields unphysical initial conditions, the velocity has a maximum on the axis and the pressure on the wall. This case will be called 'unphysical case' hereafter. Computations with these two formulations of the initial conditions are compared with the standard case, in which the state variables are constant on the inflow boundary. The input data of the standard case are also used in the other two computations.

The drawback of this formulation of different radial dependencies of the initial conditions is that the total energy flux through the inflow boundary is not the same in all three cases. The difference, with respect to the standard case, amounts to -7.6% in the unphysical and to $+6.6\%$ in the physical case. The solutions obtained in the three cases can therefore be qualitatively compared only.

The initial conditions resulting from the formulation introduced in the last paragraph, are compared in Fig. 13. On the nozzle axis the state variables assume the same values since at $\eta = 0$ the cross sectional area on which the one-dimensional solution is based, is equal in all cases. At the wall large differences are present. In the physical case the pressure, for example, is 26% smaller than in the standard case. In the unphysical case the difference is $+35\%$. In Fig. 13 only the concentration γ_O is plotted.The radial variation of the other concentrations is similar.

At the exit the dependence on the radius of the state variables is qualitatively the same (cf. Fig. 14). The differences, which are approximately independent of η, are mainly due to the differences in the total energy flux at the upstream boundary (see below). In the pressure the differences with respect to the standard case amount to -14% (physical case) and to $+11\%$ (unphysical case).

Fig. 15 shows contour lines of the temperature in an upstream section of the full computational domain. It can be seen that the curvature of the contour lines is different only in the very beginning. At $x = 0.03m$ the maximum of the temperature is already on the axis in all three cases. Behind this position the contour plots are qualitatively the same.

Finally, in Fig. 16 the temperature and the concentration γ_O are plotted along the axis. It can be seen, especially in γ_O, that the characteristic changes in these curves which are caused by the decrease in the dimension of the equilibrium reaction subspace, are the same in all cases.

In order to verify that the differences in the solutions are mainly due to different total energy fluxes at the inflow boundary, another computation is performed. In this computation the initial conditions are approximated in the usual way by exactly one one-dimensional equilibrium flow solution, thus assuming a constant state on the inflow boundary. This time, however, the one-dimensional flow solution does not correspond to the $x-$position of the upstream boundary but to some position $x_* < x_u$. Here, x_* is chosen so that the total energy flux at the inflow boundary is within 0.1% of the energy flux of the physical case. In Fig. 17a the the temperature and pressure are plotted versus the non-dimensional radius at the inflow boundary. As in the cases dicussed above, the differences between the two initial conditions are large (on the axis, e.g., temperature: 1.8%, pressure: 18.1%). Fig. 17b contains the results for the temperature and pressure at the nozzle exit. The solutions agree well both, qualitatively and quantitively. On the nozzle axis where the differences are largest, these differences are: temperature: 0.9%, pressure: 3.1%, density: 2.1%, velocity: -0.1%, γ_N: 5.0%, γ_O: 0.1%, γ_{NO}: 0.0%, γ_{NO^+}: 0.0%.

Neither of the considered initial conditions is fully correct. Nonetheless, except for a small region downstream of the inflow boundary, the solutions which are based on different formulations of the initial conditions, agree qualitatively. Differences were shown to be due to different total energy fluxes at the inflow boundary. Thus it is reasonable to approximate the initial conditions by the corresponding one-dimensional flow solution as done by Surf. If more exact initial conditions are required, this can be achieved by rewriting subroutine inicond.

6.5. On the step size in the method of lines

A finite difference method is used for solving the system of differential equations modeling partial equilibrium flows. The numerical solution depends on the step size. In the limit of vanishingly small step sizes the numerical solution should converge towards the true solution. Here, the method of lines is applied (cf. Surf report for details). The independent variable of the resulting system of ordinary differential equations is the axial coordinate ξ ($\hat{=}x$). A solver is used for solving this system of ODEs. It selects the step size (in ξ) automatically. The step size is limited by the length of the interval $\Delta\xi = (x_d - x_u)/(m_{max} - 1)$ between two succeeding output points. Thus the choice of the number m_{max} of cross sections of constant ξ at which the solution is printed to the second output file, determines the maximal step size in ξ–direction. It was shown by sample calculations that the special choice of m_{max} has no influence on the solution.

The step size in η–direction is determined by the number n_{max} of lines used in the method of lines. The dependence of the solution on n_{max} is shown in Fig. 18 by comparing results of computations with $n_{max} = 4,\ 10,\ 20,\ 30$ and 40 at the nozzle exit. Except for the value of n_{max} the standard case is assumed in all cases. It can be seen that the solution converges well with increasing n_{max}. If $n_{max} \geq 20$ the difference in the results is small. In order to obtain a quantitative measure, the difference between the total energy fluxes at the inflow and outflow boundary is compared. There should be no difference. In the case of $n_{max} = 4$ the difference amounts to 11%, whereas for $n_{max} = 40$ it is less than one percent. The difference in the total energy flux decreases slightly better than linearly with n_{max}. Further, the increase in CPU-time with n_{max} is less than quadratic. In order to obtain a resonable compromise between CPU-time and accuracy, $n_{max} = 20$ was chosen in the standard case computation.

6.6. Remarks on the nozzle contour

The program Surf cannot handle shock waves. Accordingly, in using Surf it is important to avoid conditions where shocks are formed in the flow field. If shocks are nevertheless present, this can result in strange results since the program Surf does not recognize shocks. This is demonstrated by an example.

As in the preceding chapters the expansion of high temperature air through a convergent-divergent nozzle is considered. The properties of air and the chemical reactions are the same as in the standard case. The only exception is the switch temperature which is still $T_{fit} = 6000K$ as in the computations presented in the Surf report. This time an expansion through the nozzle of the

HEG shock tunnel of the DLR, Göttingen, is examined. Actually, the HEG nozzle without boundary layer correction is considered (cf. Hannemann, 1990). The reservoir temperature and pressure are $T_0 = 13780K$ and $p_0 = 2000 \cdot 10^5 Pa$. In a first computation, the geometry of the HEG nozzle was not 'well defined'. Actually, the nozzle contour was already very smooth (cf. Fig. 19a). However, in the first derivative of the radius a small discontinuity was present (Fig. 19b). In flow direction a step like decrease of the first derivative of the radius takes place at the discontinuity. This has the same effect like a wedge and a shock will be formed in a supersonic flow. The effect of the discontinuity on the computational result is shown in Fig. 20. For comparison, the results of a computation based on a nozzle geometry with a smooth derivative of the radius (cf. Fig. 19c) are also included in Fig. 20. The corresponding two nozzle contours are practically the same, differences cannot be resolved on the scaled of Fig. 19a. In the case with the discontinuity the contour plots of Fig. 20a reveal something like a 'boundary layer effect' though an inviscid flow is considered. This effect is caused by the boundary condition at the wall which requires the flow to be tangential to the wall. For that reason, the boundary layer effect appears only in the velocity, no other state variables are affected. As an example the temperature is plotted versus the radius at the nozzle exit in Fig. 20b. This is also done for the velocity. It can be seen that the deviation of the velocity is limited to the wall point. A small difference between the solutions which can still be seen on the axis, is due to the geometries of the two computational versions of the HEG nozzle being slightly different. (At the inflow boundary the cross sectional areas of the two versions of the HEG nozzle differ by less than 0.1%. In a one-dimensional equilibrium flow this results in a difference of the velocity of $\Delta u = 8m/s$ at this position.)

Acknowledgement

The work described in this report is a continuation of a project which was begun at GALCIT. The theory of partial chemical equilibrium, however, was mainly developed at the Max-Planck-Institute for Fluid Dynamics, Göttingen, FRG. The present report is nevertheless published as a GALCIT report because it is closely connected with the GALCIT report No. FM 89-1 ('Surf Report'). Thanks are due to Prof. E.–A. Müller for letting me bring the project to an end at the Max-Planck-Institute.

I am particularly grateful to Prof. H. G. Hornung for suggesting the project of introducing partial equilibrium in reacting flows and for many stimulating discussions by e-mail.

Appendix A: Finite difference equations for method of lines

In this appendix the finite difference equations for partial equilibrium flows are listed. Since these equations are similar to the ones for nonequilibrium flows which were listed in Appendix B of the Surf report, this section of the Surf report is copied here. Included are, however, those modifications necessary for partial equilibrium.

To solve the system of equations (3.9-14) by the method of lines, the η-direction is discretized yielding n_{max} lines. The finite difference approximation of the η-derivatives is obtained according to the appropiate characteristic directions (cf. eq. (3.8)). In the method of lines formulation the dependent variables at different η_n, $\eta_n = (n-1)/(n_{max}-1)$, $n = 1,...,n_{max}$, are to be taken as different functions. For instance, now there are n_{max} different pressure functions $p_n(\xi)$, $n = 1,...,n_{max}$, replacing $p(\xi,\eta)$. The system (3.9-14) is then written separately for each line n and the corresponding dependent variables (u_n, v_n, p_n, etc.), $n = 1,...,n_{max}$. Here, first some abbreviations are introduced:

$$
\begin{aligned}
S_- &:= \sqrt{u^2 \cdot (1 + (\frac{dy_-}{d\xi})^2) - {a_f}^2} \quad , & S_+ &:= \sqrt{u^2 \cdot (1 + (\frac{dy_+}{d\xi})^2) - {a_f}^2} \\
S_0 &:= \sqrt{u^2 + v^2 - {a_f}^2} \quad , & H &:= h_\rho + \sum_{l=1}^{s} h_{\gamma_l} \; P_{eq}(\gamma_{l_\rho}) \\
S_I &:= \begin{cases} I_p \cdot \dfrac{u \; dy_-/d\xi}{y_-} & \text{for } y_- > 0 \\ I_p \cdot b \cdot \dfrac{\partial v}{\partial \eta} & \text{for } y_- = 0 \end{cases} \quad , & y &= y_- + \eta \cdot (y_+ - y_-) \\
S_k &:= 1 - \frac{1}{K_{\gamma_k}} \cdot \prod_{l=1}^{s} \gamma_l^{\beta_{lk}} \\
L_{jk} &:= \Big[\beta_{jk} \frac{\Gamma}{\gamma_j} - \sum_{l=1}^{s} \beta_{lk} + \frac{\Delta \hat{h}_k}{R\,T} - \sum_{i=1}^{c} (\beta_{ik} \frac{\Gamma}{\gamma_i} - \sum_{l=1}^{s} \beta_{lk} + \frac{\Delta \hat{h}_k}{R\,T}) \cdot \alpha_{ji} \Big] \\
G_j &:= h_{\gamma_j} - \sum_{i=1}^{c} h_{\gamma_i} \; \alpha_{ji} \; .
\end{aligned}
\tag{A.0}
$$

The second expression for S_I ($y_- = 0$) is derived from the first one in the limiting case of $y_- \to 0$ by using L'Hospital's rule. The equation for y follows from the definition of the new coordinate η (cf. chapter 3.).

At the boundaries ($n = 1$, $n = n_{max}$) the boundary conditions $v_1 = u_1 \cdot \frac{dy_-}{d\xi}$ and $v_{n_{max}} = u_{n_{max}} \cdot \frac{dy_+}{d\xi}$ replace those compatibility equations whose characteristics enter the flow field from outside. This eventually leads to the following system of ordinary differential equations where the subscript n, enumerating the lines, has been omitted:

lower boundary, i.e. $n = 1$ (at $(\xi, \eta_1 = 0)$):

$$
\Big(1 + (\frac{dy_-}{d\xi})^2\Big) \cdot \frac{\partial u}{\partial \xi} + \frac{1}{\rho u} \cdot \frac{\partial p}{\partial \xi} = -u \cdot \frac{dy_-}{d\xi} \cdot \frac{d^2 y_-}{d\xi^2} \tag{A.1}
$$

$$(A.2) \qquad -\frac{H}{{a_f}^2}\cdot\frac{\partial p}{\partial \xi}+H\cdot\frac{\partial \rho}{\partial \xi}+\sum_{j=c+1}^{s} G_j\cdot\frac{\partial \gamma_j}{\partial \xi}=0$$

$$\begin{aligned}(A.3) \qquad & \frac{S_-}{\rho a_f}\cdot\frac{\partial p}{\partial \xi}-\frac{{a_f}^2}{{a_f}^2-u^2}\cdot\frac{1}{H\ \rho}\cdot\Big(u\ \frac{dy_-}{d\xi}-\frac{u}{a_f}\ S_-\Big)\cdot u\cdot\sum_{j=c+1}^{s} G_j\cdot\frac{\partial \gamma_j}{\partial \xi}= \\ & =\Big(\frac{d\eta}{d\xi}\Big)_3\cdot\Big[-u\ \frac{dy_-}{d\xi}\cdot\Big(\frac{\Delta u}{\Delta \eta}\Big)_3+u\cdot\Big(\frac{\Delta v}{\Delta \eta}\Big)_3-\frac{S_-}{\rho a_f}\cdot\Big(\frac{\Delta p}{\Delta \eta}\Big)_3\Big]- \\ & \quad -\frac{{a_f}^2}{{a_f}^2-u^2}\cdot\Big(u\ \frac{dy_-}{d\xi}-\frac{u}{a_f}\ S_-\Big)\cdot S_I+u^2\ \frac{d^2y_-}{d\xi^2}\end{aligned}$$

$$(A.3+l,\quad l=1,...,s-c-n_e) \qquad \sum_{j=c+1}^{s} n_{j,l}\cdot\frac{\partial \gamma_j}{\partial \xi}=\frac{1}{u}\cdot\sum_{j=c+1}^{s} n_{j,l}\cdot\Big(\sum_{k=1}^{r}(1-I_{r,k})P_{jk}\Big)$$

$$(A.3+l,\quad l=s-c-n_e+1,...,s-c)$$
$$-\Big(\sum_{l=1}^{s}\beta_{lk}-\frac{\Delta \hat{h}_k}{R\ T}\Big)\cdot\frac{1}{p}\frac{\partial p}{\partial \xi}-\frac{\Delta \hat{h}_k}{R\ T}\cdot\frac{1}{\rho}\frac{\partial \rho}{\partial \xi}-\sum_{j=c+1}^{s} L_{jk}\cdot\frac{1}{\Gamma}\frac{\partial \gamma_j}{\partial \xi}=-\lambda\cdot S_k\ ,\quad k\in\overline{N_e}$$

<u>flow field, i.e. $2<n<n_{max}-1$ (at $(\xi,\eta_n=(n-1)/(n_{max}-1))$):</u>

definition: $ln:=3+s-c+(n-2)\cdot(4+s-c)$

$$(A.ln+1) \qquad \frac{\partial u}{\partial \xi}+\frac{v}{u}\cdot\frac{\partial v}{\partial \xi}+\frac{1}{\rho u}\cdot\frac{\partial p}{\partial \xi}=-\frac{d}{u}\cdot\Big(\Big(\frac{\Delta u}{\Delta \eta}\Big)_1+\frac{v}{u}\cdot\Big(\frac{\Delta v}{\Delta \eta}\Big)_1+\frac{1}{\rho u}\cdot\Big(\frac{\Delta p}{\Delta \eta}\Big)_1\Big)$$

$$\begin{aligned}(A.ln+2) \qquad & -\frac{H}{{a_f}^2}\cdot\frac{\partial p}{\partial \xi}+H\cdot\frac{\partial \rho}{\partial \xi}+\sum_{j=c+1}^{s} G_j\cdot\frac{\partial \gamma_j}{\partial \xi}= \\ & =\frac{d}{u}\cdot\Big(\frac{H}{{a_f}^2}\cdot\Big(\frac{\Delta p}{\Delta \eta}\Big)_1-H\cdot\Big(\frac{\Delta \rho}{\Delta \eta}\Big)_1-\sum_{j=c+1}^{s} G_j\cdot\Big(\frac{\Delta \gamma_j}{\Delta \eta}\Big)_1\Big)\end{aligned}$$

$$\begin{aligned}(A.ln+3) \qquad & v\cdot\frac{\partial u}{\partial \xi}-u\cdot\frac{\partial v}{\partial \xi}-\frac{S_0}{\rho a_f}\cdot\frac{\partial p}{\partial \xi}-\frac{{a_f}^2}{{a_f}^2-u^2}\cdot\frac{1}{H\ \rho}\cdot\Big(v+\frac{u}{a_f}\ S_0\Big)\cdot u\cdot\sum_{j=c+1}^{s} G_j\cdot\frac{\partial \gamma_j}{\partial \xi}= \\ & =\Big(\frac{d\eta}{d\xi}\Big)_2\cdot\Big[-v\cdot\Big(\frac{\Delta u}{\Delta \eta}\Big)_2+u\cdot\Big(\frac{\Delta v}{\Delta \eta}\Big)_2+\frac{S_0}{\rho a_f}\cdot\Big(\frac{\Delta p}{\Delta \eta}\Big)_2\Big]+\frac{{a_f}^2}{{a_f}^2-u^2}\cdot\Big(v+\frac{u}{a_f}\ S_0\Big)\cdot \\ & \quad\cdot\Big[\frac{1}{H\ \rho}\sum_{j=c+1}^{s} G_j\cdot d\cdot\Big(\frac{\Delta \gamma_j}{\Delta \eta}\Big)_1-\frac{I_p v}{y}\Big]\end{aligned}$$

$$\begin{aligned}(A.ln+4) \qquad & v\cdot\frac{\partial u}{\partial \xi}-u\cdot\frac{\partial v}{\partial \xi}+\frac{S_0}{\rho a_f}\cdot\frac{\partial p}{\partial \xi}-\frac{{a_f}^2}{{a_f}^2-u^2}\cdot\frac{1}{H\ \rho}\cdot\Big(v-\frac{u}{a_f}\ S_0\Big)\cdot u\cdot\sum_{j=c+1}^{s} G_j\cdot\frac{\partial \gamma_j}{\partial \xi}= \\ & =\Big(\frac{d\eta}{d\xi}\Big)_3\cdot\Big[-v\cdot\Big(\frac{\Delta u}{\Delta \eta}\Big)_3+u\cdot\Big(\frac{\Delta v}{\Delta \eta}\Big)_3-\frac{S_0}{\rho a_f}\cdot\Big(\frac{\Delta p}{\Delta \eta}\Big)_3\Big]+\frac{{a_f}^2}{{a_f}^2-u^2}\cdot\Big(v-\frac{u}{a_f}\ S_0\Big)\cdot \\ & \quad\Big[\frac{1}{H\ \rho}\sum_{j=c+1}^{s} G_j\cdot d\cdot\Big(\frac{\Delta \gamma_j}{\Delta \eta}\Big)_1-\frac{I_p v}{y}\Big]\end{aligned}$$

$(A.ln+4+l,\quad l=1,...,s-c-n_e)$

$$\sum_{j=c+1}^{s} n_{j,l}\cdot\frac{\partial\gamma_j}{\partial\xi} \;=\; \frac{1}{u}\cdot\sum_{j=c+1}^{s} n_{j,l}\cdot\Big(\sum_{k=1}^{r}(1-I_{r,k})P_{jk}\Big)-\frac{d}{u}\cdot\sum_{j=c+1}^{s} n_{j,l}\cdot\Big(\frac{\Delta\gamma_j}{\Delta\eta}\Big)_1$$

$(A.ln+4+l,\quad l=s-c-n_e+1,...,s-c)$

$$-\Big(\sum_{l=1}^{s}\beta_{lk}-\frac{\Delta\hat{h}_k}{R\,T}\Big)\cdot\frac{1}{p}\frac{\partial p}{\partial\xi}-\frac{\Delta\hat{h}_k}{R\,T}\cdot\frac{1}{\rho}\frac{\partial\rho}{\partial\xi}-\sum_{j=c+1}^{s}L_{jk}\cdot\frac{1}{\Gamma}\frac{\partial\gamma_j}{\partial\xi}=$$

$$=\frac{d}{u}\Big[\Big(\sum_{l=1}^{s}\beta_{lk}-\frac{\Delta\hat{h}_k}{R\,T}\Big)\cdot\frac{1}{p}\Big(\frac{\Delta p}{\Delta\xi}\Big)_1+\frac{\Delta\hat{h}_k}{R\,T}\cdot\frac{1}{\rho}\Big(\frac{\Delta\rho}{\Delta\xi}\Big)_1+\sum_{j=c+1}^{s}L_{jk}\cdot\frac{1}{\Gamma}\Big(\frac{\Delta\gamma_j}{\Delta\xi}\Big)_1\Big)$$

$$-\lambda\cdot S_k\quad,\qquad k\in\overline{N_e}$$

<u>upper boundary, i.e. $n=n_{max}$ (at $(\xi,\eta_{n_{max}}=1)$):</u>

definition: $lm := 3+s-c+(n_{max}-2)\cdot(4+s-c)$

$(A.lm+1)$

$$\Big(1+\big(\frac{dy_+}{d\xi}\big)^2\Big)\cdot\frac{\partial u}{\partial\xi}+\frac{1}{\rho u}\cdot\frac{\partial p}{\partial\xi}=-u\cdot\frac{dy_+}{d\xi}\cdot\frac{d^2y_+}{d\xi^2}$$

$(A.lm+2)$

$$-\frac{H}{{a_f}^2}\cdot\frac{\partial p}{\partial\xi}+H\cdot\frac{\partial\rho}{\partial\xi}+\sum_{j=c+1}^{s}G_j\cdot\frac{\partial\gamma_j}{\partial\xi}=0$$

$(A.lm+3)$

$$-\frac{S_+}{\rho a_f}\cdot\frac{\partial p}{\partial\xi}-\frac{{a_f}^2}{{a_f}^2-u^2}\cdot\frac{1}{H\rho}\cdot\Big(u\frac{dy_+}{d\xi}+\frac{u}{a_f}S_+\Big)\cdot u\cdot\sum_{j=c+1}^{s}G_j\cdot\frac{\partial\gamma_j}{\partial\xi}=$$

$$=\Big(\frac{d\eta}{d\xi}\Big)_2\cdot\Big[-u\,\frac{dy_+}{d\xi}\cdot\Big(\frac{\Delta u}{\Delta\eta}\Big)_2+u\cdot\Big(\frac{\Delta v}{\Delta\eta}\Big)_2+\frac{S_{\div}}{\rho a_f}\cdot\Big(\frac{\Delta p}{\Delta\eta}\Big)_2\Big]-$$

$$-\frac{{a_f}^2}{{a_f}^2-u^2}\cdot\Big(u\,\frac{dy_+}{d\xi}+\frac{u}{a_f}\,S_+\Big)\cdot\frac{I_p\;u\;dy_+/d\xi}{y_+}+u^2\,\frac{d^2y_+}{d\xi^2}$$

$(A.lm+3+l,\quad l=1,...,s-c-n_e)$

$$\sum_{j=c+1}^{s} n_{j,l}\cdot\frac{\partial\gamma_j}{\partial\xi} \;=\; \frac{1}{u}\cdot\sum_{j=c+1}^{s} n_{j,l}\cdot\Big(\sum_{k=1}^{r}(1-I_{r,k})P_{jk}\Big)$$

$(A.lm+3+l,\quad l=s-c-n_e+1,...,s-c)$

$$-\Big(\sum_{l=1}^{s}\beta_{lk}-\frac{\Delta\hat{h}_k}{R\,T}\Big)\cdot\frac{1}{p}\frac{\partial p}{\partial\xi}-\frac{\Delta\hat{h}_k}{R\,T}\cdot\frac{1}{\rho}\frac{\partial\rho}{\partial\xi}-\sum_{j=c+1}^{s}L_{jk}\cdot\frac{1}{\Gamma}\frac{\partial\gamma_j}{\partial\xi}=-\lambda\cdot S_k\;,\quad k\in\overline{N_e}$$

These are $(n_{eq}=n_{max}\cdot(4+s-c)-2)$ equations; $(3+s-c)$ equations at each of the boundaries and $(4+s-c)$ equations at each of the $(n_{max}-2)$ lines within the flow field. In this system the derivatives of the enthalpy with respect to the density and to the species concentrations will be replaced by:

$(A.n_{eq}+1)$

$$H := h_\rho = -\,c_p\cdot\frac{p}{R\;\rho^2\;\Gamma}$$

$$h_{\gamma l} = \hat{h}_l - c_p\cdot\frac{p}{R\;\rho\;\Gamma^2}\quad,\quad l=1,...,s.$$

The equation system (A.1–(lm+3+s–c)) can be written in matrix form:

$$A\,\frac{\partial f}{\partial \xi} = B \quad , \tag{$A.n_{eq}+2$}$$

where A is the coefficient matrix, B the vector containing the r.h.s. and f is a vector containing the dependent variables, $f = (u_1, p_1, \rho_1, \gamma_{c+1,1}, ..., \gamma_{s,1}, u_2, v_2, p_2, ..., u_{n_{max}}, p_{n_{max}}, \rho_{n_{max}}, \gamma_{c+1,n_{max}}, \cdots, \gamma_{s,n_{max}})^t$. Here, a solver for ordinary differential equations will be used to solve the equation system. For applying this solver, the system needs to be in the form

$$\frac{\partial f}{\partial \xi} = C \quad , \tag{$A.n_{eq}+3$}$$

which is easily obtained by solving eq.$(A.n_{eq}+2)$ for $\frac{\partial f}{\partial \xi}$ numerically.

In the course of the numerical integration of the equation system (e.g. in the form of eq. $(A.n_{eq}+3)$) by a suitable solver, the dependent variables p_n, ρ_n and $\gamma_{j,n}$, $j = c+1, ..., s$, are transformed to new variables:

$$\begin{aligned} q_{1,n} &= \sqrt{p_n} \\ q_{2,n} &= \sqrt{\rho_n} \\ q_{2+j-c,n} &= \sqrt{\frac{1}{\gamma_{j,n}} - \frac{1}{\gamma_j^\circ}} \quad , \quad j = c+1, ..., s \quad , \end{aligned} \tag{$A.n_{eq}+4$}$$

where γ_j° denotates the maximum value possible for the concentration γ_j of the dependent species. The pressure, density and species concentrations are thus always greater or equal zero, and further, always $\gamma_j \leq \gamma_j^\circ$, $j = c+1, ..., s$, holds. In this manner, these quantities do never assume unphysical values.

Appendix B: Some important new Fortran variables

Fortran variable:	Comment:
af	in subroutine nmatrix af is used as the sound speed, this may be the partially frozen or frozen sound speed
apf2	$= a_{pf}^2$
coevc(j,k)	matrix containing the reduced reaction vectors $\tilde{R}_k$, $k = 1,...,r$, (cf. chapter 4.3.) as columns ($j = 1,...,s-c$)
fm(l,j-ic)	matrix containing the formation reaction vectors F_j, $j = c+1,...,s$, as columns, $l = 1,...,s$
fmon(l,j)	matrix containing an orthonormal basis for the reaction subspace as column vectors ($l = 1,...,s$, $j = 1,...,s-c$)
ibsvc(l)	the first n_e components of this vector are the reaction numbers of the set of linearly independent equilibrium reactions which provide a basis for all equilibrium reactions
ibsvcn(l,n)	the first n_e components of this vector are the reaction numbers of the set of linearly independent equilibrium reactions which provide a basis for all equilibrium reactions (for every line n, $n = 1,...,n_{max}$)
idim	$= n_e$ (locally)
idmnsn(n)	$= n_e$ (for every line n, $n = 1,...,n_{max}$)
ie	parameter which is set ie $= 1$: equilibrium flow; ie $= -1$: partial equilibrium or nonequilibrium flow; ie $= -10$: partial equilibrium or non-equilibrium flow: at least one vector of basis for equilibrium reactions did change
iear(k)	$= 0$: reaction k is not in the equilibrium reaction subspace $= 1$: reaction k is in the equilibrium reaction subspace
iek(k,n)	= iear(k) for every line n, $n = 1,...,n_{max}$
iprint	parameter which steers output (if iprint $= 1$ some output is provided)
nline	n (number of line in method of lines)
rlmbda	$= \lambda$: proportionality factor (cf. eq. (3.15))
rmult(j-ic,l,n)	matrix containing the multipliers $n_{j,l}$, $j = c+1,...,s$, for the rate equations (for every

line n, $n = 1, ..., n_{max}$), $l = 1, ..., (s-c) - n_e$

`spon(l,j)` matrix containing a basis for the nonequilibrium reaction subspace as the last $(s - c - n_e)$ column vectors (i.e. $j = n_e + 1, ..., s - c$)

`waa(k,j-ic,n)` $= (R^{neq}_{j,k}) - \sum_{i=1}^{c} (R^{neq}_{i,k}) \cdot \alpha_{ji}$, $k = 1, ..., s - c - n_e$, $j = c + 1, ..., s$ (matrix containing coefficients of eq. (2.33) for every line n)

Appendix C: Figures

```
Nozzle: T5/100 (GALCIT), usual throat
expansion of air (8 species, 22 reactions)
c.l. (=comment line): names of output data files
yr20up1
yr20up2
c.l.: job id. no.,iequil,ifrzn,i2d,iout
   100 0 0 1 1
c.l.: xu, xd, mmax, nmax
     .01   1.  200   20
c.l.: T0, p0
   9000.       2.00E+07
c.l.: Tv
      3.D3
c.l.: ichkd, rminlt
     1 2.
c.l.: dcrit
    .1
c.l.: ic, is, ir
          4           8           22
c.l.: indep. species: symb(i), g0(i), i=1,.,ic
 E- .0D0
 N2 .78112D0
 O2 .20954D0
 AR .00934D0
c.l.: alph(j,i), j=ic+1,.,is, i=1,.,ic:
  0.   .5 0.  0.
  0. 0.    .5 0.
  0.   .5  .5 0.
 -1.   .5  .5 0.
c.l.: thermodynamic properties of (is) species:
 E-
     5.4847D-7  1       0.0000000E+00  3.D3
     1.       1.       1      0
  2.000000
 0.0000000E+00
 0.0000000E+00
 20.78675D0,0.D0,0.D0,0.D0,0.D0,
 -97.57301D0
 N2
     28.0160D-3   2       0.0000000E+00  3.D3
     2.86      2.        4     1
  1.000000        3.000000        6.000000        1.000000
 0.0000000E+00    72352.91        85843.07        88323.06
  3353.240
 28.69805D0,5.1357108D-3,-1.0604805D-6,9.1105665D-11,-2.27333721D-15,
 25.53668D0
 O2
     32.000D-3    2       0.0000000E+00  3.D3
     2.07      2.       5        1
  3.000000        2.000000        1.000000        3.000000        3.000000
 0.0000000E+00    11096.78        18996.51        51965.59        71700.80
  2238.970
 27.01839D0,8.253918D-3,-1.6716921D-6,1.4778012D-10,-4.1585184D-15,
 49.18163
```

Fig. 1: Input data file for the program Surf as used in the standard case computation

```
 AR
     39.944D-3      1       0.0000000E+00  3.D3
     1.       1.         3          0
  1.000000         5.000000         3.000000
 0.0000000E+00    134099.5         134973.2
 0.0000000E+00
 21.31292D0,-5.9728982E-4,1.8631269D-7,-2.2439826D-11,9.2875987D-16,
 33.26661D0
  N
     14.008D-3      1        471243.3268   3.D3
     1.       1.         5          0
  4.000000         6.000000         4.000000         6.000000         12.00000
 0.0000000E+00    27682.28         27758.32         41520.40         119951.2
 0.0000000E+00
 25.01829,-5.212693D-3,1.574425D-6,-1.3852965D-10,3.880839D-15,
 10.83801D0
  O
     16.000D-3      1        246857.841       3.D3
     1.       1.         6          0
  5.000000         3.000000         1.000000         5.000000         1.000000
  5.000000
 0.0000000E+00    228.9249         326.7953         22845.16         48650.70
  106202.7
 0.0000000E+00
 21.56952D0,-8.3295238D-4,2.99205D-7,-2.8873997D-11,8.9304039D-16,
 38.25274D0
 NO
     30.008D-3      2           89890.90965     3.D3
     2.42       1.         3          1
  4.000000         2.000000         4.000000
 0.0000000E+00    63296.52         66107.84
  2699.180
 31.23181D0,3.4655021D-3,-6.5841147D-7,5.6218415D-11,-1.5014366D-15,
 30.02577D0
NO+
     30.00765D-3    2         984961.9485      3.D3
     2.42       1.         6          1
  1.000000         6.000000         3.000000         6.000000         2.000000
 0.0000000E+00
 0.0000000E+00    58025.33         85093.78         105107.5         105539.5
 0.0000000E+00
  3372.950
 28.24824D0,6.2350007D-3,-1.512119D-6,1.5423789D-10,-4.6051132D-15,
 34.92642D0
c.l.: ibet(l,k) ,l=1,.,is, k=1,.,ir:
 0 2 0 0 0 0 0 0
 0 1 0 0 1 0 0 0
 0 1 1 0 0 0 0 0
 0 1 0 1 0 0 0 0
 0 1 0 0 0 1 0 0
 0 1 0 0 0 0 1 0
 0 0 2 0 0 0 0 0
 0 0 1 0 0 1 0 0
 0 1 1 0 0 0 0 0
 0 0 1 1 0 0 0 0
 0 0 1 0 1 0 0 0
 0 0 1 0 0 0 1 0
 0 1 0 0 0 0 1 0
 0 0 1 0 0 0 1 0
 0 0 0 1 0 0 1 0
 0 0 0 0 1 0 1 0
 0 0 0 0 0 1 1 0
 0 0 0 0 0 0 2 0
 0 0 1 0 1 0 0 0
 0 1 0 0 0 1 0 0
 0 1 1 0 0 0 0 0
 1 0 0 0 0 0 0 1
```

Fig. 1: continued

```
c.l.: irnp(l,k) ,l=1,.,is, k=1,.,ir:
 0 1 0 0 2 0 0 0
 0 0 0 0 3 0 0 0
 0 0 1 0 2 0 0 0
 0 0 0 1 2 0 0 0
 0 0 0 0 2 1 0 0
 0 0 0 0 2 0 1 0
 0 0 1 0 0 2 0 0
 0 0 0 0 0 3 0 0
 0 1 0 0 0 2 0 0
 0 0 0 1 0 2 0 0
 0 0 0 0 1 2 0 0
 0 0 0 0 0 2 1 0
 0 1 0 0 1 1 0 0
 0 0 1 0 1 1 0 0
 0 0 0 1 1 1 0 0
 0 0 0 0 2 1 0 0
 0 0 0 0 1 2 0 0
 0 0 0 0 1 1 1 0
 0 0 0 0 0 1 1 0
 0 0 0 0 1 0 1 0
 0 0 0 0 0 0 2 0
 0 0 0 0 1 1 0 0
c.l.: rk1(k), rk2(k), rk3(k), k=1,.,ir:
 3.0000000E+15  -1.500000        1.132942E5
 1.4999999E+16  -1.500000        1.132942E5
 9.8999996E+14  -1.500000        1.132942E5
 9.8999996E+14  -1.500000        1.132942E5
 9.8999996E+14  -1.500000        1.132942E5
 9.8999996E+14  -1.500000        1.132942E5
 3.6000000E+15  -1.500000        5.939902E4
 2.0999999E+12  -0.500000        5.939902E4
 1.2000000E+15  -1.500000        5.939902E4
 1.2000000E+15  -1.500000        5.939902E4
 1.2000000E+15  -1.500000        5.939902E4
 1.2000000E+15  -1.500000        5.939902E4
 5.2000000E+15  -1.500000        7.551270E4
 5.2000000E+15  -1.500000        7.551270E4
 5.2000000E+15  -1.500000        7.551270E4
 5.2000000E+15  -1.500000        7.551270E4
 5.2000000E+15  -1.500000        7.551270E4
 5.2000000E+15  -1.500000        7.551270E4
  1000000.       0.500000        3.625576E3
 5.0000000E+07   0.000000        3.802827E4
 9.1000002E+18  -2.500000        6.501867E4
 1.8000000E+15  -1.500000        0.000000E0
c.l.: ithb(k), k=1,.,ir:
```

Fig. 1: continued

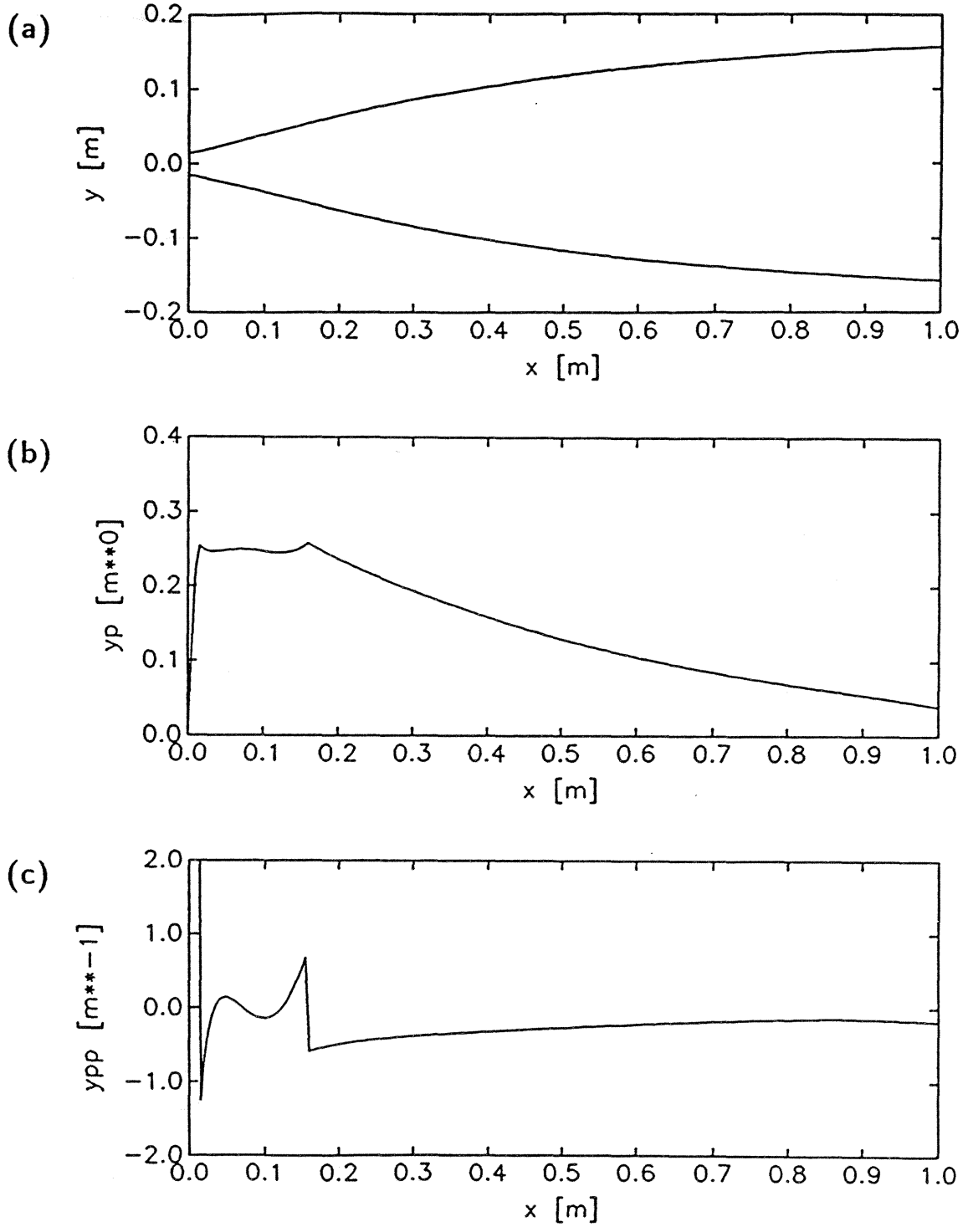

Fig. 2: Nozzle T5/100 of the GALCIT shock tunnel:
(a) nozzle contour
(b) first derivative of the radius
(c) second derivative of the radius

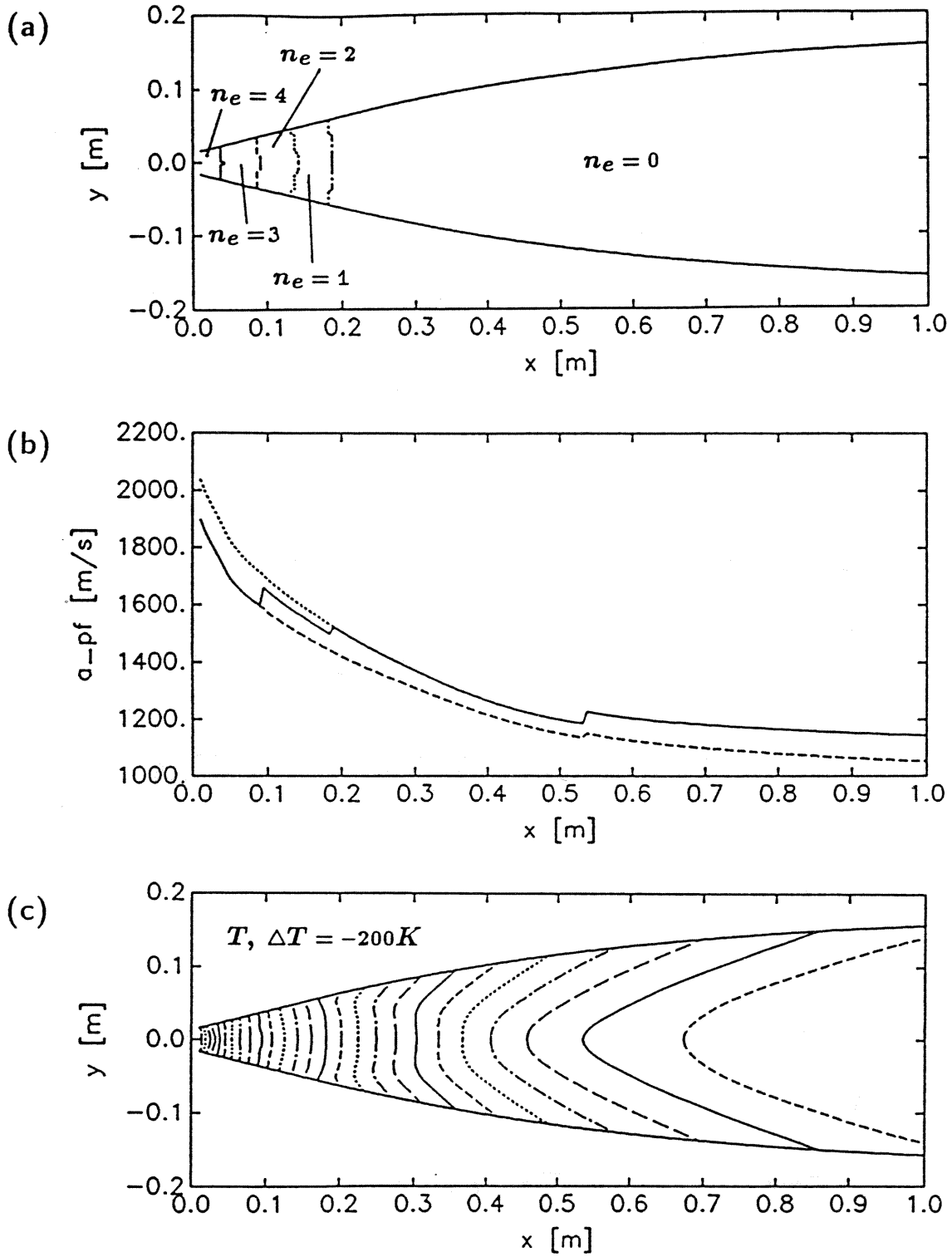

Fig. 3: Partial equilibrium flow, $\lambda_{crit} = 0.1m$ (standard case):
(a) contour lines of n_e, displaying regions of different degree of equilibrium
(b) sound speed along nozzle axis: a_{pf} (solid line), a_e (dashed line), a_f (dotted line)
(c) temperature contours: on the first upstream line $T = 7800K$

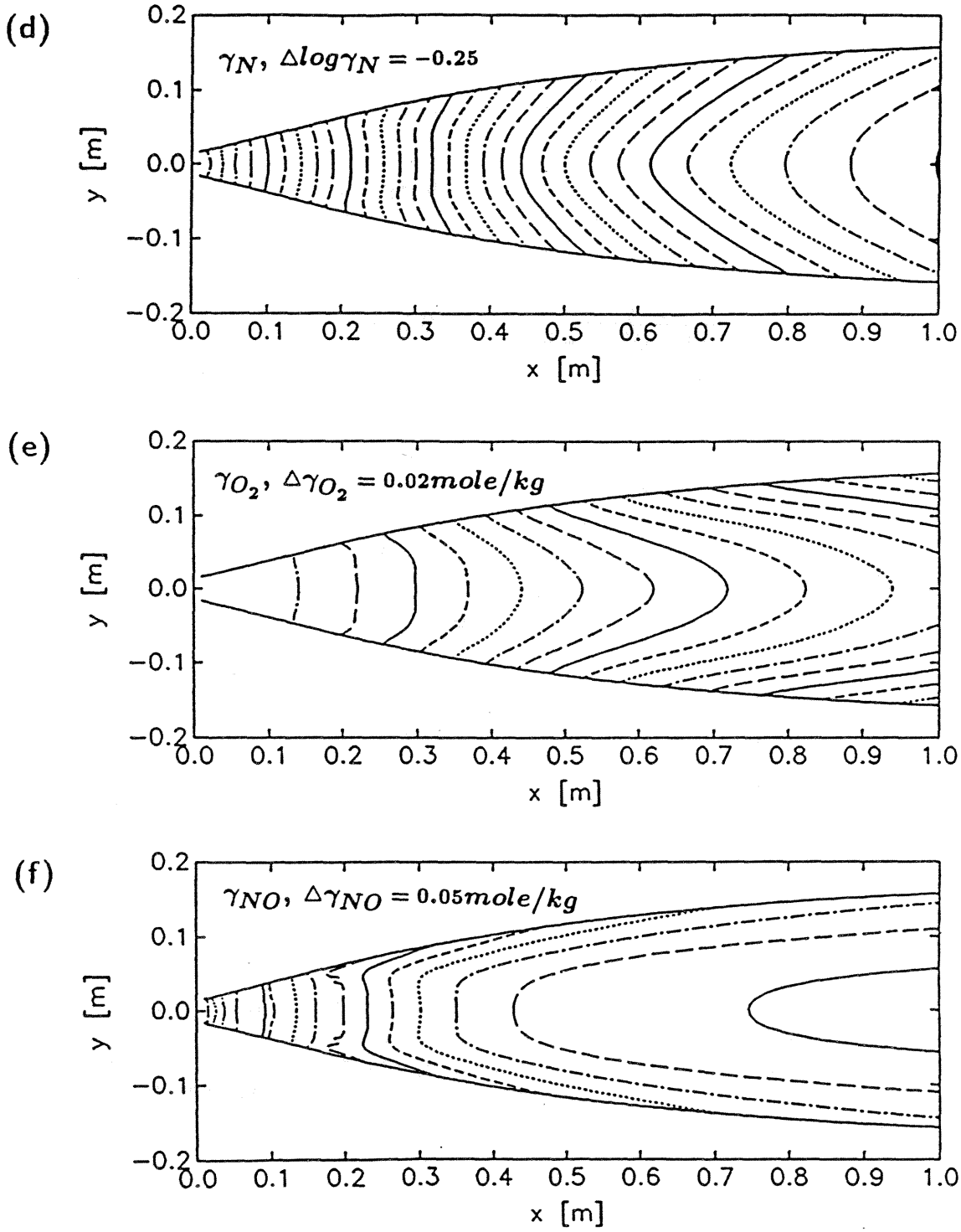

Fig. 3: Partial equilibrium flow (continued)
(d) γ_N contours: on the first upstream line $\gamma_N = 8.64 mole/kg$
(e) γ_{O_2} contours: on the first upstream line $\gamma_{O_2} = 0.062 mole/kg$
(f) γ_{NO} contours: on the first upstream line $\gamma_{NO} = 1.05 mole/kg$

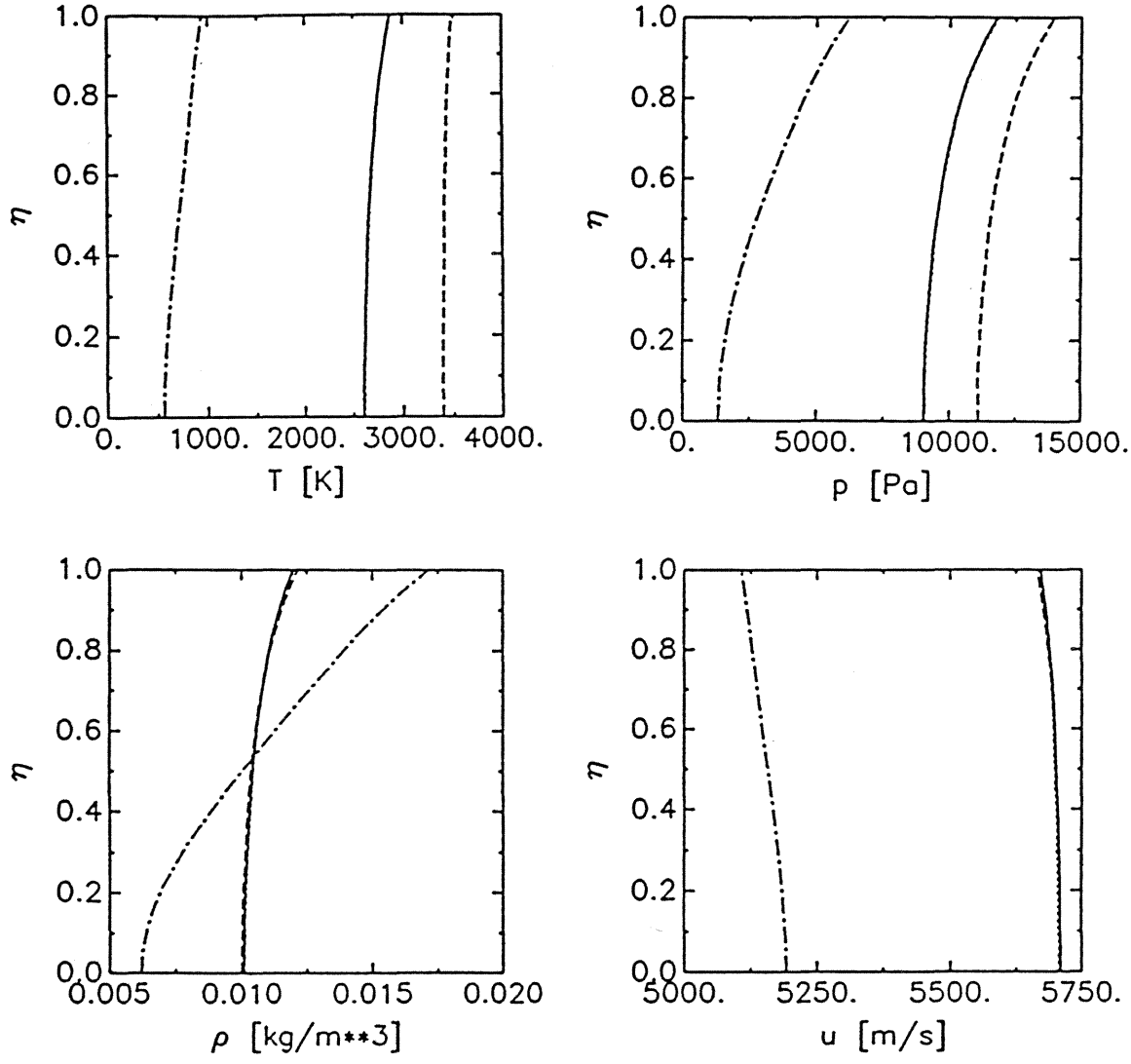

Fig. 4: Partial equilibrium flow, $\lambda_{crit} = 0.1m$ (standard case): state variables versus non-dimensional radius η at the nozzle exit (solid lines), comparison with nonequilibrium flow (dotted lines), equilibrium flow (dashed lines) and frozen flow (chain-dotted lines) [the partial equilibrium flow solution cannot always be distinguished from the nonequilibrium solution, further, the frozen flow solution is not always plotted]

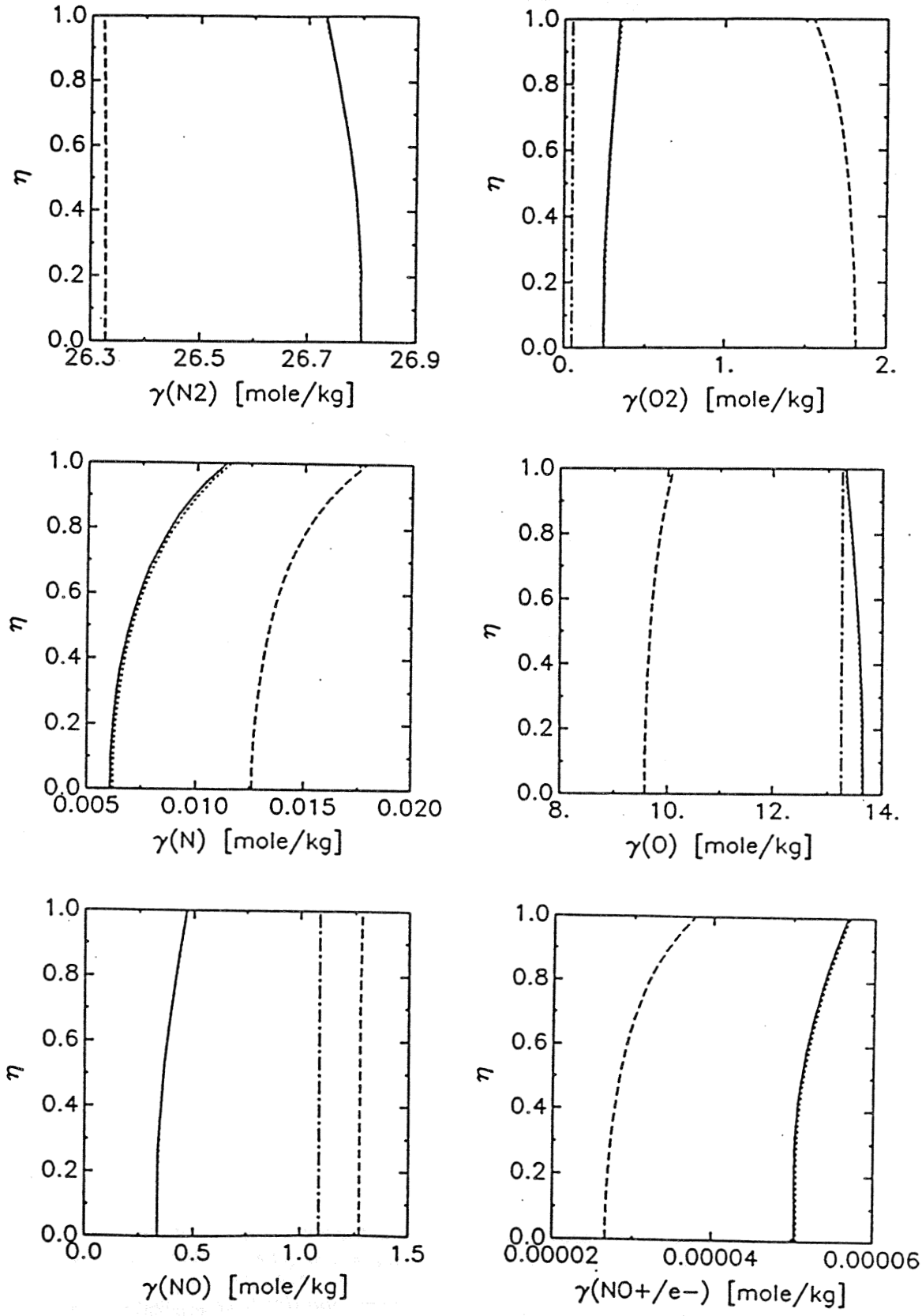

Fig. 4: Partial equilibrium flow, $\lambda_{crit} = 0.1m$ (standard case) continued

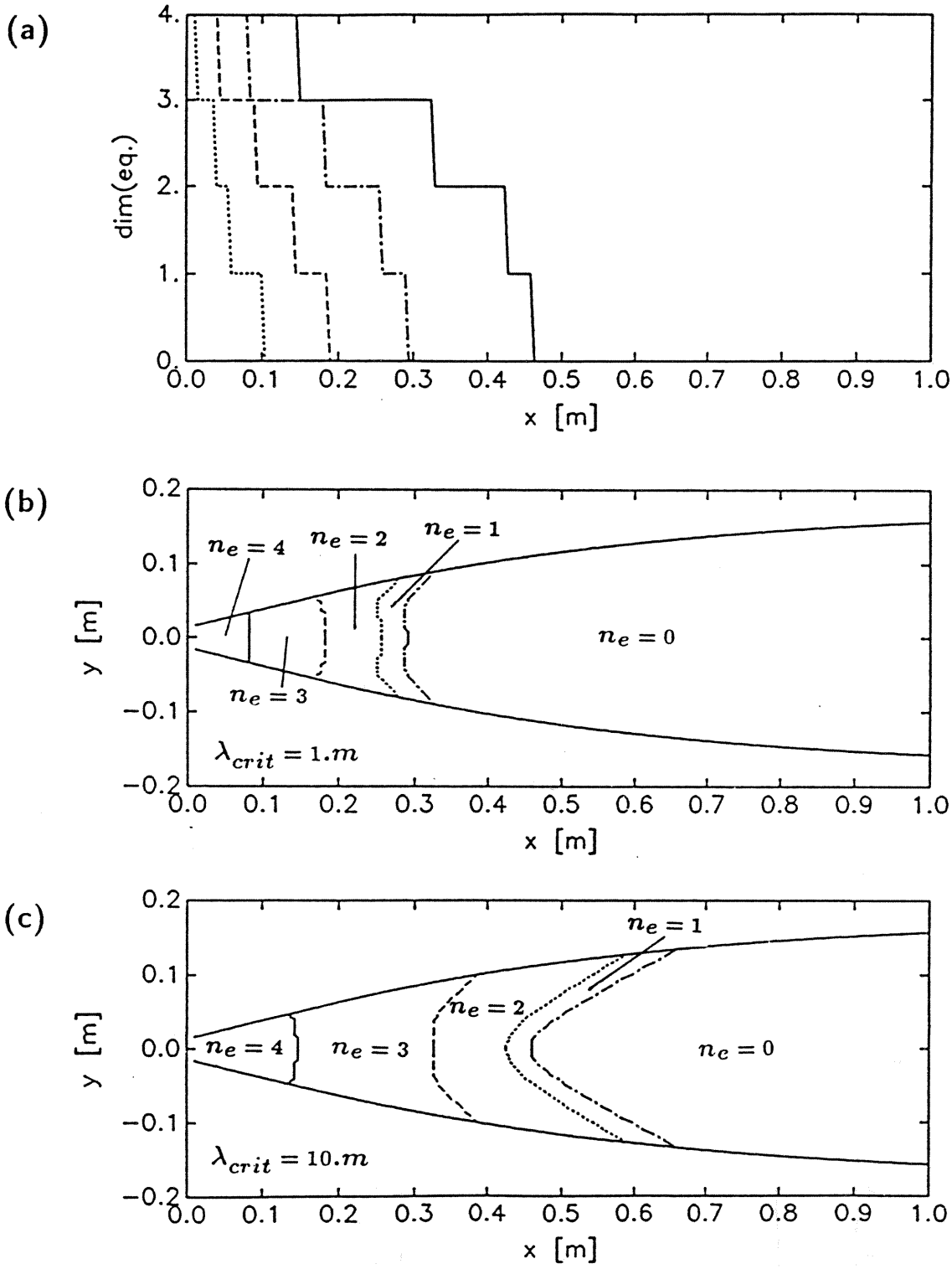

Fig. 5: Partial equilibrium flow with different λ_{crit}:
(a) dimension n_e of the equilibrium reaction subspace along nozzle axis, $\lambda_{crit} = 0.01m$ (dotted line), $\lambda_{crit} = 0.1m$ (dashed line), $\lambda_{crit} = 1.m$ (chain-dotted line), $\lambda_{crit} = 10.m$ (solid line)
(b) contour plot of n_e, displaying regions of different degree of equilibrium for the case of $\lambda_{crit} = 1.m$
(c) same as (b), this time for the case of $\lambda_{crit} = 10.m$

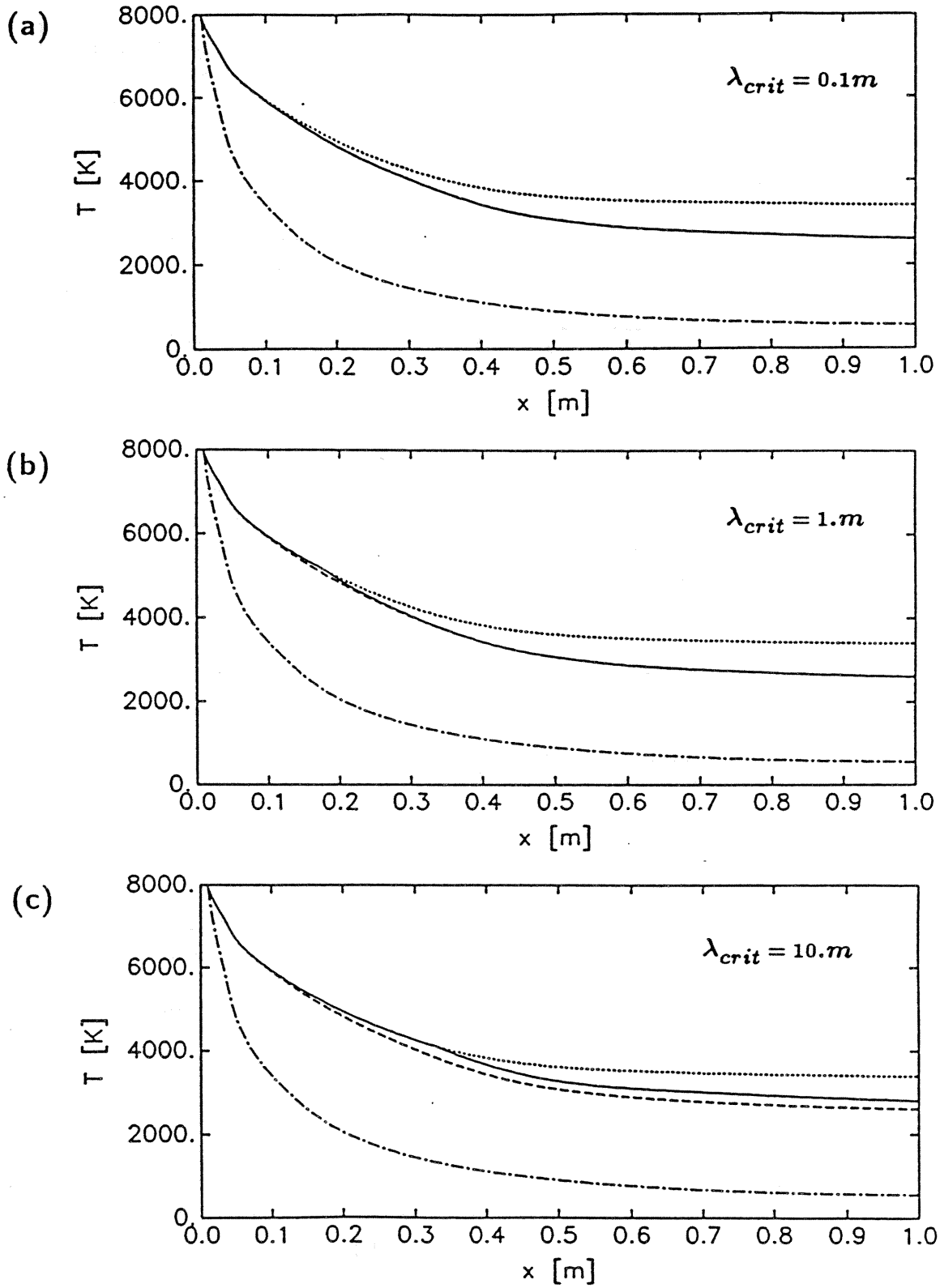

Fig. 6: Temperature along nozzle axis, comparison of partial equilibrium flow (solid line), equilibrium flow (dotted line), nonequilibrium flow (dashed line) and frozen flow (chain-dotted line): (a) $\lambda_{crit} = 0.1m$, (b) $\lambda_{crit} = 1.m$, (c) $\lambda_{crit} = 10.m$

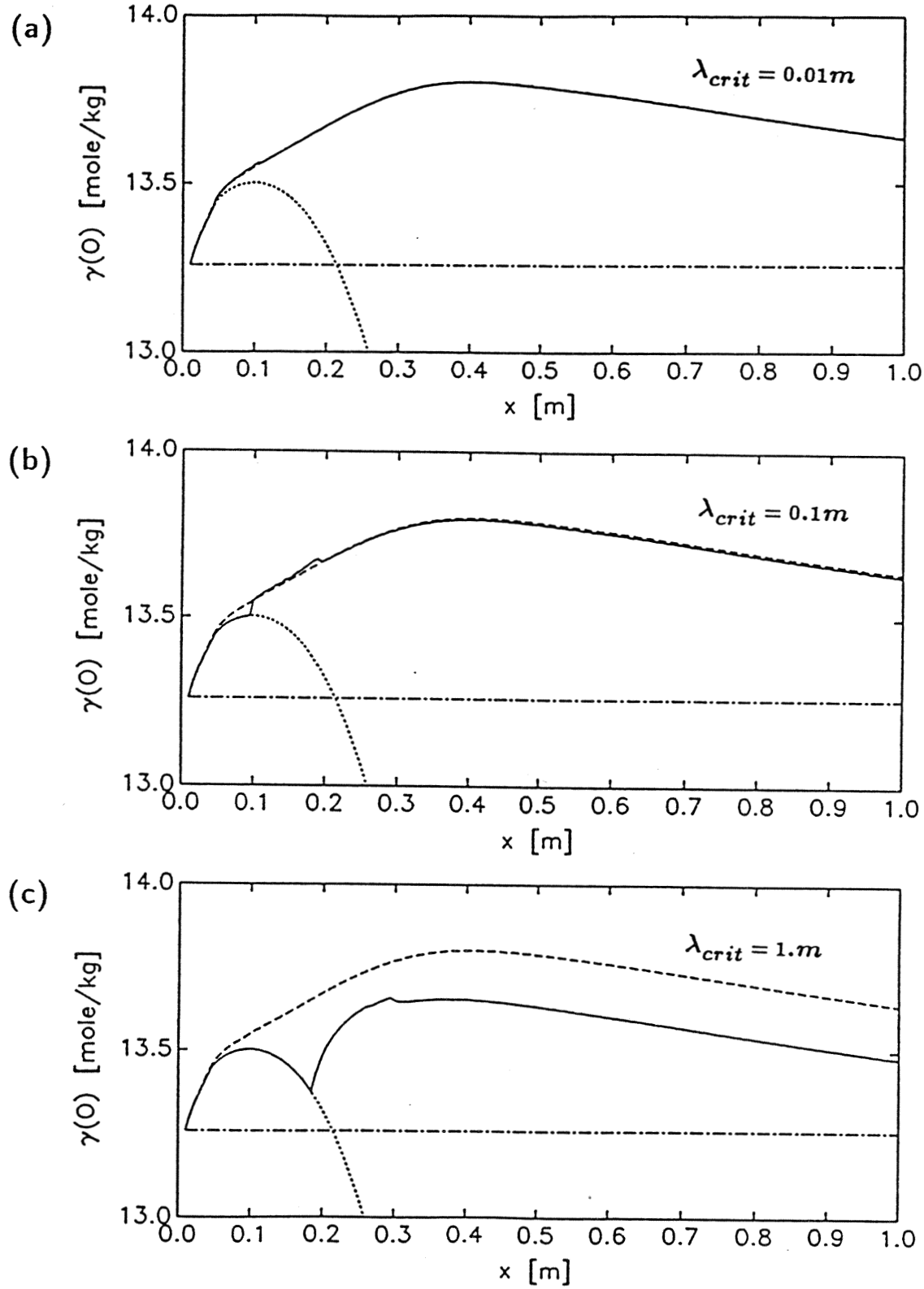

Fig. 7: Concentration γ_O of monatomic oxygen along nozzle axis, comparison of partial equilibrium flow (solid line), equilibrium flow (dotted line), nonequilibrium flow (dashed line) and frozen flow (chain-dotted line): (a) $\lambda_{crit} = 0.01m$, (b) $\lambda_{crit} = 0.1m$, (c) $\lambda_{crit} = 1.m$

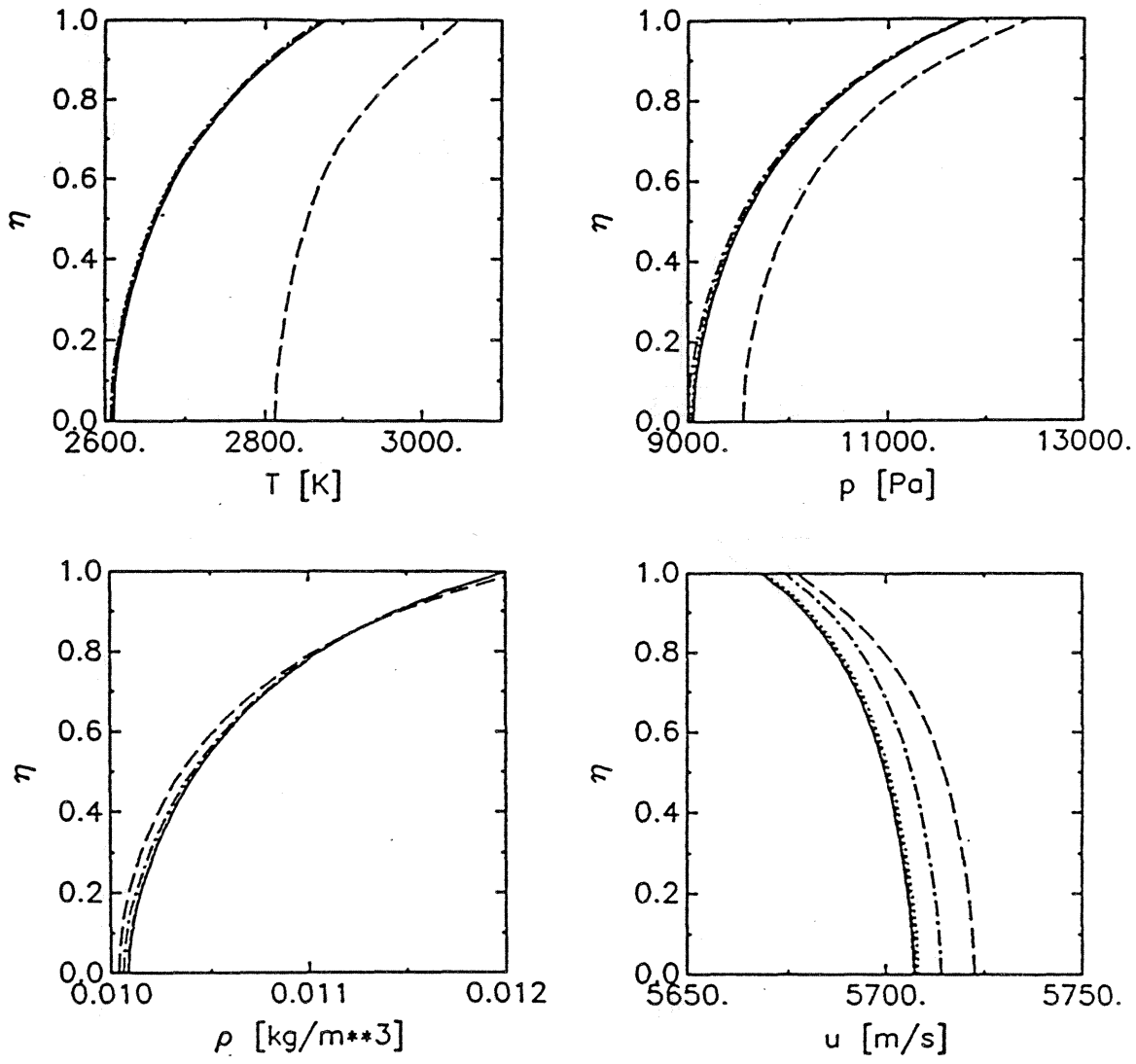

Fig. 8: State variables versus non-dimensional radius η at the nozzle exit: comparison of nonequilibrium flow (solid lines) and partial equilibrium flows with $\lambda_{crit} = 0.01m$ (short-dashed lines), $\lambda_{crit} = 0.1m$ (dotted lines), $\lambda_{crit} = 1.m$ (chain-dotted lines), $\lambda_{crit} = 10.m$ (long-dashed lines)

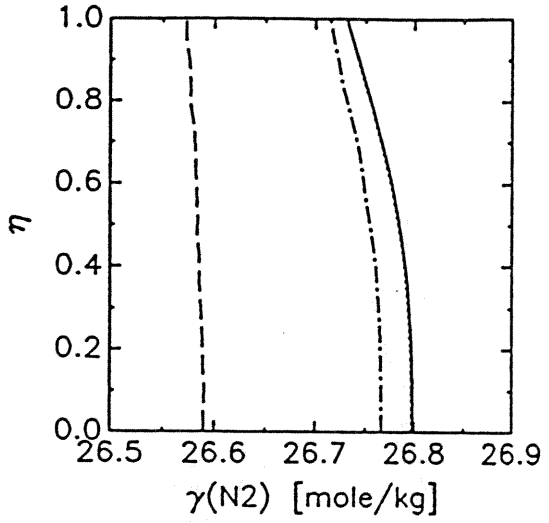

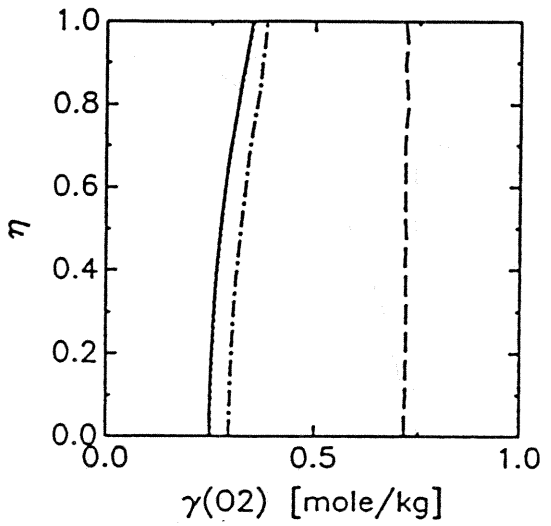

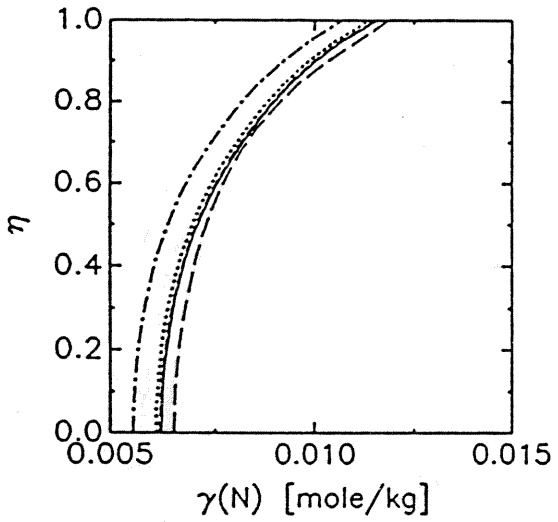

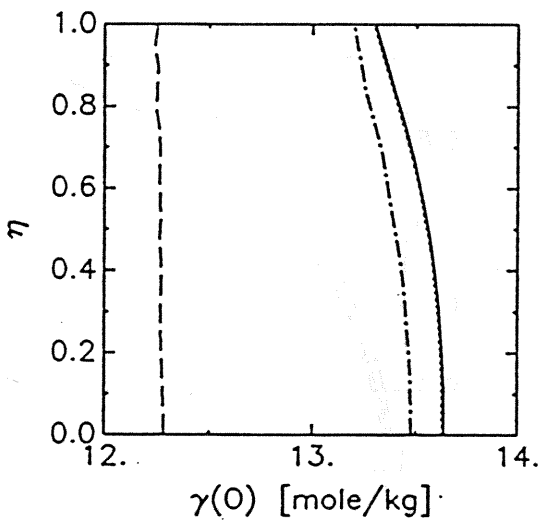

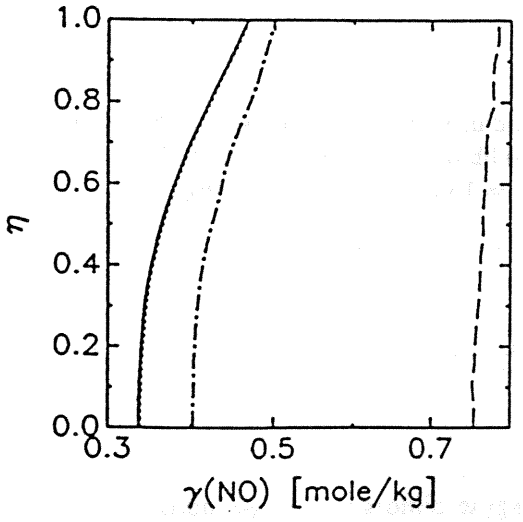

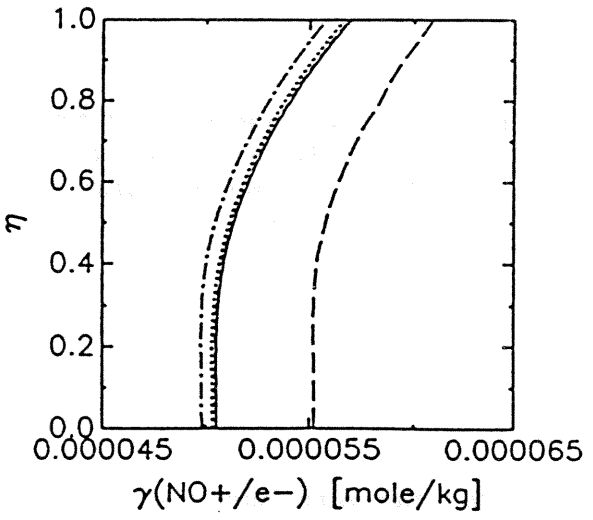

Fig 8.: continued

```
Nozzle: T5/100 (GALCIT), usual throat
expansion of an ideal gas
c.l. (=comment line): names of output data files
yrigas1
yrigas2
c.l.: job id. no.,iequil,ifrzn,i2d,iout
   106  0 0 -1 1
c.l.: xu, xd, mmax, nmax
     .01   1.   200    20
c.l.: T0, p0
   9000.       2.00E+07
c.l.: Tv
     0.D3
c.l.: ichkd, rminlt
     1 2.
c.l.: dcrit
    1.D-2
c.l.: ic, is, ir
    1       2         0
c.l.: indep. species: symb(i), g0(i), i=1,.,ic
 O2 1.D0
c.l.: alph(j,i), j=ic+1,.,is, i=1,.,ic:
 .5
c.l.: thermodynamic properties of (is) species:
 O2
     32.000D-3   2       0.     -3.D3
     2.07    2.       1        0
 2.
 0.
 0.
  O
     16.000D-3    1      246857.841E+1       -3.D3
     1.       1.       1        0
 2.
 0.
 0.
c.l.: ibet(l,k) ,l=1,.,is, k=1,.,ir:
c.l.: irnp(l,k) ,l=1,.,is, k=1,.,ir:
c.l.: rk1(k), rk2(k), rk3(k), k=1,.,ir:
c.l.: ithb(k), k=1,.,ir:
```

Fig. 9: Input data file for the program Surf as used in the ideal gas computation

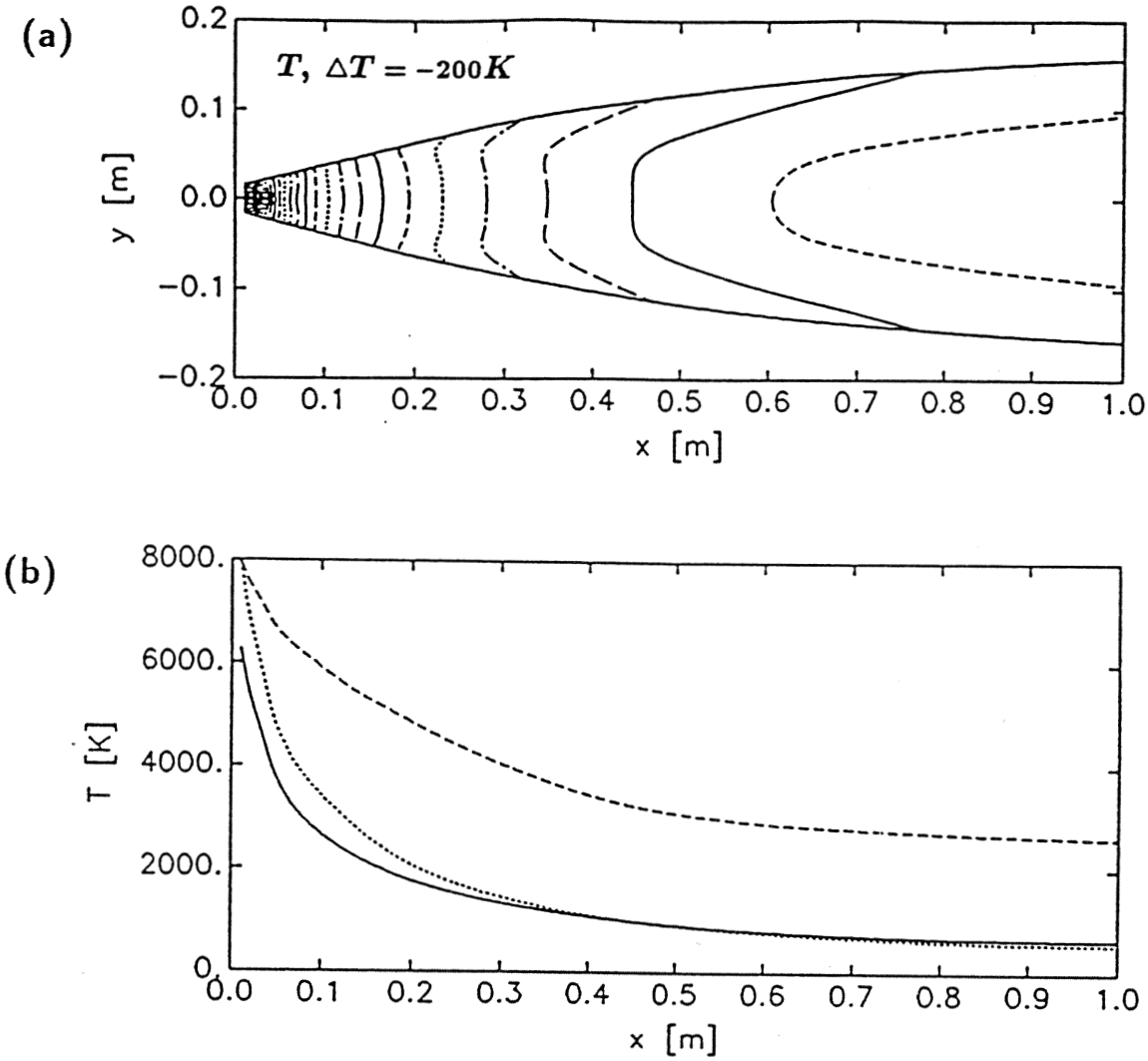

Fig. 10: Ideal gas flow:
(a) temperature contours: on the last downstream line $T = 800K$
(b)temperature along nozzle axis, comparison with frozen flow (dotted line) and partial equilibrium flow, $\lambda_{crit} = 0.1m$, (dashed line)

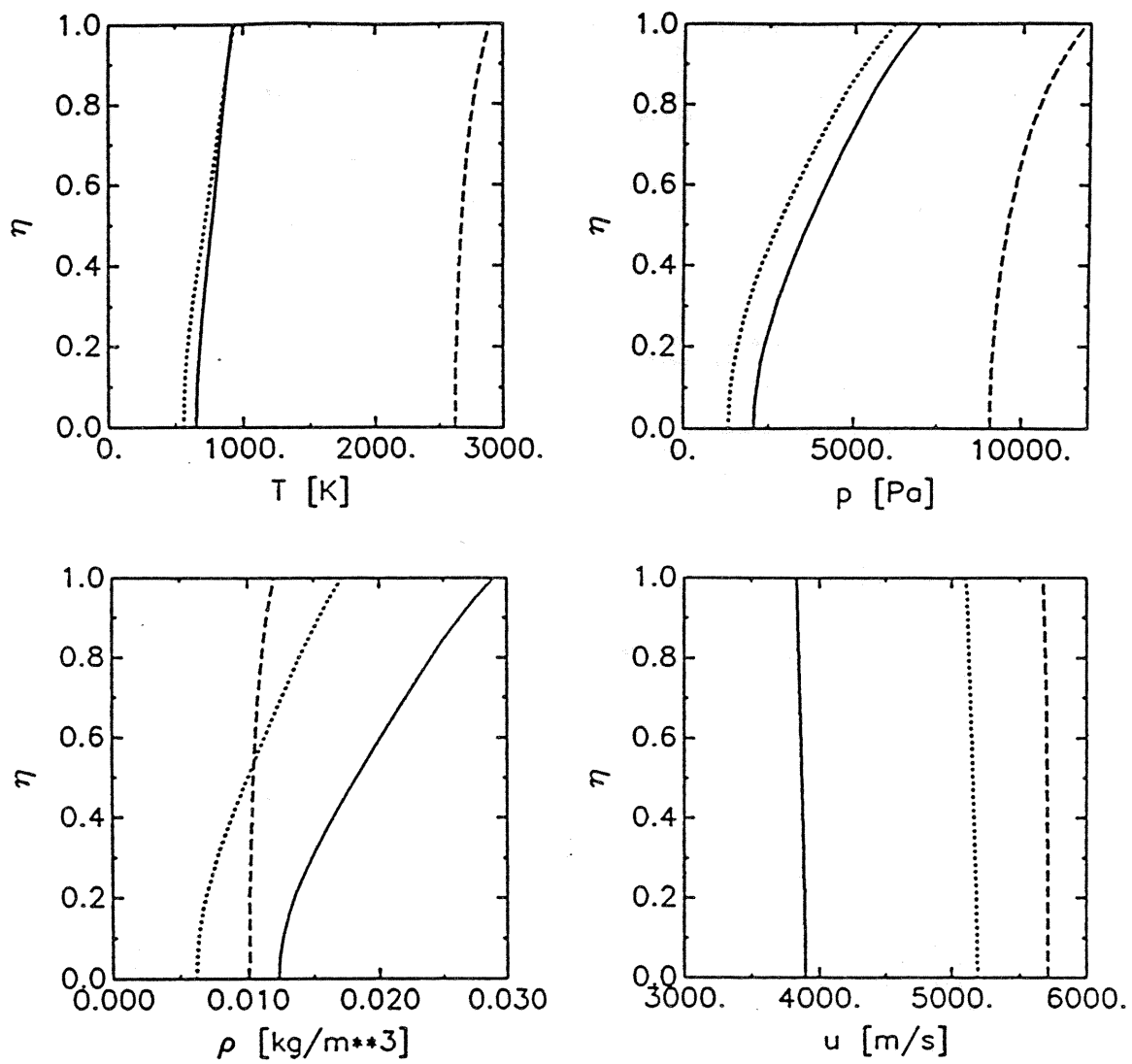

Fig. 11: Ideal gas flow, state variables versus non-dimensional radius at the nozzle exit (solid lines), comparison with partial equilibrium flow, $\lambda_{crit} = 0.1m$, (dashed lines) and frozen flow (dotted lines)

```
      subroutine inicond
c   modified version: the initial conditions at different eta-postions
c   (but constant x_u) are obtained by approximating the initial data at
c   different eta by an equilibrium solution which corresponds to different
c   cross sectional areas. At eta = 0 the assumed cross section equals the
c   actual cross section of the nozzle considered.
c
c   This subroutine determines the initial conditions for the calculation
c   of a 2-dimensional nozzle flow at x=x_u by using the solution of the
c   1-dimensional case. The initial solution is stored in twod(n,i),
c   n=1,...nmax, i=1,...,4+is-ic. The 1-D solution must be provided in
c   oned(m,i), m=1,...,mmax.
c
      implicit real*8(a-h,o-z)
c   parameter for array declarations:
      parameter (icm=10,ism=25,idscm=15,i4dscm=19,irm=100)
      parameter (mmaxm=200,nmaxm=25)
      parameter (ifem=10,ifvm=4)
c
      common /mp/iequil,ifrzn,i2d
      common /const1/ic,is,idsc,i4dsc
      common /var1/p,rho,g(ism),t
      common /var3/oned(mmaxm,i4dscm),twod(nmaxm,i4dscm)
      common /stgntn/t0,p0
      common /geom/xu,xd,mmax,nmax,ip
      data pi/3.14159/
c   geometry at x=xu:
      xusave=xu
      x=xu
      call geomtr(x,ym,yp,dymdx,dypdx,d2ymdx,d2ypdx)
      ypm=yp-ym
      dy=ypm/(nmax-1.)
c   approximate two-dimensional initial conditions by one-dimensional
c   solution:
      do 20, n=nmax,1,-1
c   determine one-dimensional equilibrium (i2d=1) or frozen (i2d=-1) flow
c   solution at x=xu:
      t=t0
      p=p0
      xu=xusave*(1.+(1.-cos(pi/2.*float(n-1)/float(nmax-1)))*.5)
      inic=1
      if(i2d.eq.1) then
        call equil(inic)
      else
        call frzn(inic)
      end if
c   total velocity (=t1):
      t1=oned(1,1)
      y=ym+(n-1)*dy
      t2=((yp-y)*dymdx+(y-ym)*dypdx)/ypm
      twod(n,1)=t1/sqrt(1.+t2**2)
      twod(n,2)=twod(n,1)*t2
      twod(n,3)=oned(1,3)
      twod(n,4)=oned(1,4)
      do 21, l=1,idsc
21    twod(n,4+l)=oned(1,4+l)
20    continue
      xu=xusave
      return
      end
```

Fig. 12: Modified version of subroutine inicond as used in computations with different initial conditions

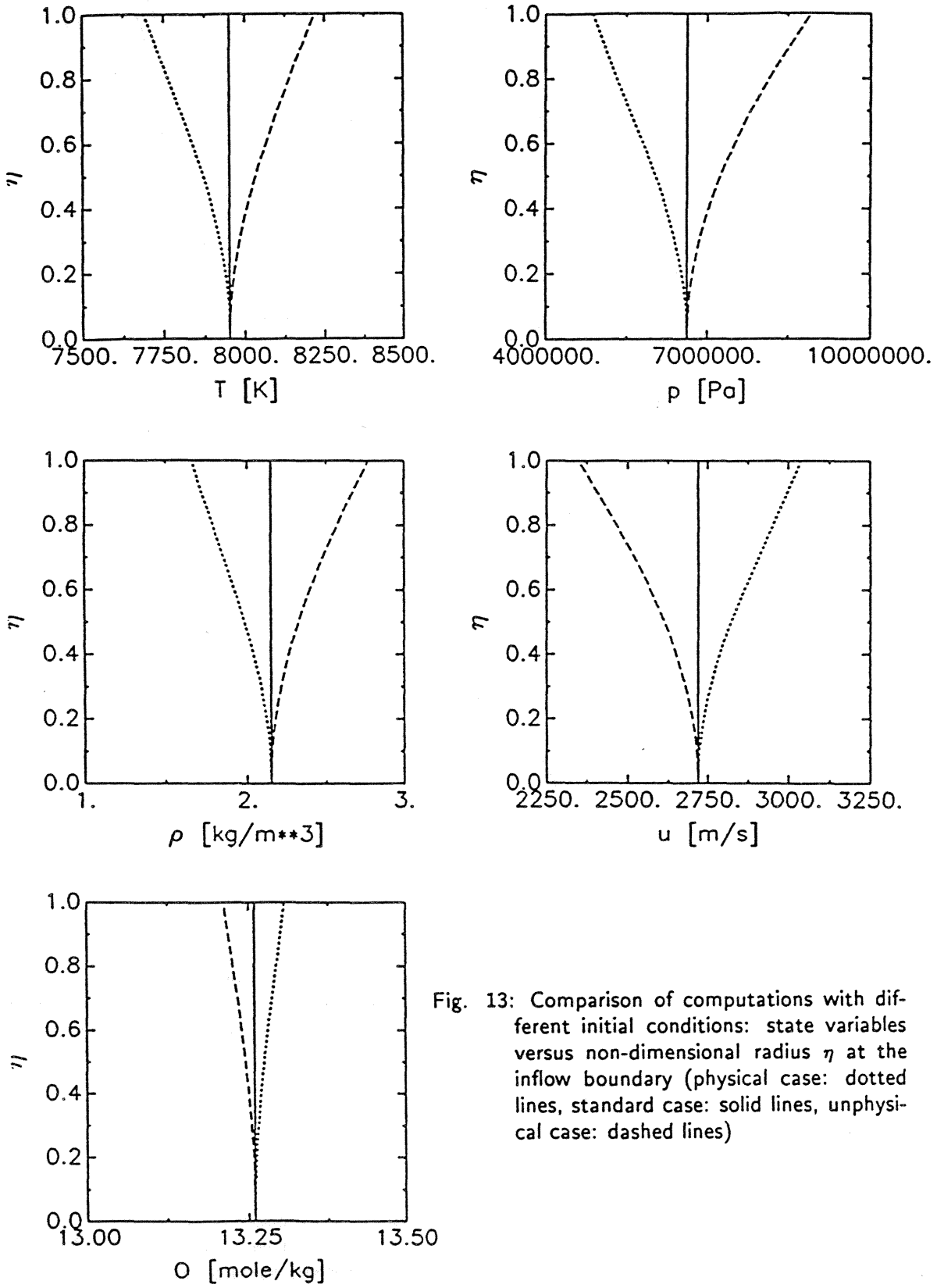

Fig. 13: Comparison of computations with different initial conditions: state variables versus non-dimensional radius η at the inflow boundary (physical case: dotted lines, standard case: solid lines, unphysical case: dashed lines)

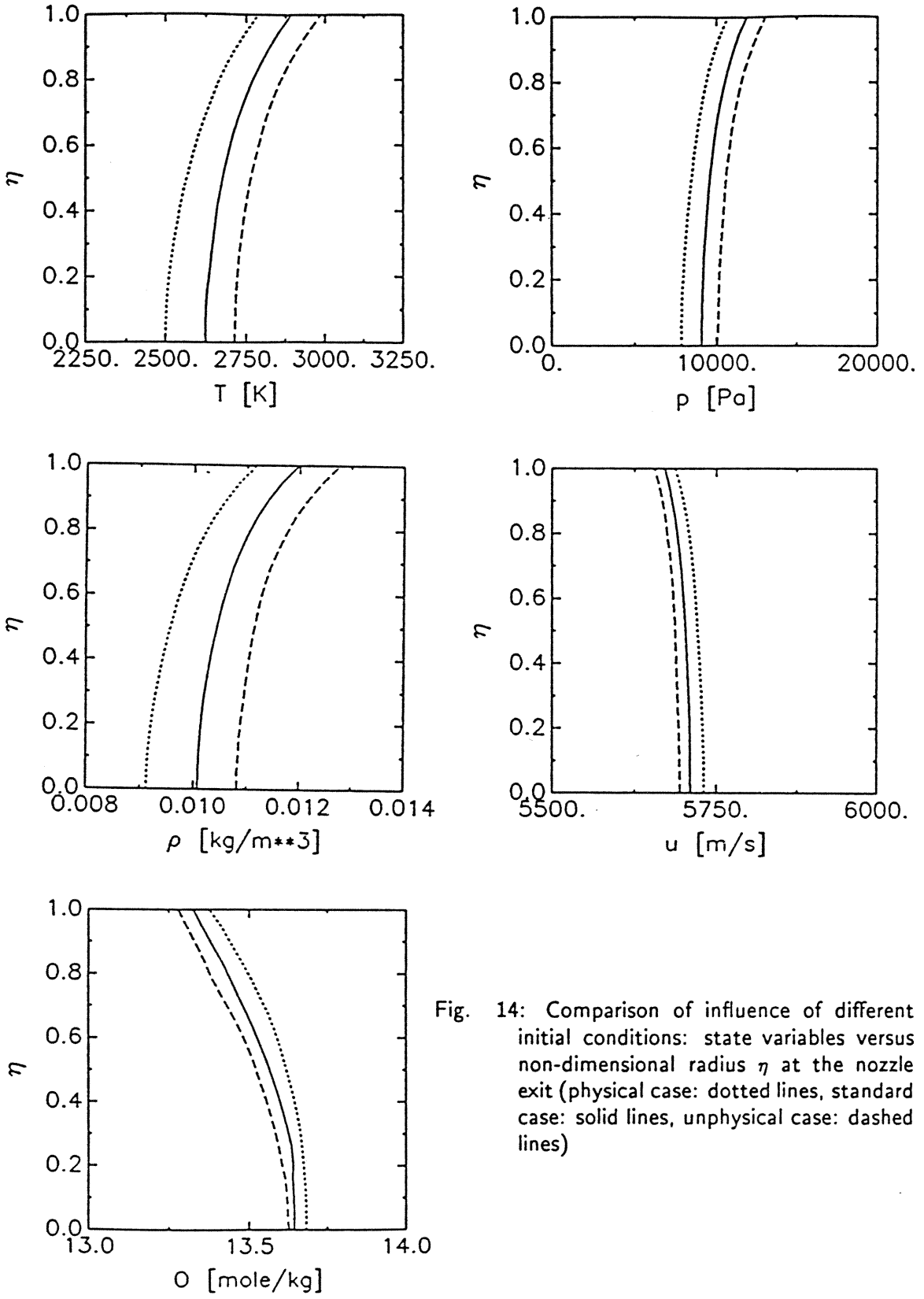

Fig. 14: Comparison of influence of different initial conditions: state variables versus non-dimensional radius η at the nozzle exit (physical case: dotted lines, standard case: solid lines, unphysical case: dashed lines)

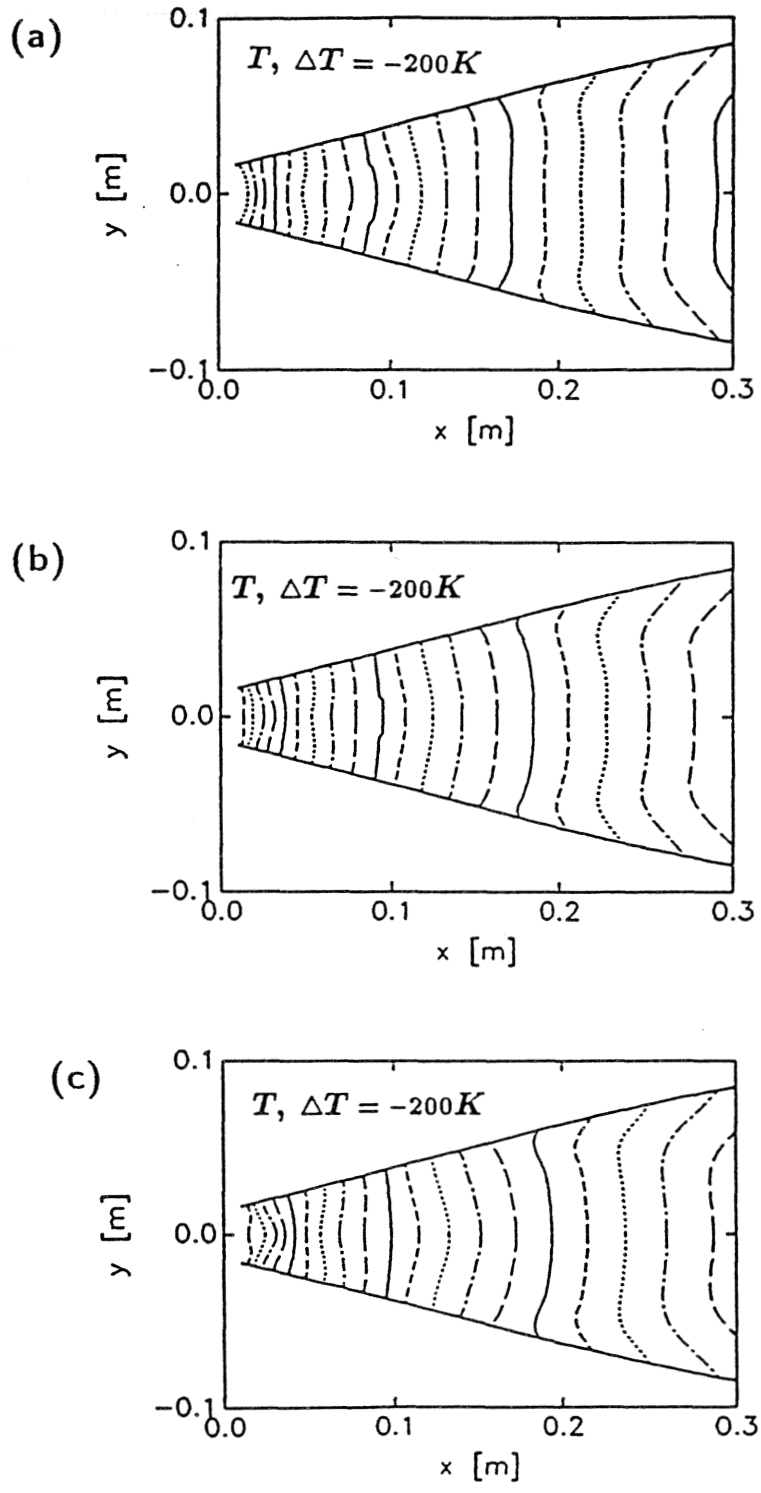

Fig. 15: Different initial conditions: temperature contours
(a) physical case: on the first upstream line $T = 7600K$
(b) standard case: on the first upstream line $T = 7800K$
(c) unphysical case: on the first upstream line $T = 7800K$

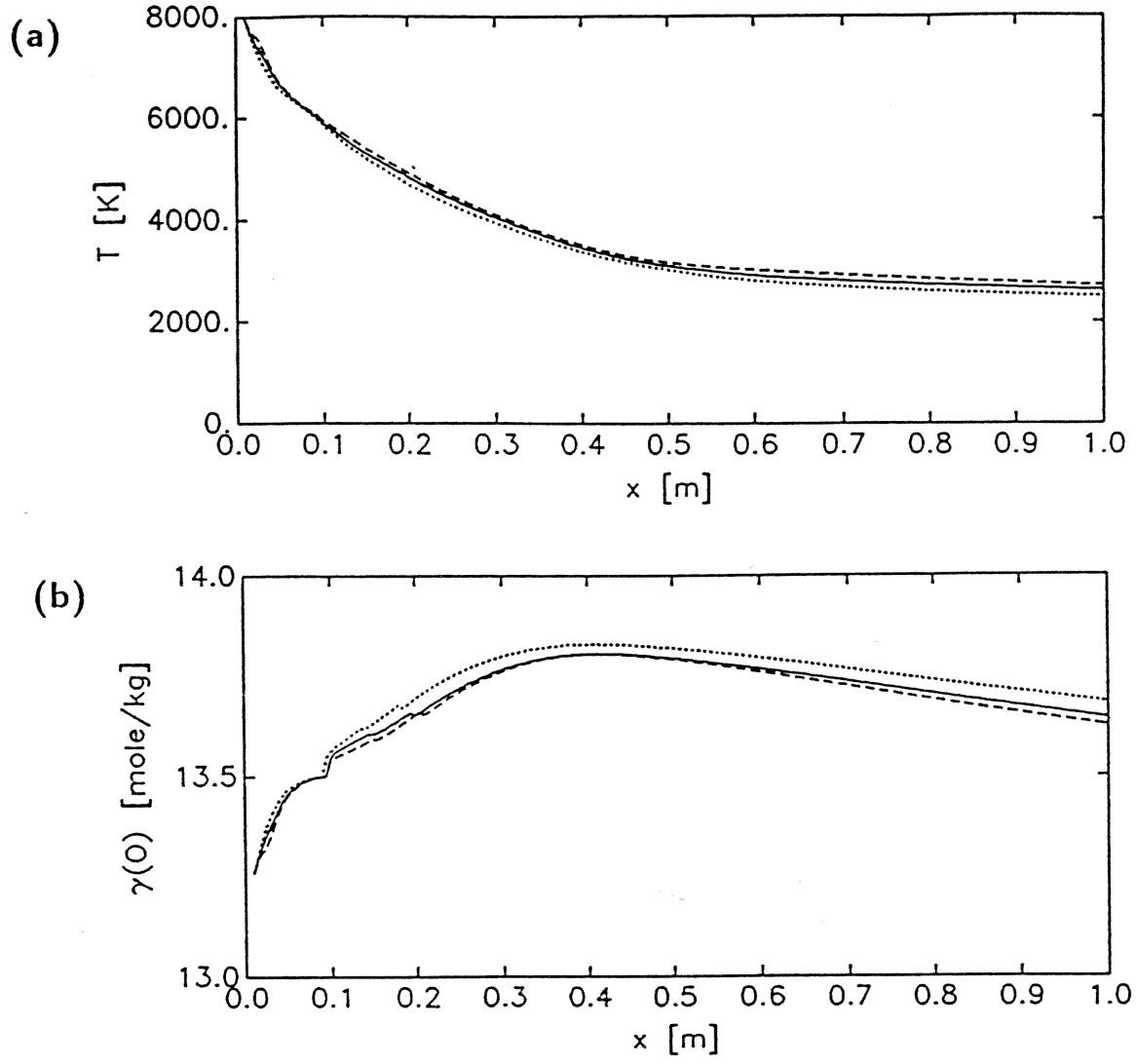

Fig. 16: Different initial conditions: physical case (dotted line), standard case (solid line), unphysical case (dashed line)
(a) temperature along nozzle axis
(b) concentration γ_O along nozzle axis

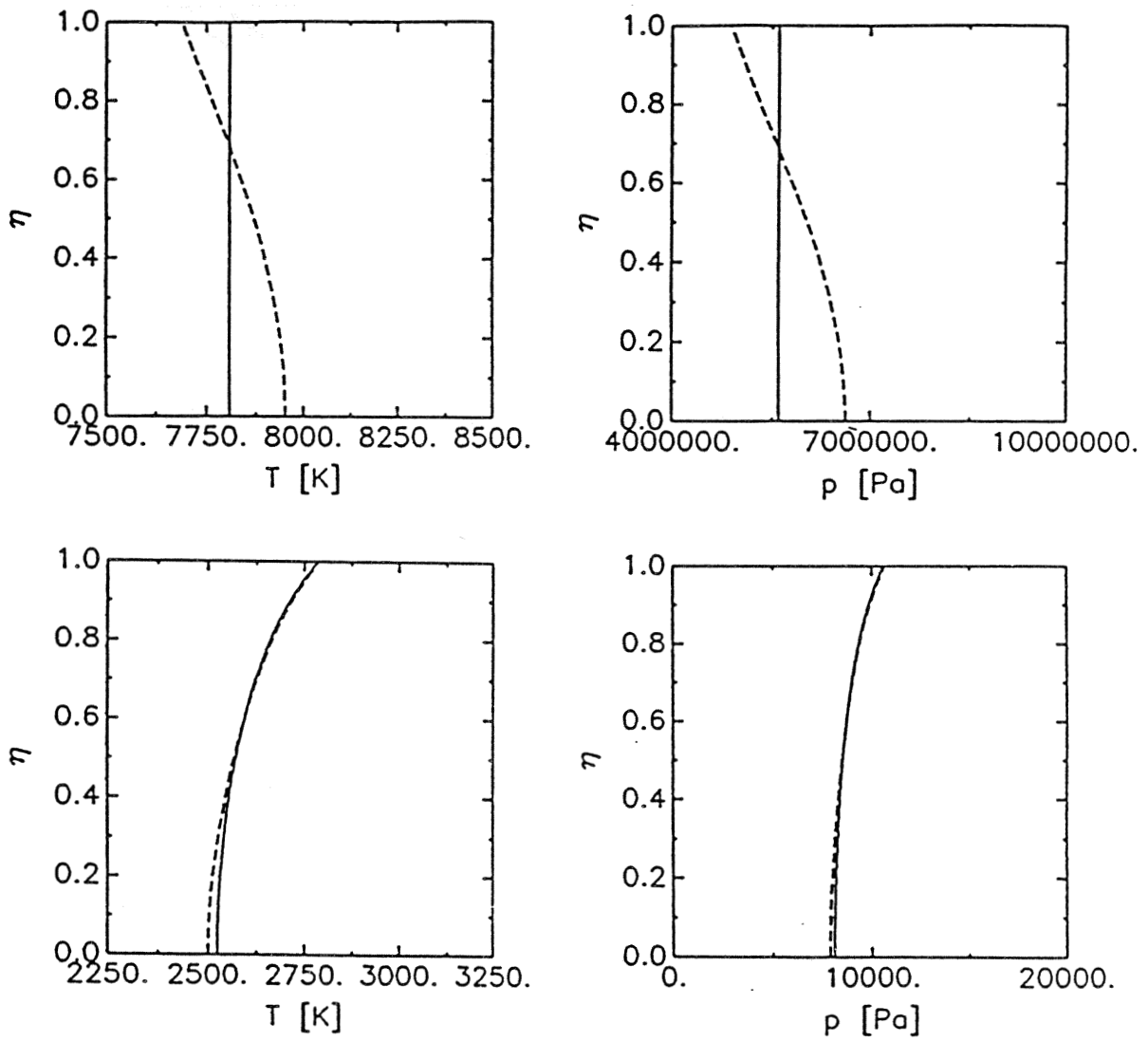

Fig. 17: Different initial conditions but same energy flux at inflow boundary: temperature and pressure versus non-dimensional radius η:
(a) at inflow boundary ($x = x_u$)
(b) at nozzle exit ($x = x_d$)

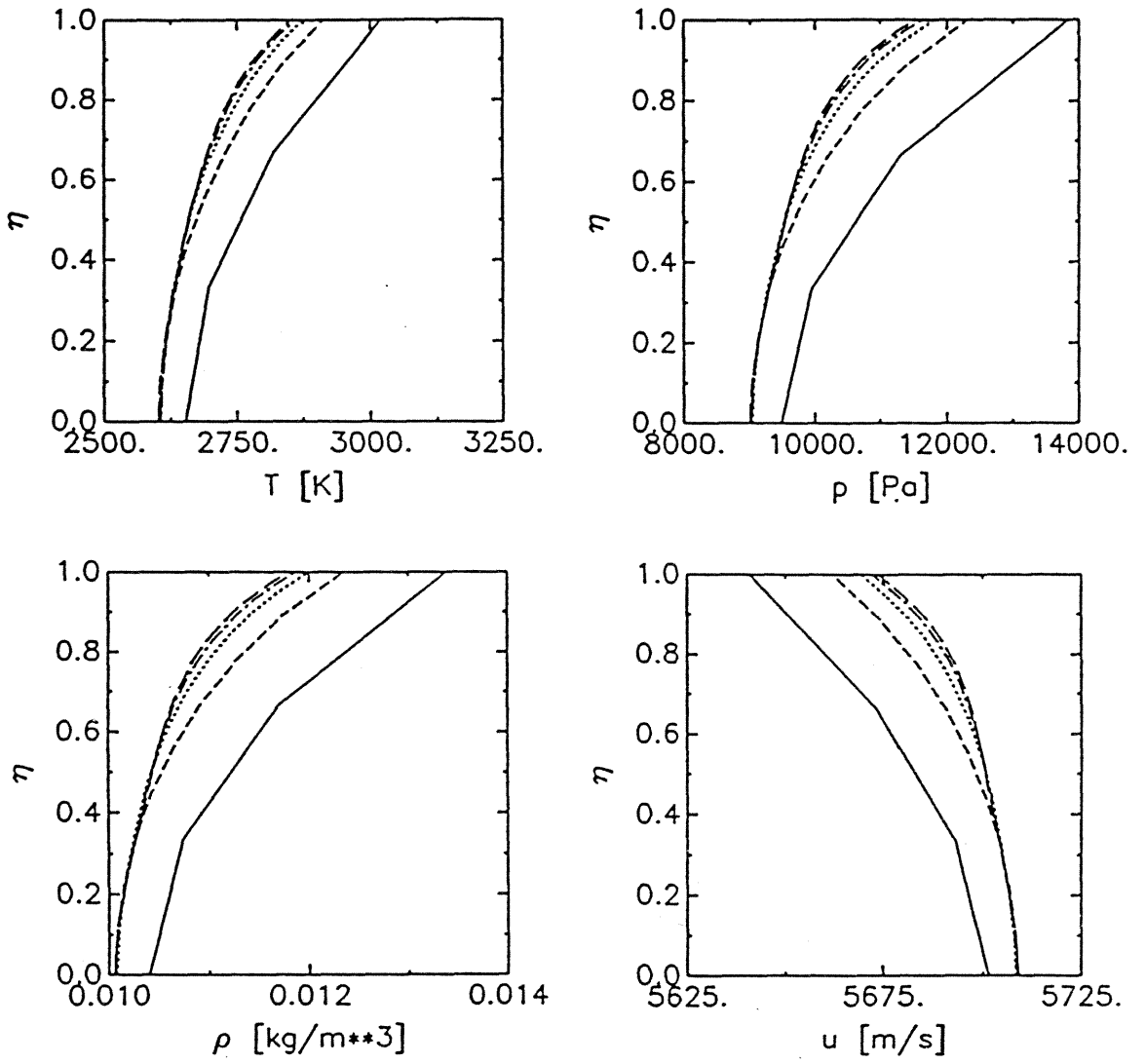

Fig. 18: Different number n_{max} of lines (standard case): state variables versus non-dimensional radius η at the nozzle exit (n_{max} = 4: solid lines, n_{max} = 10: short-dashed lines, n_{max} = 20: dotted lines, n_{max} = 30: chain-dotted lines, n_{max} = 40: long-dashed lines)

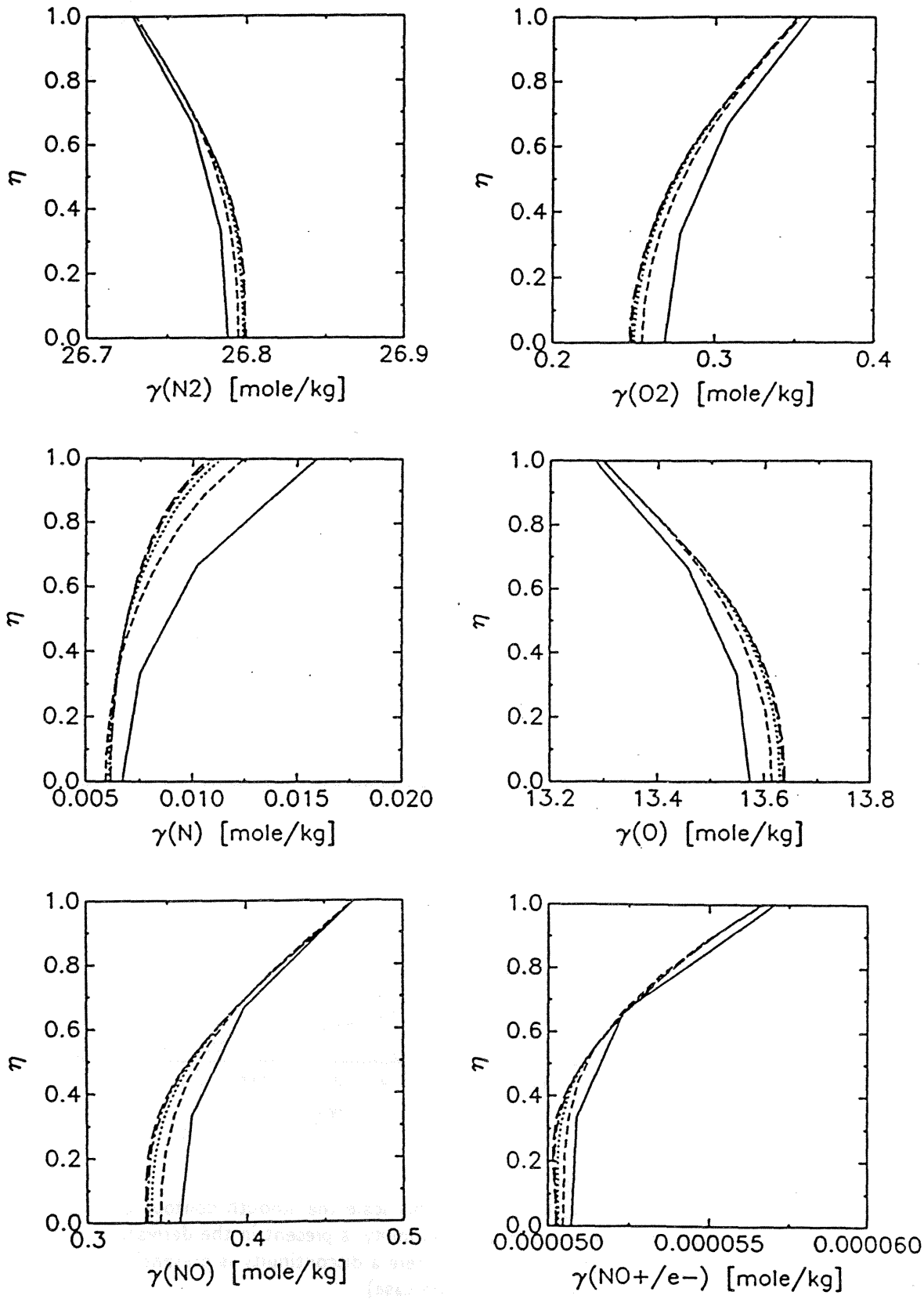

Fig. 18: different number n_{max} of lines (standard case) (continued)

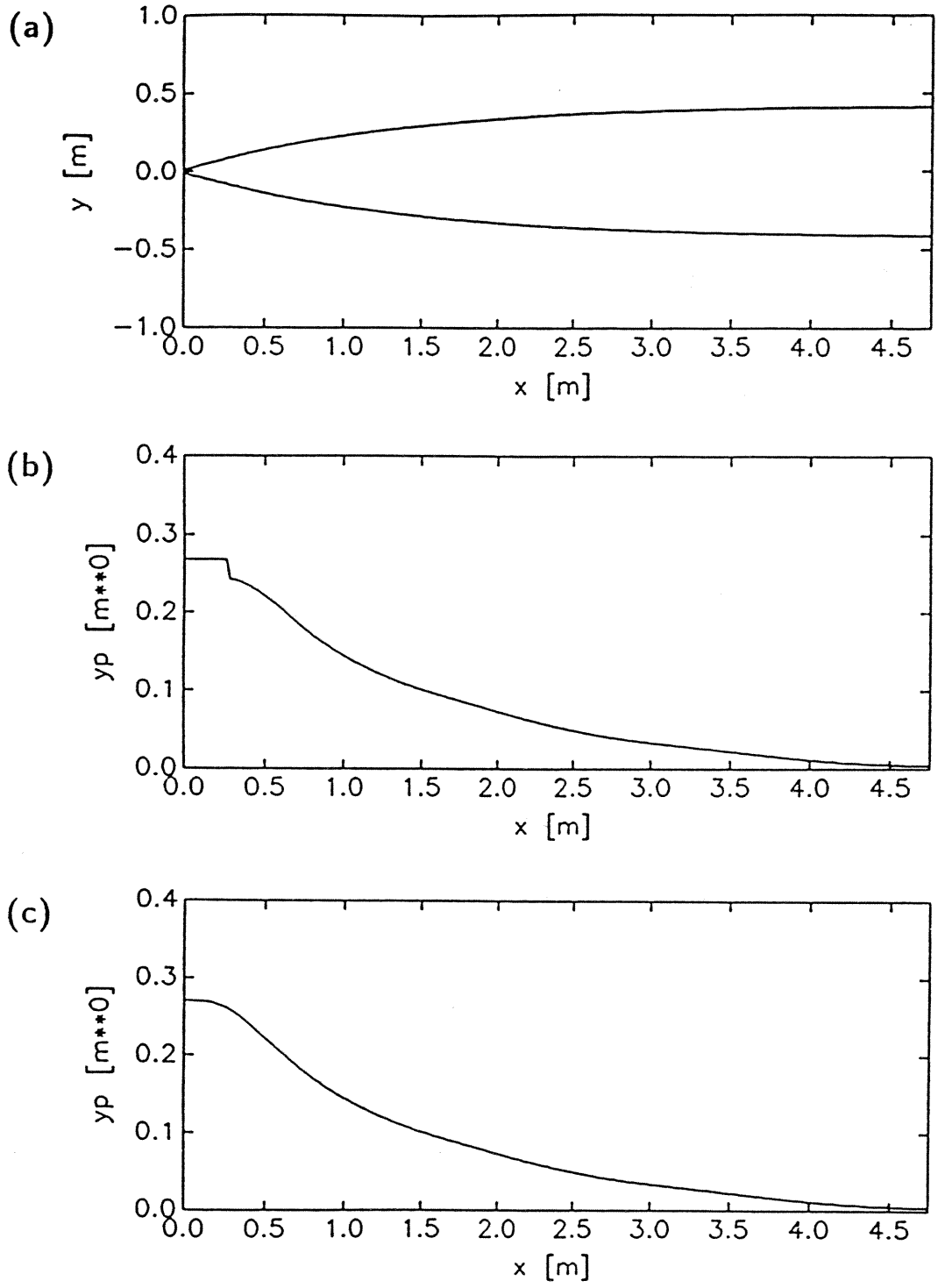

Fig. 19: Nozzle of the HEG shock tunnel:
(a) nozzle contour (smooth case): on this scale the smooth contour cannot be distinguished from the one in which a discontinuity is present in the derivative of the radius
(b) first derivative of the radius (case where a discontinuity is present)
(c) first derivative of the radius (smooth case)

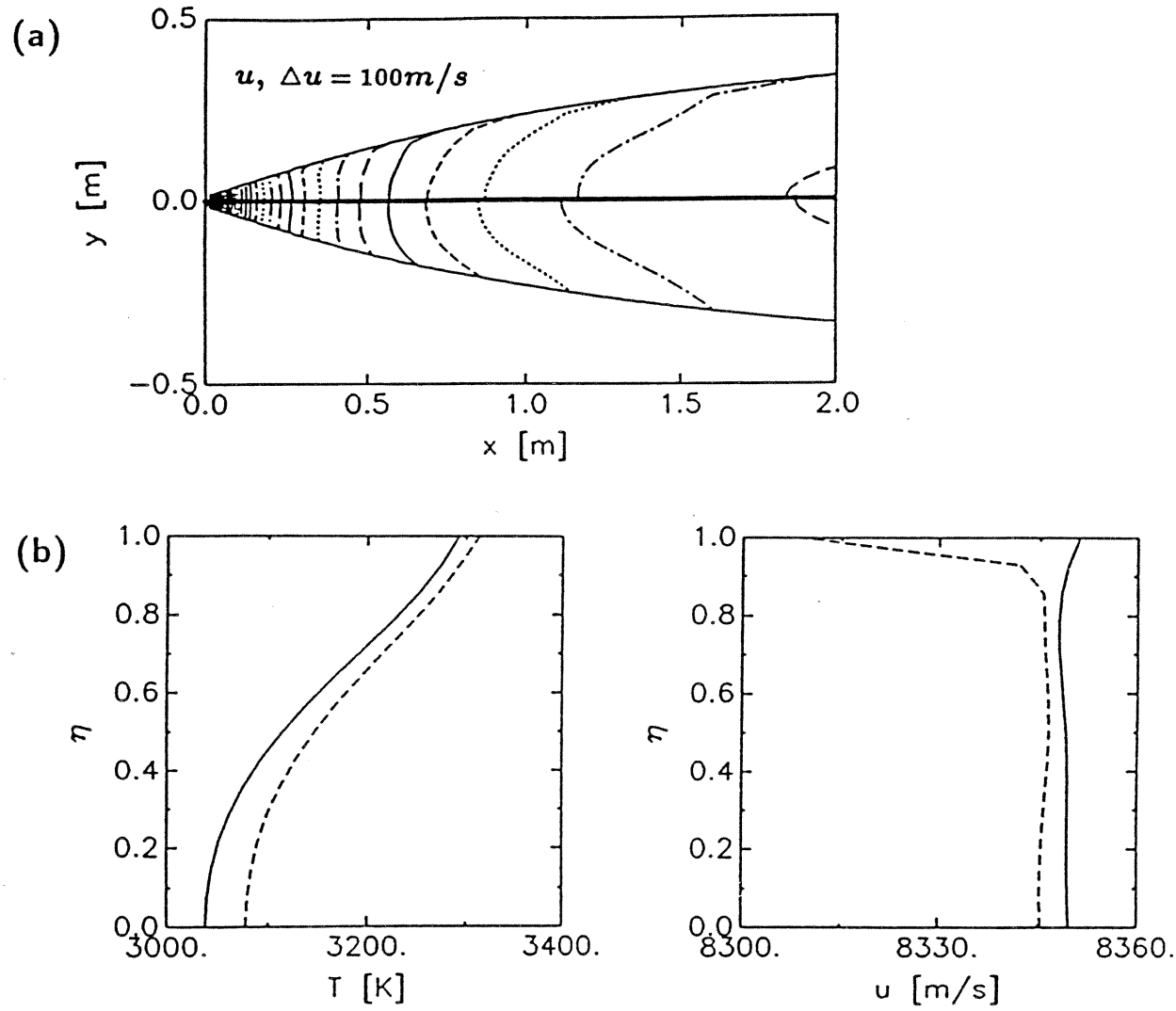

Fig. 20: Comparison of results obtained by a computation of a flow through two different versions of the nozzle of the HEG shock tunnel:
(a) velocity contours (section showing upstream part of nozzle), upper half: case in which a discontinuity is present in the derivative of the radius, lower half: smooth case, on the last downstream line $u = 8300m/s$
(b) temperature and total velocity versus non-dimensional radius at the nozzle exit: smooth case (solid lines), case in which a discontinuity is present in the derivative of the radius (dashed lines)

References

Amsden, A. A., Ramshaw, J. D., O'Rourke, P. J. and Dukowicz, J. K. (1985) KIVA: A Computer Program for Two- and Three-Dimensional Fluid Flows with Chemical Reactions and Fuel Sprays. Los Alamos National Laboratory Rep. No. LA–10245-MS

Dongarra, J. J., Bunch, J. R., Moler, C. B., Stewart, G. W. (1979) LINPACK User's Guide. SIAM, Philadelphia

Hannemann, K. (1990) Design of an Axisymmetric, Contoured Nozzle for the HEG. Deutsche Forschungsanstalt für Luft- und Raumfahrt, Rep. no. DLR-FB 90-04

Hornung, H. G. (1988) private communication

Lordi, J. A., Mates, R. E. and Moselle, J. R. (1966) Computer Program for the Numerical Solution of Nonequilibrium Expansions of Reacting Gas Mixtures. NASA CR-472

Moretti, G. (1979) The λ-Scheme. Computers and Fluids, Vol. 7, 191-205

Ramshaw, J. D. (1980) Partial Chemical Equilibrium in Fluid Dynamics. Phys. Fl., Vol. 23, 675-680

Rein, M. (1989) Surf: A Program for Calculating Inviscid Supersonic Reacting Flows in Nozzles. GALCIT Rep. No. FM 89-1